FACULTY OF ENGINEERING
AND ARCHITECTURE

Monitoring Vietnamese Bridges Using Vibration Based Damage Detection Method and Machine Learning

Huong Duong Nguyen

Doctoral dissertation submitted to obtain the academic degree of
Doctor of Civil Engineering

Supervisors
Prof. Magd Abdel Wahab, PhD* - Prof. Tien Thanh Bui, PhD**

* Department of Electromechanical, Systems and Metal Engineering
Faculty of Engineering and Architecture, Ghent University
** Department of Bridge Engineering and Underground Infrastructure
Faculty of Civil Engineering, University of Transport and Communications, Vietnam

June 2021

GHENT
UNIVERSITY

FACULTY OF ENGINEERING AND ARCHITECTURE

Monitoring Vietnamese Bridges Using Vibration Based Damage Detection Method and Machine Learning

Huong Duong Nguyen

Doctoral dissertation submitted to obtain the academic degree of
Doctor of Civil Engineering

Supervisors
Prof. Magd Abdel Wahab, PhD* - Prof. Tien Thanh Bui, PhD**

* Department of Electromechanical, Systems and Metal Engineering
Faculty of Engineering and Architecture, Ghent University

** Department of Bridge Engineering and Underground Infrastructure
Faculty of Civil Engineering, University of Transport and Communications, Vietnam

June 2021

GHENT UNIVERSITY

ISBN 978-94-6355-501-2
NUR 956
Wettelijk depot: D/2021/10.500/49

Members of the Examination Board

Chair

Prof. Patrick De Baets, PhD, Ghent University

Other members entitled to vote

Prof. Guido De Roeck, PhD, KU Leuven
Samir Khatir, PhD, Ghent University
Yong Ling, PhD, Ghent University
Prof. Hung Nguyen Xuan, PhD, Ho Chi Minh City University of Technology, Vietnam
Yunlai Zhou, PhD, Xi'an Jiaotong University, China

Supervisors

Prof. Magd Abdel Wahab, PhD, Ghent University
Prof. Tien Thanh Bui, PhD, University of Transport and Communications, Vietnam

Dedicate to my whole family ….

Acknowledgements

This thesis has been carried out in the Finite Element Modelling Research group, Department of Electrical Energy, Systems and Automation, Faculty of Engineering and Architecture, Ghent University, Belgium in the framework of the VLIR-UOS team project VN2018TEA479A103, ‘Damage assessment tools for Structural Health Monitoring of Vietnamese infrastructures’.

Firstly, I would like to express millions of thanks to my advisors, Prof. Magd Abdel Wahab, Prof. Thanh Bui-Tien, and Prof Guido De Roeck for having me as their PhD student and for their guidance, encouragement, support, valuable advice through my research. Without their guidance, this thesis would not have been completed.

I would like also to acknowledge the financial support of the VLIR-UOS scholarships. Moreover, I would like to acknowledge the Bridges and Roads Department, National University of Civil Engineering (NUCE), Hanoi, Vietnam. They have encouraged and provided the best conditions to facilitate my research.

I would like to thank the research team at Ghent university, Long Viet Ho, Hoa Tran-Ngoc, and Samir Khatir. Discussing and collaborating with them help me to improve my research skills and knowledge. I also really appreciate my colleagues in Vietnam, Dr. Quoc Bao Nguyen, Phuc Thanh Trinh, Tien Phat Nguyen, and Van Thinh Nguyen, who stand behind my experiments in this research.

Living and studying in Ghent is an unforgettable memory for me. I would like to send my appreciation to all members of the Soete

Laboratory. There is a very good atmosphere in our office. Especially, I would like to thank Mrs. Georgette D'hont, who is our laboratory secretary. You have offered me a lot of help. Your words, your assistance can comfort me when I have a difficult time. The lockdown of Belgium because of Covid-19 made the life of foreign students harder. I would like to thank my Vietnamese friends, who shared with me this hard time, Ms. Huynh Le Thao Tran, Mr. Le Tuan Anh, Mrs. Le Phuoc Cat Tuong, Ms. Nguyen Thi Phuong among others. Thank you all for the time we spent together.

Finally yet importantly, I would like to express my biggest gratitude to my family. Without their love, unconditional support, and encouragement, I would not have this success today. This doctoral thesis is also for you.

Huong Duong Nguyen

Ghent, March 2021

Contents

Summary

Condition assessment and evaluation of existing bridges is often treated by the bridge administrators during their lifetime. If their reliability and functionality can not be guaranteed based on the structural assessments made, the bridges need to be replaced or strengthened. Structural health monitoring helps to early detect damage in a bridge, which can be upgraded or repaired on time, therefore reducing the maintenance cost and extending the life cycle of structures. The non-destructive methods, such as X-ray, ultrasound, visual inspection are local techniques, which can only detect damage on or near the surface of the structure. Whereas, the vibration based damage detection (VBDD) methods are global damage detection methods that can be applied for complex structures and long term monitoring. Transmissibility and modal curvature methods are two VBDD methods that were chosen to review in this work.

The objective of this thesis is to detect damage in bridges and structures using vibration measurement data. Therefore, to improve the accuracy and level of damage identification, machine learning has been considered as a promising approach to combine with VBDD methods. Machine learning involves computers discovering how they can perform tasks without being explicitly programmed to do so. It involves computers learning from data provided so that they carry out certain tasks. Machine learning approaches are traditionally divided into three broad categories, i.e. supervised learning, unsupervised learning and reinforcement learning. Among many machine learning algorithms, ANNs, and CNNs are the most popular techniques, which have been widely used in SHM during the last decades. Deep learning is a part of a machine learning method based on neural networks, which use multiple layers in the network. Nowadays, deep learning has become

the principal approach for much ongoing work in the field of machine learning.

The achievements of this research are explained as follows:

- Firstly, two approaches are proposed in this thesis. The first one combines transmissibility and artificial neural network (ANN) and the second one combines gapped smoothing method and convolutional neural network (GSM-CNN). A neural network is a series of mathematical constructions that attempts to create a process that mimics the way the human brain operates. The simplest neural network has at least three layers: one input layer, one hidden layer and one output layer. After training, neural networks can predict the damage and its severity with high accuracy.

  In the transmissibility -ANN method, the neural networks are trained by input data got from transmissibility functions. Damages are presented in the numerical model to obtain training data. The targets of the network are the damage location and severity.

  In the GSM-CNN method, the neural networks are trained by images converted from damage indicators and calculated based on the modal curvatures. This method does not require the data from an intact structure. CNN is a class of deep neural networks, which process data that has a grid pattern, such as images. Therefore, the images adapted from damage indicators are used as the input of CNN, wheras the output is the damage location and severity. After training, CNN can predict correctely the damage when it got input data from a laboratory beam and bridge girders.

  Additionally, the procedure for applying these two methods in a structure is described in details. It should be noted that each step should be adjusted depending on structural types.

- Secondly, two proposed methods are validated using FEM and laboratory beams. Damages in a simply supported beam are successfully found using the transmissibility-ANN method. A laboratory beam with free-free boundary conditions is set up to verify the GSM-CNN method. Fifteen accelerometers are used to collect the vibration of the beam. The damages in this beam are detected using the measured vibration data. The accuracy of the GSM-CNN method in the beam structure is more than 90%.

- Thirdly, three Vietnamese bridges including Ca-Non bridge, Nam O bridge, and Bo Nghi bridge are presented as case studies.

Ca-Non is a simply supported girder bridge. It has eight main girders. ANNs can predict damage location and severity in the main girders after being trained by using data from transmissibility functions. In this research, transmissibility functions evaluated directly from the simulated measurements of the responses at analyzed nodes. The load excitation is the moving truck, running across the bridge with constant velocity.

Nam O is a truss bridge. The transmissibility function is calculated between two truss joints. The measurement data of the Nam O bridge is used to update the finite element model. Multiple damages are introduced in this bridge. The transmissibility-ANN method is applied for this bridge to find the damage location and severity. Sensors are installed in the truss joints in order to measure the bridge vibration responses. Therefore, in this research, the displacement response at each node is transformed into the frequency domain to calculate the transmissibility functions.

Bo Nghi is a simply supported girder bridge. It has four main girders. Five accelerometers were attached to the bridge to identify the bridge's natural frequencies. Damage is introduced in the main girder of the bridge. CNN only trains using a finite element model of a single girder, not the whole bridge. Therefore, the size of the training and validation data will be reduced. The images reshape from the damage indicators of the first three modes of the bridge are the input data of CNN. Damage indicators are calculated based on GSM. After training, CNN can predict the location of damage in the bridge girders.

- Finally, the results and discussions for applying the proposed methods for bridges are presented. This success opens the wide road to improve the combination between the vibration-based damage detection method and machine learning for bridge health monitoring.

Samenvatting

Toestandbeoordeling en evaluatie van bestaande bruggen wordt vaak gedurende hun levensduur door de brugbeheerders uitgevoerd. Als de betrouwbaarheid en functionaliteit op basis van de gemaakte bouwkundige beoordelingen niet kan worden gegarandeerd, moeten de bruggen worden vervangen of versterkt. Structurele gezondheidsmonitoring helpt om vroegtijdig schade in een brug op te sporen, die op tijd kan worden opgewaardeerd of gerepareerd, waardoor de onderhoudskosten worden verlaagd en de levensduur van constructies wordt verlengd. De niet-destructieve methoden, zoals X-ray, ultrasound en visuele inspectie zijn lokale technieken die alleen schade op of nabij het oppervlak van de constructie kunnen detecteren. Trillingsgebaseerde schadedetectie-methoden (VBDD) zijn echter globale schadedetectiemethoden die kunnen worden toegepast voor complexe constructies en monitoring op lange termijn. Methoden voor overdraagbaarheid en modale kromming zijn de twee geselecteerde VBDD-methoden om in dit werk te bestuderen.

Het doel van dit proefschrift is om schade aan bruggen en constructies te detecteren met behulp van trillingsmeetgegevens. Om de nauwkeurigheid en het niveau van schade-identificatie te verbeteren, wordt machine learning daarom beschouwd als een veelbelovende benadering om te combineren met VBDD-methoden. Machine learning houdt in dat computers ontdekken hoe ze taken kunnen uitvoeren zonder daarvoor expliciet te zijn geprogrammeerd. Hierbij leren computers van de verstrekte gegevens om bepaalde taken uit te voeren.

Benaderingen met machine learning worden traditioneel onderverdeeld in drie brede categorieën, namelijk leren onder toezicht, leren zonder toezicht en leren met versterking. Van de vele algoritmen voor machine learning zijn ANN's en CNN's de meest populaire technieken, die de afgelopen decennia op grote schaal in SHM zijn gebruikt. Deep learning is een onderdeel van een machine learning-methode op basis van neurale netwerken, die meerdere lagen in het netwerk gebruiken. Tegenwoordig is deep learning de belangrijkste benadering geworden voor veel lopende werkzaamheden op het gebied van machine learning.

De resultaten van dit onderzoek worden als volgt toegelicht:

- Ten eerste stelt dit proefschrift twee nieuwe methoden voor. De eerste combineert transmissibiliteit en een artificieel neuraal netwerk (ANN) en de tweede combineert de afvlakkingsmethode met tussenruimte en een convolutioneel neuraal netwerk (GSM-CNN). Een neuraal netwerk is een reeks wiskundige constructies die proberen een proces te creëren dat de werking van het menselijk brein nabootst. Het eenvoudigste neurale netwerk heeft minimaal drie lagen: een inputlaag, een verborgen laag en een outputlaag. Na training kunnen neurale netwerken de schade en de ernst ervan met hoge nauwkeurigheid voorspellen.

In de transmissibiliteit-ANN-methode worden de neurale netwerken getraind door inputgegevens die zijn verkregen via overdraagbaarheidsfuncties. Schade wordt weergegeven in het numerieke model om trainingsgegevens te verkrijgen. De doelen van het netwerk zijn de locatie van de schade en de ernst van de schade te bepalen.

Bij de GSM-CNN-methode worden de neurale netwerken getraind door afbeeldingen die zijn geconverteerd uit schade-indicatoren en berekend op basis van de modale krommingen. Deze methode vereist geen gegevens van een intacte structuur. CNN is een klasse van diepe neurale netwerken die gegevens verwerken die een rasterpatroon hebben, zoals afbeeldingen. Daarom worden de afbeeldingen aangepast van schade-indicatoren gebruikt als de input van CNN, terwijl de output de locatie van de schade en zijn niveau is. Na training kan CNN de schade correct voorspellen wanneer het inputgegevens kreeg van een laboratoriumbalk en brugliggers.

Bovendien wordt de procedure voor het toepassen van deze twee methoden in een structuur in detail beschreven. Elke stap moet wel worden aangepast afhankelijk van het type constructie.

- Ten tweede worden twee voorgestelde methoden gevalideerd met behulp van de finiete-elementenmethode (FEM) en laboratoriumbalken. Beschadigingen in een eenvoudig ondersteunde balk worden met succes gevonden met behulp van de transmissibiliteit-ANN-methode. Een laboratoriumbalk met vrije randvoorwaarden wordt opgesteld om de GSM-CNN-methode te verifiëren. Vijftien versnellingsmeters worden gebruikt om de trilling van de balk te verzamelen. De beschadigingen in deze balk worden gedetecteerd met behulp van de gemeten trillingsgegevens. De nauwkeurigheid van de GSM-CNN-methode in de balkstructuur is meer dan 90%.

- Ten derde worden drie Vietnamese bruggen, waaronder de Ca-Non-brug, de Nam O-brug en de Bo Nghi-brug, gepresenteerd als casussen.

Ca-Non is een eenvoudig ondersteunde liggerbrug met acht hoofdliggers. ANN's kunnen de locatie van de schade in de hoofdliggers voorspellen nadat ze zijn getraind met behulp van gegevens van overdraagbaarheidsfuncties. In dit onderzoek werden transmissibiliteitsfuncties rechtstreeks geëvalueerd op basis van de gesimuleerde metingen van de responsen op geanalyseerde knooppunten. De ladingsexcitatie is een rijdende vrachtwagen, die met constante snelheid over de brug rijdt.

Nam O is een truss-brug. De overdraagbaarheids functie wordt berekend tussen twee truss-verbindingen. De meetgegevens van de Nam O-brug worden gebruikt om het finiete-elementenmodel bij te werken. Bij deze brug zijn er meerdere beschadigingen aangebracht. Voor deze brug wordt de transmissibiliteit-ANN-methode toegepast om de locatie van de schade en de ernst te bepalen. Sensoren worden in de truss-verbindingen geïnstalleerd om de trillingsreacties van de brug te meten. Daarom wordt in dit onderzoek de verplaatsingsrespons op elk knooppunt getransformeerd naar het frequentiedomein om de transmissibiliteits functies te berekenen.

Bo Nghi is een eenvoudig ondersteunde liggerbrug met vier hoofdliggers. Er werden vijf versnellingsmeters aan de brug bevestigd om de natuurlijke frequenties van de brug te identificeren. Er is schade aangebracht in de hoofdligger van de brug. CNN traint alleen met een finiete-elementenmodel van een enkele ligger, niet de hele brug. Daarom zal de omvang van de trainings- en validatiegegevens worden verkleind. De afbeeldingen die zijn omgevormd van de schade-indicatoren van de eerste drie modes van de brug zijn de inputgegevens van CNN. Schade-indicatoren worden berekend op basis van GSM. Na training kan CNN de locatie van schade in de brugliggers voorspellen.

- Ten slotte worden de resultaten en discussies voor het toepassen van de voorgestelde methoden voor bruggen gepresenteerd. Dit succes opent de brede weg om de combinatie te verbeteren tussen de trillingen-gebaseerde schadedetectiemethode en machine learning voor het monitoren van de gezondheid van bruggen.

List of Figures

List of Tables

Nomenclature &Abbreviations

SHM	:	Structural Health Monitoring
FEM	:	Finite Element Method
ANN	:	Artificial Neural Network
CNN	:	Convolutional Neural Network
VBDD	:	Vibration Based Damage Detection
MAC	:	Modal Assurance Criterion
GSM	:	Gapped Smoothing Method
TFs	:	Transmissibility Functions
ROC	:	Receiver Operating Characteristic
TP	:	True Positive
FP	:	False Positive
TN	:	True Negative
FN	:	False Negative
$\mathbf{M}_{\mathrm{b}}$	:	Mass matrix
$\mathbf{C}_{\mathrm{b}}$	:	Damping matrix
$\mathbf{K}_{\mathrm{b}}$	:	Stiffness matrix
$\mathrm{T}(\omega)$	:	Transmissibility after Fourier transform
$T_{i,j}$	:	Transmissibility function
ω	:	Natural frequency
$\mathrm{X}(\omega)$	:	Response after Fourier transform

W	:	Weight matrix
f(x)	:	Activation function
b	:	Bias parameters
R	:	Coefficient of determination,
mse	:	Mean square error
DI	:	Damage Index
TI	:	Transmissibility damage Index
MC	:	Modal Curvature
ϕ	:	Modal displacement
EI(x)	:	Bending stiffness
M	:	Bending moment
ϕ''	:	Modal curvature
U	:	Modal strain energy

List of Publication

No	Publication	Impact Factor
1	Nguyen, D.H., T.T. Bui, G. De Roeck, and M.A. Wahab, *Damage detection in Ca-Non Bridge using transmissibility and artificial neural networks.* Structural Engineering and Mechanics, 2019. **71**(2): p. 175-183	2.984
2	Nguyen, D.H., H. Tran-Ngoc, T. Bui-Tien, G. De Roeck, and M.A. Wahab, *Damage detection in truss bridges using transmissibility and machine learning algorithm: Application to Nam O bridge.* Smart Structures and Systems, 2020. **26**(1): p. 35-47.	3.557
3	Nguyen, D.H., Q.B. Nguyen, T. Bui-Tien, G. De Roeck, and M.A. Wahab, *Damage detection in girder bridges using modal curvatures gapped smoothing method and Convolutional Neural Network: Application to Bo Nghi bridge.* Theoretical and Applied Fracture Mechanics, 2020. **109**: p. 102728.	3.021
4	Nguyen, H. D., Bui, T. T., De Roeck, G., & Wahab, M. A. (2020). *Damage detection in structures using modal curvatures gapped smoothing method and deep learning*. Structural Engineering and Mechanics, 2021. **77**(1): p. 47-56	2.984
5	Nguyen, D. H., Ho, L. V., Bui-Tien, T., De Roeck, G., & Wahab, M. A. (2020). *Damage Evaluation of Free-Free Beam Based on Vibration Testing*. Applied Mechanics, 2020, **1**(2), 142-152.	

6	Nguyen, H.D., T.T. Bui, G. De Roeck, and M.A. Wahab. *Damage Detection in Simply Supported Beam Using Transmissibility and Auto-Associative Neural Network*. in International Conference on Numerical Modelling in Engineering. 2018. Springer.	

Besides, I have contributed in some other publications during my Ph.D time at Ghent University:

No	Publication	Impact Factor
1	Ho, L.V, Nguyen, D.H., T.T. Bui, G. De Roeck, and M.A. Wahab, *Damage detection in steel plates using feed-forward neural network coupled with hybrid particle swarm optimization and gravitational search algorithm.* Journal of Zhejiang University SCIENCE A, 2020. doi=10.1631/jzus.A2000316	

Chapter 1

Introduction

1.1 Problem outline

Vietnam is an Asian country and the easternmost country on the Indochinese Peninsula. The country long is from the North to the South with a complex transport network. As a developing country, Vietnam wants to attract investment funds. Therefore, Vietnam focuses on modernizing the country's infrastructure. Nowadays, the highway system helps to reduce the time travel from the North to the South. Many large bridges have been built and become the symbol of the city or the country. For example, in Hanoi the capital of Vietnam, across the Hong river, there are three large bridges Dong Tru bridge (the concrete arch bridge); Nhat Tan bridge (a cabe-stayed bridge), and Thang Long bridge (a truss bridge). Da Nang is a city in the middle of Vietnam and is known as a city for tourism. Rong bridge over the Han River is the symbol of this city. In the South, some cable-stayed bridges, such as My Thuan bridge, Can Tho bridge have been constructed, which help to improve the condition of the highway. Besides, many other less known bridges are working as critical transportation links of a region.

Back in history, the first concrete bridge in Vietnam was constructed in the French colonial period. The simply supported beam, the cantilever beam or truss constructed by the cast in place method was very popular at that time. However, these bridges had been destroyed or failed and were replaced by new ones. After the war, Vietnam built many simply supported girders shape T or I. The prestressed concrete was investigated and used in many bridges. Before the year 1975, many prestressed concrete bridges were produced in concrete manufacture companies and erected around the country. Some truss bridges such as Ham Rong bridge, Long Bien bridge using steel material have been erected. After re-gaining the independence, to recover the economy, bridges that were destroyed or failed during the wars, were rebuilt. Besides, many new bridges were constructed along the country to improve the transport from the North to South and expected as determinants of economic development. The spans are longer, the structure types are more modern, and the construction technique has been improved. Using new material, such as high-performance concrete -HPC, high strength steel - HPS, improving the bridge design, applying information technology, ameliorating construction technique, are some of the directions for building future bridges in Vietnam.

To conclude, bridges in Vietnam are very diverse in terms of structural types, materials, and construction time period. Bridges are ones of the most important and expensive structures in the transport network of the country. However, many of the bridges that are currently in use were built during the 1970s and have now reached the end of their design life. Most bridges also carry significantly more and heavier vehicles than originally expected. This makes bridge maintenance, inspection and monitoring of critical importance.

Assessing bridge condition frequently is a mandatory requirement. A bridge or a component of the bridge can be damaged because of extreme events like floods, storms, and earthquakes or due to hazard that the bridge was not designed for. For a long time, some of the bridge components are reduced in stiffness, which affects the lives of the whole bridge. Monitoring the structural damage can be achieved through conventional visual, local, or global methods. Non-destructive testing included vibration-based monitoring is a global monitoring method for damage identification. The changes in modal properties of the damaged structure are identified through the vibration measurement campaign. In the project "Improved operational safety of natural resources infrastructure by Structural Health Monitoring" 2014-2016 (VLIR-UOS 2014-123), measurement campaigns on Vietnamese infrastructures were successfully conducted. After performing vibration measurements on a structure, the next step in SHM is to assess the condition of the structure, detect and localize damage, and quantify its severity. This step is done in the team project VN2018TEA479A103, 'Damage assessment tools for Structural Health Monitoring of Vietnamese infrastructures'. This PhD dissertation is a part of the project.

Damage detection methods can be divided into two main categories, namely physical model-based and statistical/data model-based approaches. Natural Frequency Based Methods, Mode Shape-Based Methods, Mode Shape Curvature/Strain Mode Shape-Based Methods, Dynamically Measured Flexibility Based Methods, are the physical model-based approaches. Whereas, Statistical techniques have neural network-based methods (ANN, CNN). Statistical methods are mathematical formulas, models, and techniques that are used in statistical analysis of raw research data. Neural network learns from the training data to detect damage. This method does not require a deep understanding of structural behavior. However, a significant database of intact, and damaged structure responses are required. That can be supported by the improvement of FEM software and machine learning algorithms. The input data of neural network is the vibration measurements of the real bridge, which are successfully archived. Therefore, some novel methods should be proposed using this data for the health-monitoring step.

1.2 Objectives and contributions

The main objective of this research is to develop novel methods to assess bridge health using vibration measurement data. That is the methodology using the vibration measurements for the existing infrastructures in Vietnam and developing damage assessment techniques. In the past years, although the vibration-based damage method has been proved to have the potential to apply for a real structure, the number of research is limited. Combining machine learning and vibration-based damage method to improve the accuracy in detecting, localizing, and quantifying structural damage is the goal of this research. Moreover, not only numerical examples, but also bridge case studies are the subject of this work.

The original contributions of this research can be summarized as follows:

- Proposing a damage detection method, which combines transmissibility and ANN. TFs are calculated for each bridge damage scenario and used as input of ANN. After training, ANN can predict the damage location and severity of the bridge based on given input. TFs is an output-only method. Therefore, this method does not require knowledge about the input force or structure modal properties, and it has a high potential to be applied to real case studies.

- Proposing a damage detection method, which combines GSM and CNN. CNN learns from images. Therefore, the images converted from GSM has been used as the input of CNN. This method improves the accuracy in localizing the damage compared with using only GSM. The damage location can be found exactly. Using GSM to build the input data does not require the data measurement of intact structure.

- Using two proposed methods to detect damage in a beam structure. Damage in a beam is assessed using both the transmissibility-ANN method and the GSM- CNN method. The proposed methods are verified using a laboratory beam, which is equipped with accelerometers.

- Vibration measurements are set up in the measurment campaign for bridges. From the measured data, the FEM of the bridge can be updated and used for SHM.

- Three Vietnamese bridges: Ca-Non bridge, Nam O bridge, Bo Nghi bridge are monitored. The damages in these bridges are detected by using different methods. This success opens the wide road to improve the combination between vibration-based damage detection method and machine learning for bridge health monitoring.

1.3 Organization of the thesis

This thesis content six chapters. The outline of each chapter, after the introduction chapter, is given below.

Chapter 2: This chapter is the literature review chapter. Firstly, the literature review of the vibration-based damage detection method is presented. Two well-known methods, that are transmissibility and modal curvature method, are reviewed in Section 2.1.2 and 2.1.3, respectively. Secondly, Section 2.2 presents vibration-based SHM using machine learning. Furthermore, many state of art references are reviewed in this chapter.

Chapter 3: In this chapter, the transmissibility and ANN method are proposed, and detailed. The combination of these two methods is explained clearly. The procedure of applying this method for SHM is presented in this chapter.

Chapter 4: In this chapter, the GSM and CNN method are proposed. This chapter provides the methodology of GSM, CNN, and the details of combining these two methods. The procedure of the GSM-CNN approach for damage detection is also presented.

Chapter 5: The results of this research are summarized in this chapter, which has two sections. Section 5.2 presents the damage detection results for a simply supported beam and a laboratory free-free beam, which are assessed using the transmissibility- ANN method and GSM-CNN method, respectively. Section 5.3 presents the results of applying the proposed methods for the three bridges, i.e. Ca-Non bridge, Nam O bridge and Bo Nghi bridge.

Chapter 6: The main conclusions and suggested future work are summarized in this chapter.

Chapter 2

Literature review

2.1 Vibration-based damage detection method

2.1.1 Introduction

Vibration-based damage detection method appeared during the late 1970s, was applied in aerospace and offshore oil industries [1]. In terms of civil engineering, bridges and bridge management systems are the subject of infrastructural monitoring using vibration data in many kinds of research [2-4]. The vibration data of a structure can be measured by a variety of sensors, such as LDVTs, accelerometers, and strain gauges. The measurement data are always made in the time domain and can be converted to the frequency domain by using a Fourier transform. Modal parameters such as natural frequencies, mode shapes, modal damping, etc. are the functions of physical properties of the structure, i.e. mass, damping, stiffness, and boundary conditions. Therefore, by examining the changes of modal parameters, the damage can be detected and located. For example, the natural frequencies of the first three modes of a 355 m span suspension bridge, Tamar bridge, show variations due to damage [5]. The potential of VBDD methods applied to a real-life bridge is high and got the attention of many researchers [6-8].

However, the VBDD methods are influenced by many factors such as temperature, wind, traffic, and data quality (signal to noise ratio). Several different VBDD methods were perfomed using natural frequencies, mode shapes, mode shape curvatures, dynamically measured flexibilities. The number of sensors required for data collection depends on VBDD methods. Single or a few sensors may be enough to identify the natural frequencies of one structure. Whereas, multiple sensors are required for the mode shapes. A literature review written by Doebling et al. [9] presented an extensive survey that used VBDD methods. Referred to Doebling et al. [9], most of the research at the time pre-1996, limited to laboratory exercises, although these were still able to provide useful insights for potential full-scale applications. Many researchers attempted to investigate the VBDD method for civil structures. Mazurek [10], Doebling and Farrar [11] examined the statistical significance of VBDD results in 40 highway bridges in Albuquerque, New Mexico. Since then, the experimental data obtained from existing bridges have been used to investigate different aspects of VBDD methods [12]. The presence of scouring under foundations was assessed using the dynamical behavior of a bridge. The promising applications of VBDD methods in bridge monitoring were showed in this research results [13]. The transmissibility functions between pairs of accelerometers were used to obtain the damage detection in a masonry arch bridge [14]. The vibration of the damaged and undamaged bridge were measured and provided the signals for the VBDD method. The modal strain energy and the modal flexibility method were proved to work well on real structures [7, 15]. The mode shape curvature were used to detect the damage in bridges and successfully applied to Z24 bridge [16]. In these recent years, methods used to detect damage in a bridge using vibration measurement got a lot of researchers' interest [17-20] . The state-of-the-art review of VBDD methods were provided in Ref. [21]. The aim of this framework is to guide the researchers step by step to implement the VBDD methods.

VBDD is a simple method to apply and suitable for real bridges. There are several different VBDD methods. However, in preparing this thesis, the author decided to emphasize on two methods that are transmissibility method and the modal curvature method.

2.1.2 Transmissibility

The transmissibility in a single-degree-of-freedom system is defined as as the ratio between the modulus of the response amplitude and the modulus of the imposed amplitude of motion. The idea of transmissibility can be extended to a system with *N* degrees-of-freedom. Transmissibility use output only response measurements, defined as output to output relationship. Transmissibility makes it possible to detect damage without any assumption about the nature of excitations even though different loading conditions are applied during the experiments. Moreover, it is demonstrated that the transmissibility function is less sensitive to environmental variables [22]. The limitation of transmissibility is that it depends on the location of excitations. A change in the excitation location might cause a significant change in the TFs under healthy conditions. The transmissibility functions are sensitive to damage because they are the ratios of FRFs, which are known to be sensitive to damage, however it is difficult to prove their localization capabilities.

Research on transmissibility has been raised decades ago. Transmissibility functions (TFs) have been first proposed as potential features for damage detection in [23]. Since then, many damage detection methods base on TFs have been defined and developed by many research group, such as the group of Keith Worden at the University of Sheffield [24-27], the research team of Maia at IST in Porto [28-32], and the group of Adams at Purdue University [22, 33, 34]. For damage detection, transmissibility can be used directly [35, 36], or combined with other novel approaches such as deep learning [30, 37-40].

For vibration modal analysis, the concept of TFs have been developed from a single degree of freedom to multiple degrees of freedom [41]. The motivation for using transmissibility for damage detection relies on the fact that the transmissibility is a local quantity, suggesting a higher sensitivity than the modal parameters in detecting changes in the dynamic behavior of structures [29]. In 1999, Ribeiro et al. [42] showed how the transmissibility matrix could be evaluated directly from the measurement of the responses in time domain, rather than in frequency domain. Therefore, the modal parameters of a structure can be identified from output only transmissibility that only requires the output information. The transmissibility could be calculated from measurement data [43-45], under variable load conditions in [46]. The modal properties of a bridge were identified using transmissibility measurement in [47, 48].

For civil engineering structures, the importance of SHM is to extend the lifetime, to enhance safety and to reduce the cost of maintenance. The application of transmissibility in structural health monitoring has been presented in [26, 32, 36, 38, 40, 49-60] . Large civil structures were the subject of many researches. For example, damage in a three-story aluminum frame structure was detected and qualified using transmissibility coherence analyzed from system response [60]. Transmissibility calculated both from bridge and vehicle response in a vehicle and bridge coupled systems were successfully used to detect damage in a bridge [36]. The damage in a simple supported girder bridge and a truss bridge was assessed using transmissibility combined with machine learning [38, 40].

The review on transmissibility can be found on some article, such as in Refs. [61, 62]. Although the potential to apply transmissibility to SHM of bridges is high, not many related articles are available.

2.1.3 Modal curvature methods.

The changes in the curvature mode shapes have been shown to be more sensitive to damage than the natural frequencies or the mode shapes themselves [63]. From the 1990s, some researchers were applied this method to bridges SHM, such as in Refs. [16, 64, 65].

A drawback of using the changes in the curvature mode shapes for damage detection is that the measurement data of healthy structure needs to be known. Ratcliffe [66] proposed a method that uses a finite difference Laplacian function to identify the location of stiffness damage without the prior knowledge of the intact structure and then successfully locates delamination in an experimental composite beam [67]. This is called Gapped Smoothing Methods (GSM). The global smoothing method for the one-dimensional beam using mode shape data has been developed by Yoon et al. [68, 69]. In order to locate the damaged regions in a plate, Yoon et al. extended the methods to the two-dimensional gapped smoothing technique [70].

The combination of modal curvature with other approaches to identify damage has also been raised by many researchers. The mode shape curvatures in conjunction with static displacements could improve the results of damage assessment in a bowstring truss [71]. A Gaussian process (GP) regression model was used to build smoothed (noise-free) curvature mode shapes from noisy experimental modes [72]. Multiple damages in plate structures can be localized by generating a damage index based on GSM [73]. GSM is an effective method for localizing damage by curvature damage index. The images extracted from the GSM can be used to train the network to detect and quantify the damage [74].

Wahab and De Roeck were the two first researchers who applied a modal curvature method to a bridge [16]. A damaged indicator called “Curvature Damage Factor” (CDF) was proposed. This indicator summarizes the difference in modal curvature between intact and damaged structures for all modes. The fault position is the location of the high peak at the CDF plots. This method was successfully applied not only in beam-like structures, but also on a real pre-stressed concrete structure, i.e. the Z24 bridge. The data from an intentionally damaged bridge, I-40 bridge over Rio Grande in Albuquerque, NM, USA was used to test the mode shape curvature methods. Thirteen accelerometers were mounted equally along the girder to get the FRFs data. The results showed that the method worked well. The applications of modal curvature have been presented to assess bridge damage, such as a small curved bridge [75], Dogna bridge [17, 76], and Bo Nghi bridge [74]. Although the ability for applying GSM to bridges is high, the number of relevant applications is limited.

2.2 Vibration-based structural health monitoring using machine learning

SHM is a technology to automate the inspection process in order to assess and evaluate the health condition of structures in real-time or at specified time intervals. SHM limits the number of collapsed structures, gives an opportunity to repair them, extends their lives and therefore it avoids demolishing them and constructing new structures. Thus, money will be saved, and the environment will be protected as well. There are four different sequential SHM levels: detection, identification, quantification, and prediction. The higher levels of SHM, the more complicated SHM technology is.

The review on SHM can be found in many publications [6, 9, 21, 77-81]. Some state of art SHM methods using measured vibration response data, machine learning based, and other methods based on statistical process control, fuzzy logic were reviewed.

SHM with non-destructive evaluation could include long term monitoring with a small set of instruments [82] or short term vibration measurement campaign. For civil engineering structures, vibration data provides a rich source of data for structural investigation. Vibration based monitoring is a subset of SHM, which focuses on the dynamic part of structure [83]. The elaborate vibration based monitoring has been done in some bridges, such as Stonecutters Bridge [84], Rion Antirion Bridge [85] and the London Millennium Bridge [86], and others [87-94]. This will help to investigate the condition of the bridge and to provide useful knowledge for future bridge designs.

In recent years, the interest in applying machine learning to SHM has increased [95]. Several studies have been undertaken to combine machine learning and vibration-based damage detection methods to detect damage in beams [37, 96] and bridges [18, 38, 97].

The human brain has about 10^{12} neurons and about 10^{14} neural connections between them. This complex pairing system gives us the ability to analyse, process information, emotions, etc. The brain is able to organize and control its basic elements (single neurons) to perform tasks such as identification, control, and analysis in a much more effective way than the current computer. For example, the human brain is able to identify familiar faces in the crowd, estimating the distance of the observed object's moving velocities in the period from 100 ms to 200 ms, the speed at which the computer and computational software are still not available today. The ability to analyse handwriting, audio, and sound analysis, understand foreign languages and dialects is also a difficult task to simulate.

Machine learning attempts to bring computer a little closer to brain's capacity by imitating certain aspects of information processing in the brain, in a highly simplified way. The neural network investigates the capabilities of the human brain and reproduces those capabilities on machines, equipment or software. Once trained, the neural network is able to recognize similarities presented with a new input pattern, resulting in a predicted output pattern. One neural network has two basic processes: the learning process and the testing process. Learning process is the process of creating knowledge from existing information. This process is done for a set of sample data called metrics. Learning consists of three tasks; a) compute output, b) compare output with desired target then adjust weight and c) repeat the process. The quality of the learning process is expressed by a target function or a function error. The learning process will reduce the error of this function. The learning process is usually learned on learning algorithms to optimize target functions. To evaluate the effectiveness of the learning process, one needs to use an additional testing process. A trained network is tested with a new set of data, called the test data set. The test variance will show the operability of neural network with new data, which has not appeared during the learning process. The low-test error corresponds to the ability to handle new good cases. Application process consists of:

1. Collect data

2. Separate into training and test sets

3. Defined a network structure

4. Select a learning algorithm

5. Set parameters, values, initialize weights

6. Transform data to network input

7. Start training, and determine and revise weights

8. Stop and test

9. Implementation: use the network with new cases

Deep learning is a data-based approach for structural health monitoring. The measured data from the structure are attempted to relate to the estimated data from models to identify the damage. Auto-Associative Neural Network (AANN) and Convolutional Neural Network (CNN) are two machine learning algorithms that can be referred to as deep learning methods when they are more than one hidden layer. The neural network model is trained to learn the structural behaviour from the trained data (numerical data, past data, experience data), following the principle of the human brain. The model is built and trained to make the best accurate prediction of structural behaviour. In recent years, neural networks have been the most frequently used machine learning algorithms for damage assessment [95]. The drawbacks of a deep learning network are the need for training and validation, which takes a decent amount of time and the dependence of accuracy on the underlying FEM. There are several ‘classical' approaches, which can handle quite complex 3D problems even for coupled problems [98]. These approaches need the user to have deep knowledge about structural analysis, whereas deep learning does not require prior knowledge.

ANN and vibration-based methods are employed to deal with many structural health monitoring problems [38, 99-103]. For example, transmissibility combined with ANN was proposed to detect damage in a simply supported beam [102] and in a simply supported girder bridge [38]. In these papers, the transmissibility indicators were used to train the network with the purpose of identifying the location and severity of the damage. The ANN training parameters were improved by employing Cuckoo search algorithm [103]. In terms of damage assessment, ANN combined with Cuckoo search can predict accurately damage and requires shorter computational time. ANN has been developed and adapted to industrial fields. ANN is proved to be successfully used in SHM [96, 99, 104].

While ANN works with numerical matrices, CNN works with images, and has been proved to be effective when being applied in many research fields, such as object detection, image classification and face recognition [105]. So far, the applications of CNN in SHM are limited. Most of them are crack detection based on the analysis of images. By classifying images of crack in composite materials, the type of damage could be found [106]. CNN has been proposed to detect cracks in concrete structures [107]. Verstraete *et al.* [108] fed a time-frequency image into a CNN for faults diagnosis of rolling element bearing. Images of transmissibility functions obtained from a FE model were successfully used to train the CNN to localize and quantify damage in two case studies involving a mass-spring system and a structural beam [39]. The structural damage was detected by a CNN that was trained with images of raw acceleration signals [109]. CNN combined with a vibration-based method has been used in many types of research and proved to be robust and sensitive to damage [110, 111].

Chapter 3

Transmissibility and ANN method

3.1 Introduction

Bridges may suffer from damage due to environmental influences, accidental actions, service loads, and natural hazards. SHM provides an objective evaluation of the overall performance and condition of a bridge. This could protect a bridge from collapse, allow proper maintenance, make the bridge safe and extend its lifetime. SHM process, generally, has three main stages. Stage 1 is the survey step, measuring the actual structural state. Stage 2 is data analysis, using appropriate algorithms to treat the data collected in Stage 1. Stage 3 is based on the analysis results from the second phase. The engineer makes decisions on the status, working conditions, as well as measurements to improve the performance of the structure, ensure the safe exploitation of the bridge. To analyze the data, we can use two methods namely physical model-based method and non-model based method. Physical model-based approaches concentrate on the understanding of the structure from its physical characteristics, such as natural frequencies [112, 113], mode shapes [114], damping and stiffness [115, 116]. Moreover, if combined with optimization algorithms to reduce the difference between model results and results extracted from measurements, this approach will provide more accurate and efficient results [117-121]. Some authors also combined optimization algorithms with the cloud model [122] or improved the existing global optimization technique [123] for better structural damage identification. When the structure appears to be damaged, the physical variables change. However, these parameters are very sensitive to temperature, environment, and load condition. Therefore, sometimes, we do not get enough evidence to conclude whether the structure is damaged or not. In addition, creating physical models that accurately represent structural behavior is time-consuming, which slows down the detection of failures and potentially increases the cost of analysis.

Statistical approach or non-model based method is concerned with the collection, organization, analysis, and presentation of the response data. In this approach, the condition of the structure can be determined without the in-depth knowledge of the expert as well as the direct geometry and material properties. Some methods based on this approach have been developed in recent years, including Cross-correlation, Auto-Regressive, Principle Component Analysis Method, Computer vision – based, ANN. Cross- correlation is a measure of similarity of two time series, two functions or two random vectors. This analysis explored for structural health monitoring and damage detection. Yang *et al.* [124] used Cross-correlation method to detect the damage of a laboratory composite beam under random excitation. In the Auto-Regressive (AR) model, the structural response is modeled using a mathematical function [125]. It is seen that if the structure is altered for example due to damage or deterioration, the mathematical parameters in the AR model will be changed. In Principle Component Analysis (PCA) method, a model is constructed based on major components. Using an orthogonal projection, the original set of variables in an N-dimensional space is transformed into a new set of uncorrelated variables, in a P-dimensional space such as $P<N$. Although the data information is reduced, the main characteristic of the data, as well as the basic characteristic of the structure, still maintains. PCA was used to detect damage by using two separated vectors corresponded to the two biggest individual values of the data correlation matrix and compared with other methods [126]. Recently, computer vision-based method with data collected through the camera, camcorder, and data processing algorithms, was also of great interest because of technical and economic issues [127, 128]. The ANN method combined with statistical probability theory is a method of detecting structural damage through analytical algorithms, which identifies mutation factors or novel elements. ANN is a set of mathematical models that work on the principle of the biological neural network [129]. ANN is also a method to solve the inverse problem. ANN starts with the results and then calculates or predicts the causes. Besides ANN, there are many other methods that can be used to solve the inverse problem. Nanthakumar *et al.* [98] used regularized level set method for detecting damage in material interfaces, Vu-Bac *et al.* [130] used a NURBS-based inverse analysis for a shell thin structures. Data, after analysis in stage 1, will be used to design and training ANN, which

are trained to predict future values of the features. Following the validation of the best trained network, ANN will decide by itself on the results in stage 3. Numerous ANN techniques have been applied to SHM [9] and become a powerful tool for damage identification. Zang and Imregun [131] used measured frequency response functions as input data to ANN and applied PCA technique to measured FRFs. Hakim and Abdul Razak [97] combined ANN and adaptive neuro-fuzzy inference system (ANFIS) to identify damage in a model of steel girder bridge using dynamic parameters. The natural frequencies are obtained from experimental modal analysis used as input data. ANN was used for structural damage detection in the girders of a vehicular bridge and then could predict the location and severity of the damage in the studied bridge with high accuracy [132]. In recent years, more and more applications of machine learning algorithms were reported and became the most frequently used technique [95, 99, 133].

Damage assessment of bridge structures using vibration-based method has been studied since the early 1980s [134]. Modal properties such as frequency response functions (FRF) [135], mode shape curvatures [16], stiffness matrix [136, 137], modal data [138], correlation and cross-correlation coefficients [139] are usually used to identify damage in bridge structures. However, these properties are very sensitive to the environment and operating condition of the bridge. Applying these methods for small localized damage areas faces challenges [140]. Three new parameters including kurtosis, skewness of signals, and statistical density function are proposed for evaluating crack defects [141]. On the other hand, the advantages of transmissibility in detecting damage are remarked in many research works [22, 142]. The response ratio between two degrees of freedom is described as the transmissibility function. Local damage, which affects the local responses between these degrees of freedom, is expected to be more sensitive to transmissibility than

FRF. The damage index based on changes in transmissibility function between undamaged and damage structure is normally used to detect damage. Maia *et al.* [29] proposed a damage indicator based on correlations of the transmissibility functions and the modal assurance criterion (MAC) in modal analysis. These researchers are in the team of Maia at IST, Porto [28] and focus on the study of using transmissibility functions to detect and locate damage. Zhou *et al.* [32] proposed a new method combining transmissibility, hierarchical clustering analysis, and similarity measure to detect damage. Ten-floors structure simulated results and free-free beam laboratory tests were used to prove the good performance of transmissibility in detecting damage. Transmissibility has been studied to explore structural damage in many research provided by Zhou *et al*. [30, 60, 143, 144]. The more recent review on the application of transmissibility-based system identification for SHM was provided in Ref. [145]. This paper categorized global, local transmissibility functions, and limited the usage of several methodologies to the following principal features: model updating, modal analysis, and damage detection.

The vibration responses of the bridge under excitation could be used to identify the bridge dynamic parameters. The recent developments in vibration measurement instruments and analysis computing technology support this concept [146]. Most of the new improvements in the field of SHM has a high contribution from machine learning technology. ANN are among the most widely used machine learning techniques and has been trained to discover, localize, and quantify damage in bridge structures. A method of identifying damage through the evaluation of response data from an instrumented bridge was proposed in Ref. [147]. Lee *et al.* [148] assessed damage of multiple-girder simply supported bridges by using the input of the neural network as the ratios of the mode shape components between damaged and undamaged scenarios.

Mehrjoo *et al.* [149] presented a method using a back-propagation based neural network for estimating the damage intensities of truss bridge joints. ANN worked well for assessing the damage in a simply supported beam [37]. Vibration-based damage method are based on the principle that can change both the physical properties and dynamic properties. These changes can be used as input for ANN and the output are the structure conditions, damaged or undamaged, location, and severity of the damage [150]. In the last 10 years, many researchers used natural frequencies and mode shape curvatures as inputs for ANN [151]. FRF data was applied to present the healthy conditions of each member in a three-story building and used as the input of ANN [152]. The measured FRF data reduced via principal component project was handled as the ANN input variable alternatively of raw FRF [131]. The results showed that the trained ANN could distinguish between intact and damaged states with a high degree of accuracy.

As discussed above, transmissibility is proved to be more sensitive with local damage than FRF. Therefore, in this section, a novel method that makes use of transmissibility damage index as input data of ANNs is proposed. Using transmissibility combined with machine learning has been done before by some authors. Meruane [153] used transmissibility information to identify anti-resonant frequencies. The changes in the anti-resonant frequencies with respect to the intact were used as the input of ANN, which could locate and quantify the structural damage. Zhou and Wahab [104] used the indicators taken from the transmissibility function as input and then predicted the damage. A new approach method is proposed in this section and makes use of the input parameters calculated from the transmissibility function. The network not only can predict the existence of damage, but also can classify the damage types and identity the location of the damage.

3.2 Transmissibility

Firstly, we consider the relationship between responses and forces in term of receptance. If one has a vector F_A of magnitudes of applied forces at coordinates A, a vector X_U of unknown response amplitudes at coordinates U and vector X_K of known response amplitudes at coordinates K, one may establish the following relationship:

$$X_U = H_{UA} F_A \tag{3.1}$$

$$X_K = H_{KA} F_A \tag{3.2}$$

Where H_{UA} and H_{KA} are the receptance frequency response matrices related coordinates U and A, and K and A, respectively. Eliminating F_A in two equation, we have:

$$X_U = H_{UA}\, H_{KA}^{+} X_K \tag{3.3}$$

Or

$$X_U = T_{UK} X_K \tag{3.4}$$

Thus, the transmissibility matrix is defined as:

$$T_{UK} = H_{UA}\, H_{KA}^{+} \tag{3.5}$$

The transmissibility matrix could be evaluated directly from the measurement of responses. From equation (3.4), we also have:

$$T_{UK} = X_U\, X_K^{-1} \tag{3.6}$$

Dynamic model of the structure can be obtained through finite element modelling. The equation of motion can be written as:

$$\boldsymbol{M}_b\ddot{U}_b + \boldsymbol{C}_b\dot{U}_b + \boldsymbol{K}_b U_b = f_b \tag{3.7}$$

Where $\boldsymbol{M}_b$, $\boldsymbol{C}_b$, $,\boldsymbol{K}_b$ denote mass, damping and stiffness of the structure, respectively; f_b is an excitation force.

Solving Eq. (3.7), we can calculate the structure dynamic responses. These responses can be measured by attaching sensors to the structure on field measurement as well as by numerical simulations. Displacement, acceleration response time-histories were collected based on the impact of the excitation force. The time-history of the response data is then transformed to the frequency domain using a fast-Fourier transform. The transmissibility $T_{i,j}$ is then calculated as the ratio between two locations as shown in Eq. (3.8):

$$T_{(i,j)}(\omega) = X_i(\omega)X_j^{-1}(\omega) \tag{3.8}$$

Where X_i and X_j are the response in the frequency domain at location i and j, respectively.

Transmissibility functions can be computed from numerical simulations and then generating the data to train the ANNs.

3.3 Artificial Neural network (ANN)

3.3.1 Machine learning algorithm

The scientific study of algorithms and analytical models that can be learned from experience to improve its performance, without human intervention is called Machine Learning (ML). “Training data” is a mathematical model of sample data built by machine learning algorithms. Supervised learning, semi-supervised learning, and unsupervised learning are three main categories of the machine learning algorithm. Supervised learning algorithms using a collection of data carry both the inputs and the desired outputs to create a mathematical model. Semi supervised learning algorithms work with half-done training data, where a part of the sample inputs does not have desired outputs. In unsupervised learning algorithms, the training data only contains the inputs and no desired outputs. In this section, we use classification and regression algorithms, which are types of supervised learning. The first task is called classification, which includes designating input originals to one of the discrete classes. These classes are the number and location of damages in the bridge. The second task, which we mention as regression, is treated with foretelling the severity of the damage.

3.3.2 Artificial Neural Networks structure

ANNs are estimating a mapping function based on the knowledge of some example input-output pairs. This study intends to train the neural networks using the training set composed of pairs of values for the independent (input) and dependent (output) variables [154]. ANNs were designed to contain a family of mathematical models. The structure of biological neural networks is the source of ANNs creation. Pattern recognition problem, as we have indicated, must find out the non-linear mapping between a collection of input and output variables. The mapping is therefore created as mathematical functions. Adjustable parameters in these functions are resolved from training data. The output variables of ANNs are the results of the combination functions between the bias function or hidden functions with weight parameters.

In general, the neural network will be playing the role of *f(.)* as:

$$y = f(x) \tag{3.9}$$

Where x is a vector of inputs and y is a vector of outputs.

The network consists of many layers:

- One input layer that receives the indicator got from the transmissibility functions.
- One or more hidden layers that analyzes the data
- One output layer that provides the results of the analysis. In this work, the output is the location and the severity of the damage.

One layer has many neurons, which behave as functions. They transform an input signal into an output signal *f(x)*. The weights are incrementally adjusted to decrease the error, and this process is iterated until the error can no longer be minimized. The process can be expressed as:

$$x_i^{(k)} = f\left(\sum_j w_{ij}\, x_j^{(k-1)} + b_j\right) \tag{3.10}$$

Where: $x_j^{(k-1)}$ is the signals from preceding layer k-1, passed through a nonlinear activation function f to emerge as the output of the node $x_i^{(k)}$ to the next layer. w_{ji} and b_j are the weight and bias parameters.

If the network has more than one hidden layer, the procedure will continue with more hidden functions. The function *f(.)* is called an activation function. Many kinds of activation function can be examined to optimize the network parameters. The most common used functions are expressed below.

$$f(a) = tan^{-1}(a) \quad g(a) = \frac{1}{1+e^{-a}}$$
$$f(a) = \tanh(a) = \frac{e^{2a}-1}{e^{2a}+1} \tag{3.11}$$

During the training process, the value of the weights ω_{ij} are continuously adjusted to optimize network performance. The default performance function for feedforward networks is mean square error *mse*, i.e. the average squared error between the network outputs *y* and the target outputs *t*. It is defined as follows:

$$mse = \frac{1}{N}\sum_{i=1}^{N}(e_i)^2 = \frac{1}{N}\sum_{i=1}^{N}(t_i - y_i)^2 \tag{3.12}$$

There are numbers of training algorithms that can be used to train the neural network. The chosen training algorithm was the Levenberg-Marquardt backpropagation algorithm. This algorithm is fast and performs well on function fitting (nonlinear regression) problems [155].

The neural network has a number of the layers. The first layer is the input layer and the last layer is the output layer. The hidden layers are between these two layers. Each layer has a series of nodes. Each node represents one neuron. The number of hidden layers and the number of nodes are decided based on the relationship between input and output data and on the number of nodes in the input and output layers. The goal is to train the network maps new inputs correctly and not to over-fit the data. The ANNs structure is illustrated in Figure 3.1.

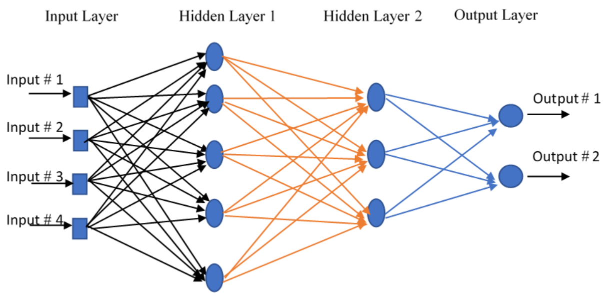

Figure 3.1–A neural networks structure

3.3.3 Pattern classification

The ANNs considered above for classifying the types and locations of damages was designed to take the input data and to assign it to one of those classes, i.e. Damage Case 1 (DC1), Damage Case 2 (DC2), Damage Case 3 (DC3), etc. We can present the outcome of the classification in terms of variable y_k (output variable), where k is the number of class. If the sample represents DC1, then y_1 takes the value 1, whereas y_2 and y_3 take the value 0. Similarly, if the sample represents DC2 then y_2 takes the value 1, whereas y_1 *and* y_3 take the value 0.

Consider the problem of two classes' prediction between Damage Case 1 (DC1) and other Damage Cases (DC#). The two classes are labelled as DC1 (Positive) and DC# (Negative). Figure 3.2 illustrates the Probability Density Functions of this case. For each threshold, there are four achievable results from a binary classifier. It is named a true positive (*TP*) if the actual class is DC1 and the result from the prediction is also DC1. It is named a false positive (*FP*), if the actual class is DC# and the result from the prediction is also DC1. For a negative results, there can be either true negative (*TN*) if prediction class is the same as actual class as DC# or false negative *(FN*).

Both TP and FP are zero if the threshold is located at the right of the null distribution and DC1 is not detected. The area below the null distribution extends if the threshold moves to the left. The four outcomes can be formulated in a confusion matrix, as show in Table 3.1, where the correct classifications are presented by numbers along the major diagonal.

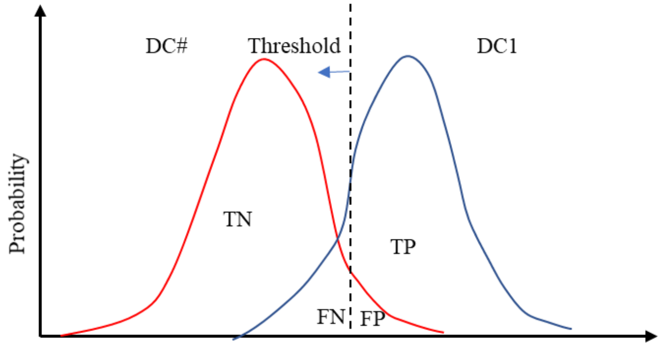

Figure 3.2–Distributions from the class DC1 and other classes DC#

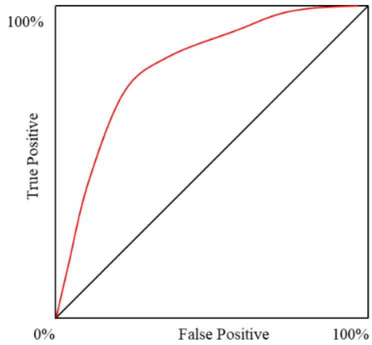

Figure 3.3–The receiver operating characteristic (ROC) curve

Table 3.1 –The confusion matrix for classifying DC1 and DC#

Outcome	Observed		
	Positive	Negative	
Positive	TP	FP	PPV FDR
Negative	FN	TN	FOR NPV
	TPR FNR	FPR TNR	ACC

Where:

PPV: Positive Predictive value; $PPV = \frac{TP}{TP+FP}$

FDR: False Discovery Rate; $FDR = \frac{FP}{TP+FP}$

FOR: False omission rate; $FOR = \frac{FN}{FN+TN}$

NPV: Negative Predictive value $NPV = \frac{TN}{FN+TN}$

TPR: True Positive Rate; $TPR = \frac{TP}{TP+FN}$

FNR: False Negative Rate; $FNR = \frac{FN}{TP+FN}$

FPR: False Positive Rate; $FPR = \frac{FP}{FP+TN}$

TNR: True Negative Rate; $TNR = \frac{TN}{FP+TN}$

ACC: Accuracy; $ACC = \frac{TP+TN}{TP+FN+FP+TN}$

Another general and graphical way to review the achievement of classifiers is by using receiver operating characteristic (ROC) curves [156]. Figure 3.3 plots the ROC curve, where the horizontal axis is the false positive rate (FPR) versus the vertical axis, which is the true positive rate (TPR). The TPR and FPR are often called sensitive and specificity, respectively. The ROC space is divided into two parts by the diagonal line. If the classifier understands the classes, the points in ROC is in the upper left triangle. The practical way to see the accuracy of the method is to analyze the area under the curve; i.e. the value 1 for perfection and value 0.5 for worthless.

3.3.4 Regression analysis

Assigning new inputs to one of the discrete classes is the main task of classification problems. However, if there are many other pattern recognition tasks, we shall refer to as regression problems, in which the outputs represent the value of continuous variables. The output of the network should be continuous variables corresponding to the target output (t), i.e. the severity of damage.

Linear regression is the simplest form of regression. Assuming that n observations $(y_i, x_i), i = 1, \dots, n$ have been used to train the network, the estimated linear regression line can be written as:

$$y_i = \beta_0 + \beta_1 x_i + \varepsilon_i \tag{3.13}$$

Where ε_i is random variable; $\beta_0 + \beta_1 x_i$ presents a straight line, and β_1 is the slope of the regression line.

Linear regression tasks are finding two parameters: the intercept (β_0) and the slope (β_1) of the regression line. The goal of these tasks is to minimize the value of mse as presented in Eq. (3.12).

Finally, the coefficient of determination, R^2, is commonly used to evaluate the goodness of fit within a simple linear regression model. It is defined as follows:

$$R^2 = 1 - \frac{SSE}{SST} \tag{3.14}$$

Where: $SSE = \sum_{i=1}^{n}(t_i - y_i)^2$ is the sum of squared error,

$SST = \sum_{i=1}^{n}(t_i - \bar{t})^2$ is the sum of squared total and $\bar{t}$ is the mean of t value.

From this definition, $R \in [0,1]$. $R = 0$ indicates that the model cannot fit the target of the network. Whereas, R =1 indicates that the model is perfectly fit.

3.4 Transmissibility- ANN approach for structural damage assessment

3.4.1 Transmissibility damage index as input data for ANN

Consider the structural vibration, as discussed in Section 3.2, the transmissibility $T_{i,j}(\omega)$ is described simply as the ratio between two responses in the frequency domain when an excitation force is applied.When used for detecting damage, the transmissibility is more effective if restricted to specific frequency bands [26]. The indicator $TI_{i,j}$ is defined in Eq. (3.15) to enhance the sensitivity of transmissibility associative with the structural deterioration or damages.

$$TI_{i,j} = \int_{f_{min}}^{f_{max}} T_{i,j} df \tag{3.15}$$

Where f_{min} and f_{max} are the low and high boundary of frequency band.

The choice of f_{min} and f_{max} greatly influences the results. This is usually done by using engineering's experience. The frequency range was chosen based on the regions of high similarities between different transmissibility functions in a structure.

The indicator $TI_{i,j}$ of intact bridge at all locations is used to calculate the damage indicator. The damage indicator value is the difference between the transmissibility indicators at all locations of the damaged bridge and intact bridge for a given frequency band. The damage indicators $DI_{i,j}$ are calculated using the following equation:

$$DI_{i,j} = \frac{TI_{i,j}^{u} - TI_{i,j}^{d}}{TI_{i,j}^{u}} \tag{3.16}$$

Where, $TI_{i,j}^{u}$ is the transmissibility indicator of the undamaged bridge and $TI_{i,j}^{d}$ is the transmissibility indicator of the damaged bridge.

The damage indicator should take the mean value of all measurement times. The damage indicators of all transmissibility functions will be stored and then used as the input data of ANN.

3.4.2 Target for ANN

In this work, the location and the severity of damage are the targets of the network. The severity of damage is shown by the percentage decrease in the stiffness of the damaged section. All input parameters for the network are calculated based on the damaged position and the severity of the damage, respectively. The network diagram is shown in Figure 3.1.

3.5 Procedure of Transmissibility-ANN methods for damage detection

This section provides the general steps for damage detection using the transmissibility-ANN method. Depends on each type of structure (simply supported bridges, continuous bridges, buildings, etc.), each step should be adjusted.

Step 1: Data collection

Transmissibility is estimated from Eq. (3.8) for all measurements.

Step 2: Calculate the input of ANN and define the target

The transmissibility damage index is calculated based on section 3.4.1 and used as input data for ANN. This process is performed repeatedly with multiple defect locations and varying severity of damages.

Damage locations and deterioration levels are retained as a target for ANN.

Step 3: ANN working

The ANN works as described in Sect 3.3.

Step 4: Analysis of results

Based on the objective function that evaluates whether the network is performing well or not. If the operation is not good, we can change the number of neuron in each layer or change the frequency domain when calculating the transmissibility damage index. If the result is satisfactory, the calculation is finished, and the network can be used.

Step 5: Applying for new data

Applying the new transmissibility index as the input data of trained ANN, the outputs of the network are the desired damage locations and deterioration levels.

Chapter 4

GSM-CNN method

4.1 Introduction

Bridges are amongst the most crucial and expensive infrastructures in a country. Early detection of damage can help to maintain in due time, so extending, the lifetime of a bridge and saving money. Vibration-based monitoring has been proved to be a useful method for providing valuable information about bridge dynamic response characteristics [83]. Vibration-based damage detection is a subset of vibration based monitoring. In the last decades, vibration-based damage detection got a lot of attention, showing the potential to real-life applications in general and bridges in particular [6, 7]. The changes in vibrational characteristics, such as, natural frequencies, modal curvatures, flexibilities and flexibility curvatures can be used to detect damage [8]. Some methods require the baseline of a healthy structure, which is not always available. Gapped Smoothing Method (GSM) was proposed by Ratcliff and Bagaria [67] with the basic assumption that the mode shapes of the beam are smooth and can be approximated by polynomials. This method was then improved by many other researchers and became one of the most commonly used techniques for damage detection. It is a good damage indicator for 1-D beams [66], beam-like structures [63] and plate-like structures [70, 73, 157]. Some attempts were done for applying the method in real-life structures despite the existing noise in measurement data [16, 158, 159]. The GSM also succeeded in locating the bridge damage [17, 75, 76]. Wahab et al. applied the modal curvatures technique to measurement data of the Z24 bridge and concluded that this method seemed to be promising for detecting damage in civil engineering structures [16]. GSM could realize the damage location in a small radius curved bridge [75]. Dilena et al. first applied the modal curvature method to Dogna bridge, a four-span simply supported concrete bridge. Only experimental data was used and confirmed that modal curvatures could be applied on a full-scale bridge. The location of damage along the main girders was identified by the changes in modal curvatures of the first two modes [76]. GSM was then applied in the FRF experimental data of Dogma bridge and showed the ability to detect the damage location in specific conditions [17]. Although the ability for applying GSM to bridges is high, the number of relevant applications is limited. This chapter proposes a novel method combining GSM and CNN to locate the damage in a bridge.

In recent years, the interest in applying machine learning to structural health monitoring has increased [95]. Several studies have been undertaken to combine machine learning and vibration-based damage detection methods to detect damage in beams [37, 96] and bridges [18, 38, 97]. Convolution neural network is different from ordinary neural network in the way that the inputs of CNN can be images, which are read as a three-dimension matrix based on the number of pixels and color (Grey or RGB (Red Green Blue)) by machines. Some CNN applications have successfully emerged with vibration-based damage detection [109, 160-163]. Several attempts have been made to assess damage in the bridge using the CNN technique. CNN classified images of a reinforced concrete bridge system from post-disaster inspection into different system-damage locations and failure levels [164]. The thermal images were used to train CNN to predict the surface damage of steel members in a truss bridge [165]. Therefore, a combination of CNN and vibration-based methods to assess damage in the bridge is possible and has the potential to be applied in practice.

In this section, we propose a method that combines CNN and a vibration-based damage detection method, namely gapped smoothing method. CNN is used to predict the location of damage based on images obtained from GSM damage indices.

4.2 Modal curvature calculation from mode shape data

The modal curvature (MC) of beam cross-section is related to the local bending stiffness. The modal curvature, $\phi''(x)$, at a point can be defined as:

$$\phi''(x) = \frac{d^2\phi(x)}{dx^2} = -\frac{M}{EI(x)} \tag{4.1}$$

Where: $\phi(x)$ is the modal displacement, $EI(x)$ is the bending stiffness and M is the bending moment at a section.

If damage exists in a structure, the bending stiffness of the structure will reduce in the damaged region and therefore the magnitude of curvature at that section of the structure will increase. The modal curvature only changes locally and can be used to detect damage.

The modal curvature can be computed from the displacement mode shapes using the central difference method:

$$\phi_i'' = -\frac{\phi_{i-1} - 2\,\phi_i + \phi_{i+1}}{\Delta x^2} \tag{4.2}$$

Where ϕ_i is the vertical component of the displacement mode shapes at the measured point i and Δx is the distance between two measurement points. For the first and last grid points, three contiguous data points are used to estimate the curvature.

Modal curvatures have been claimed to contain local information on damage and to be less sensitive to environmental variables than natural frequencies. However, simply using the difference between modal curvatures in the undamaged and damaged states can result into localization errors, due to the complex pattern that this quantity presents when considering broad damages or higher order modes.[166].

4.3 Curvature gapped smoothing method

The mode shapes can be used to locate the damage in the structure. The gapped smoothing method fits the modal curvature of mode shape to the gapped cubic polynomial. The damage index is then calculated as the difference between the measured shape and the calculated polynomial [70]. The cubic polynomial C_i for the ith element of the curvature, at position x_i is the distance from the beam end, is defined as:

$$C_i = a_0 + a_1 x_i + a_2 x_i^2 + a_3 x_i^3 \tag{4.3}$$

The coefficients a_0, a_1, a_2, a_3 are determined using neighbor curvature element ϕ_{i-2}'', ϕ_{i-1}'', ϕ_{i+1}'', ϕ_{i+2}'' from the damaged structure. For the first grid point, the cubic polynomial is determined using the modal curvatures ϕ_2'', ϕ_3'', ϕ_4'' and ϕ_5''. For the second point the curvature elements, ϕ_1'', ϕ_3'', ϕ_4'', and ϕ_5'' are used to determine the polynomial coefficients. For the last grid point and the point before the last point, a similar calculation is used. The damage index δ_i is calculated as the squared differences between the damaged curvature and the cubic polynomial.

$$\delta_i = (\phi_{di}'' - C_i)^2 \tag{4.4}$$

The measured displacement mode shape contains real and imaginary parts. These two parts are separately converted to modal curvatures by applying a gapped smoothing method.

$$\begin{aligned} \delta_i = (\phi_{di\,REAL}'' - C_{i\,REAL})^2 \\ + \ (\phi_{di\,IMAGINARY}'' - C_{i\,IMAGINARY}\,)^2 \end{aligned} \tag{4.5}$$

The damage index is determined for each grid point in turn. Figure 4.1 shows the damage index versus the location of damage in a numerical free-free beam as a reference. The figure shows clearly that the damage is somewhere between node 4 and node 7, whereas the real damaged is between node 5 and node 6. The damage index increases when the severity of the damage increases. In this chapter, GSM method will be improved by combining it with CNN. The GSM-CNN method can show the exactly location of damaged element and the severity of the damage. Figure 4.2 shows the contour plot, which will be used as the input for the CNN. This image plots the damage index of each point in the four observed modes. The horizontal axis is the grid point location, whereas the vertical axis is the natural frequency of observed mode and the colours indicate the values of damage index after normalization.

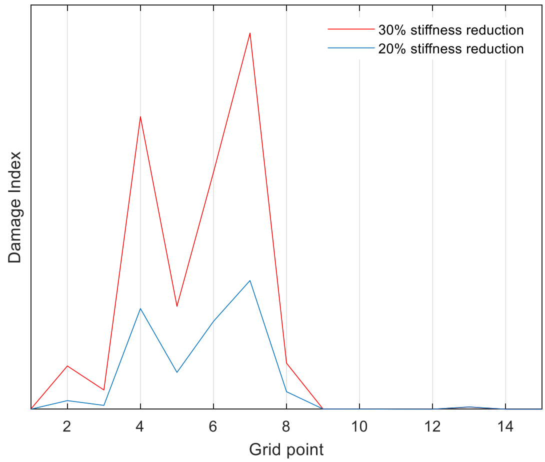

Figure 4.1– Damage index for mode 1 of a free-free beam - damage is located between nodes 5 and 6

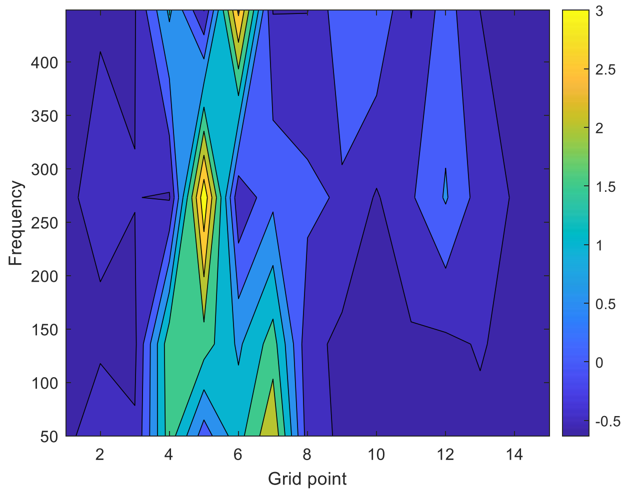

Figure 4.2– Contour plot of the damage index - damage is located between node 5 and 6 with 30% stiffness reduction

4.4 Modal strain energy and gapped smoothing method

The modal strain energy of an Euler- Bernoulli beam can be defined as:

$$U = \frac{1}{2}\int_0^l EI\left(\frac{\partial^2\phi}{\partial x^2}\right)^2 dx \tag{4.6}$$

Where l is the beam length, *EI* is the bending stiffness of the beam and ϕ is the displacement mode shape. For a subdivided beam, the strain energy U_i from measurement point *j* to *j+1* due to the ith mode is given by:

$$U_{ij} = \frac{1}{2}\int_{x_j}^{x_{j+1}} (EI)_j\left(\frac{\partial^2\phi_i}{\partial x^2}\right)^2 dx = \frac{1}{2}\int_{x_j}^{x_{j+1}} (EI)_j\,\phi_{ij}''^2 dx \tag{4.7}$$

Where ϕ_i is the displacement mode shape, ϕ_i'' is the curvature mode shape and x_j is the location of measurement point *j*. The damage leads to reducing bending stiffness. However, the bending stiffness is interrelated with the curvature (Eq.(4.7)), the damage increases the curvature. Therefore, the square of curvature can be used as an indicator of damage. The damage index is defined as the absolute differences between the square of curvature of the damaged structure and the square of that of the intact structure as in the equation below:

$$D_{ij} = \left|\phi_{dij}''^2 - \phi_{0ij}''^2\right| \tag{4.8}$$

Where ϕ_{dij}'' and ϕ_{0ij}'' are the modal curvature for mode number *i*, at measurement point *j* of damaged and intact beam, respectively. Operational modal analysis (OMA) results in unscaled mode shapes since the loads on the structure are not measured. Therefore, scaling the OMA mode shapes, for example, scaling it to maximum unit value should be done before applying Eq.(4.7). Based on this method, damage can be detected, but baseline data of healthy structure is required. Unfortunately, this data does not always exist.

Local damage results in a mode shape that has a local change in slope. This means a jump in the modal curvature. Various methods such as cubic spline, cubic polynomial (section 4.3), and piecewise linearization were used to locate the sudden change in the modal curvature. The section below introduces the method that uses a Fourier series approximation to estimate the mode shape curvatures of the intact structure.

The fitting modal curvature ϕ''_{fi} can be reconstructed in Fourier series form as:

$$\phi''_{fi}(x) = a_0 + \sum_{k=1}^{n}(a_k.\cos(k\omega x) + b_k.\sin(k\omega x)) \qquad (4.9)$$

Where a_0 models a constant (intercept) term in the data, ω is the fundamental frequency of the signal, n is the number of terms (harmonics) in the series ($1 \leq n \leq 8$). The coefficients appearing in this equation will be chosen to create the best-fit smooth curve from the original data by using the 'fit function' from Matlab.

From Eq. (4.8) and Eq.(4.9) , the damage index can be calculated based on the absolute difference between the square of measured data and the square of the smoothed fitted curvature value:

$$D_{ij} = \left|{\phi''_{dij}}^2 - {\phi''_{fij}}^2\right| \qquad (4.10)$$

Figure 4.3a shows an example of the Fourier fitting modal curvature constructed from the damage modal curvature of a simply supported girder for mode 1. The local damage around point x_j makes the modal curvature unsmooth. The Fourier function helps to create the smooth modal curvature curve of the healthy girder based on the modal curvature of the damaged girder. Figure 4.3b shows the damage index calculated from Eq. (4.10) and normalized to have mean 0 and standard deviation 1.

Therefore, the damage index can be extracted from the mode shape and does not need the baseline data from healthy structure. To overcome the false peaks because of measurement noise, the damage index for each mode is normalized using standard deviation.

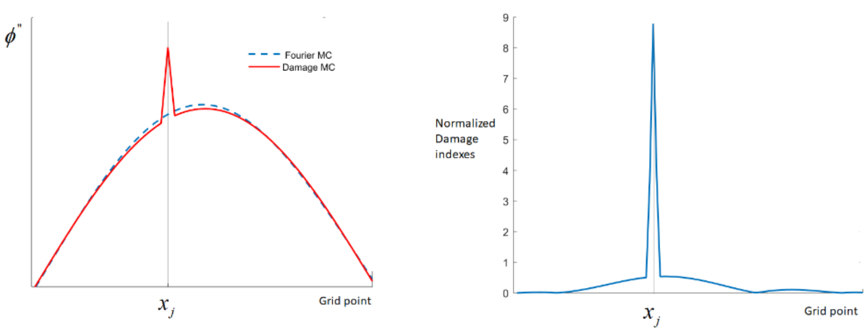

a. The modal curvature of the damaged structure and Fourier fitting modal curvature

b. Damage index

Figure 4.3– Damage index for mode 1 of a free-free beam - damage is located between nodes 5 and 6

4.5 Convolutional Neural Network (CNN)

The source of deep learning is a neural network, a branch of machine learning. Deep learning has become popular since 2006 after the fast development of high-performance parallel computing systems, such as GPU clusters. The most representative model of deep learning is Convolutional Neural Networks (CNN).

CNN is the Feed Forward Network (FFN) that uses the convolution operation instead of the matrix multiplication in its layers [167]. The computer reads the images in the input layer then passes through to the convolution layer. Image is considered as a numeric matrix, the size of this matrix is the pixels of the image. The convolution is performed using a weights matrix W, also known as filter or kernel. These filters are trained by a backpropagation algorithm. Each neuron output of the convolutional layer in layer l can be calculated as:

$$y_{i,j}^{l} = g\left(\sum_{a=0}^{n-1}\sum_{b=0}^{n-1} w_{a,b}\, y_{(i+a),(j+b)}^{l-1} + b_{a,b}\right) \tag{4.11}$$

Where y^{l-1} is the output of the previous layer, n is the filter matrix size. g is an activation function (sigmoid, tanh and ReLu) and the bias matrix b is added.

The typical structure of a five-layer CNN is shown in Figure 4.4. The input layer of CNN is a 3D matrix of pixel intensities for different colour channels. For example, a colour image size 64 × 64 pixels, can be presented as a tensor 64 × 64 × 3 (in RGB colour channel). To get all features of the image, all pixels are added to the input layer. Consequently, the input layer has 12288 nodes. Then, the number of nodes in hidden layer must be large enough to get all the data transformed from the input nodes. Many weights and bias must be used. To reduce the numbers of parameters in the network, while maintaining the main features of the image, the convolutional operation is applied for each layer. The final responses are obtained after going through a filter matrix (learned weights). Sigmoid and ReLU are the most common activation functions. Pooling layers are used between convolution layers to keep the main features, while reducing the number of parameters. Both sizes of the data representation and data computation are reduced and non-maximum values are eliminated by max-pooling computation [168]. No learning occurs in the max-pooling layer. A fully connected layer is the last layer being a vector. This final layer with different activation function is used to calculate the output layer of the model. The CNN composed of input images, convolutional layers, pooling layers, fully connected layer, and output layer. According to the tasks involved, the whole network can be optimized based on an objective function (e.g. mean squared error or cross-entropy loss) to minimize the differences between the output layer and target. Trained CNN can be stored and used to predict new cases.

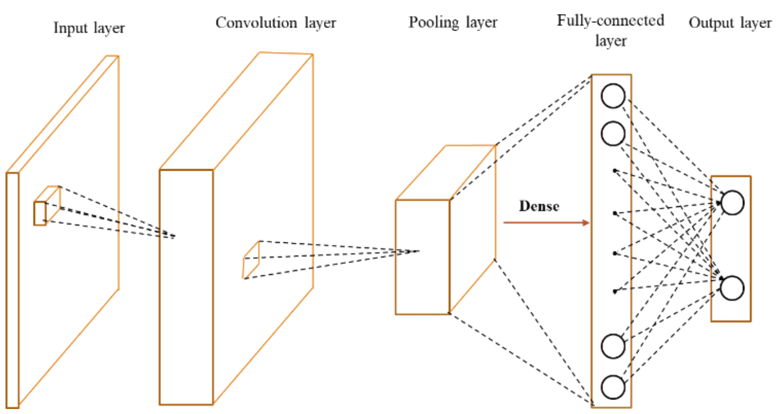

Figure 4.4– Structure of a Convolutional Neural Network

4.6 Procedure of GSM-CNN approach for damage detection

This part will propose a four-step procedure using GSM combined with CNN to locate the damage and estimate the severity of the damage.

Step 1: FE model.

FE model of the structure is created.

Step 2: Data collection.

Damage is simulated in the FE model. The damage indexes are calculated based on the curvature gapped smoothing method. The contour plot of damage index is saved for each damage scenario.

The mode shapes in the real structure are measured, the damage index is calculated and the contour images of the damage index in the real case are plotted.

Step 3: Build, train and valid the CNN model.

All images from FEM are classified into different damage locations and damage severities. These images are used as the input layer of CNN. The target of the output layer is the damage location and damage severity. After training and validation, CNN can predict the location and severity of the damage based on the contour image of the damage index.

Step 4: Test the CNN model.

Images of the damage index in the real case are converted into the CNN, which has been trained successful. The outputs of the CNN are the location and severity of the damage.

Chapter 5

Results and Discussion

5.1 Introduction

The methodology of the Transmissibility-ANN method and GSM-CNN method is presented in chapter 3 and chapter 4, respectively. This chapter will present the results and discussion and has two main sections. In the first section, the two proposed methods will be applied to detect damage in a beam. The laboratory beam was set up to verify the methods. Then, the method was improved to apply for real bridges. Different types of the bridge were considered such as simply supported bridge, truss bridge, concrete bridge, and steel bridge.

5.2 Damage detection in beams

5.2.1 Simply supported beam

5.2.1.1 Introduction

In this section, a simply supported beam is analyzed using a transmissibility-based damage detection methodology combined with Artificial Neural Network (ANN). Firstly, the transmissibility is calculated between two points in the examined beam. Then a transmissibility indicator is taken as input for the neural network, which accounts only for the response data and is sensitive to damage. The target of ANN is the location and the severity of the damage. It is found that the network, after being trained, shows good results and can be used to detect and localize damage.

5.2.1.2 Numerical model

A FE model of an experimentally tested simply supported beam, shown in Figure 5.1, is divided in 18 elements as shown in Figure 5.2. The beam is made of steel and has I100 cross-section. Young's modulus is 190.98 GPa, the density is 7800 kg/m^3, and the length is 3 m. The beam is fitted with acceleration sensors in fixed positions. The frequency of the first mode identified from FEM in SAP 2000 is 34.26 Hz, similar to the one obtained from experimental data. The dynamic force is applied to the beam at node 3 and, in turn, the accelerations are obtained at the other nodes. To investigate the damage in the beam, we reduce the stiffness of each element. For each element, a stiffness reduction from 0% to 50% with an interval of 1% is recorded. For each single damage, there will be 51 scenarios, i.e. from D1 to D50, and D0 is for the intact case.

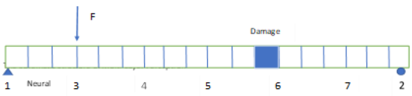

Figure 5.1– Experimental beam Figure 5.2– FEM beam

5.2.1.3 Input for ANN

As discussed above, the transmissibility matrix T34, T35, T36, T37 could be evaluated directly from the measurement of the responses at nodes 3, 4, 5, 6 and 7 using Eq. (3.8). The indicator takes the sum of transmissibility along the specific frequency range described in Eq.(3.15) and is used as the input for ANN.

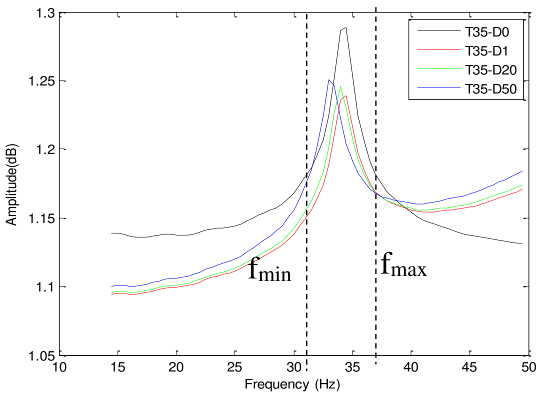

Figure 5.3– A description of the frequency band

As discussed in section 3.2, the choose of f_{min} and f_{max} greatly influences results and this is usually done through experience. With 4 functions

T34, T35, T36, T37 we have 4 indicators TI1, TI2, TI3, TI4 that can be used as input for the network. The intact beam natural frequency of mode 1 is 34.26 Hz. From Figure 5.3, we used the first peak which frequency ranges between 31 Hz and 35 Hz to calculate the ANN input.

As we know in advance, natural frequencies are important factors in assessing structural failure. There are also number of studies that make use of frequencies as damage indicators. However, in many cases, they are changing very slightly and then we do not have enough evidence to conclude whether a structure is damaged or not. The natural frequencies of a simple beam can be determined using acceleration sensors located on the beam. In this section, the natural frequencies are used as an input for the network.

5.2.1.4 Target for ANN

The first two levels of SHM are detection and localization of damage. This chapter concentrates on those two indexes as the target for the network. The severity of damage is shown by the percentage decrease of the stiffness of damage section. Damages are introduced in four elements 4, 5, 6, 7. For each damage case, we have 50 scenarios as explained earlier. All input parameters for the network are calculated based on the damaged position and the severity of the damage, respectively. The network diagram is shown in Figure 5.4.

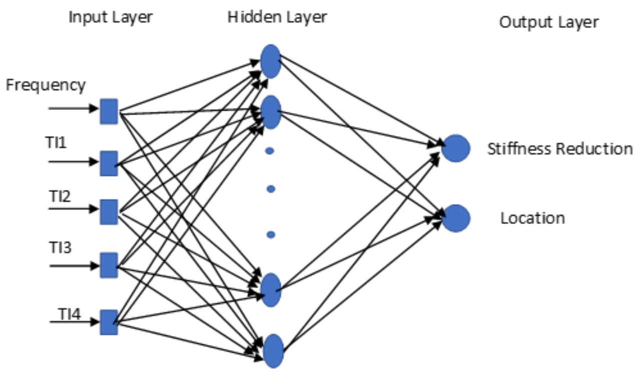

Figure 5.4– The schematic structure of multi-layer perceptron neural networks model

5.2.1.5 Results

a. Intact beam

Figure 5.5 plots different transmissibility functions when applying an impact force at node 3. Because of symmetry, the T34 is almost the same with T36, and T37 is a horizontal line. From Figure 5.5 and Figure 5.6, it is clearly recognized that although the applied force is different, the transmissibility function remains unchanged. This emphases that the transfer function can be determined from the response only, which can be characterized by the dynamic effect of the system and the independence of the input force. This makes it easier to apply it in practical cases because sometimes it is extremely difficult to measure the applied force on a structure in service.

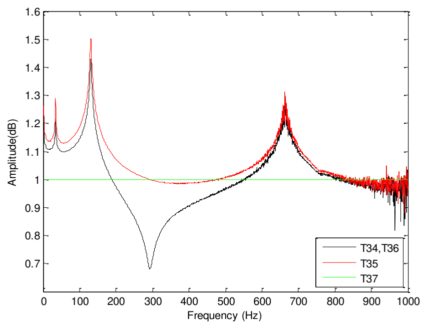

Figure 5.5– The transmissibility with impact force at node 3

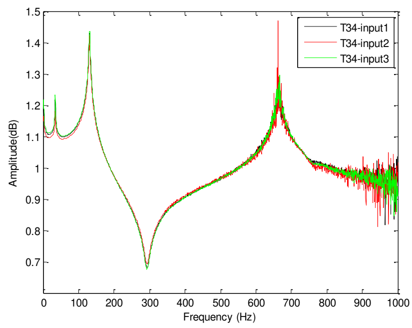

Figure 5.6– The transmissibility T34 with difference inputs

b. Damaged beam.

The TFs of damaged beam with different level of damage (the location of damage section is node 6) are shown in Figure 5.7 and Figure 5.8. It is easy to see that even when the damage is very small, the TFs change immediately. As the stiffness decreases, the peak of the transfer function moves slightly to the left (Figure 5.9). This suggests that the TFs are more sensitive to the detection of damage than to the severity of damage.

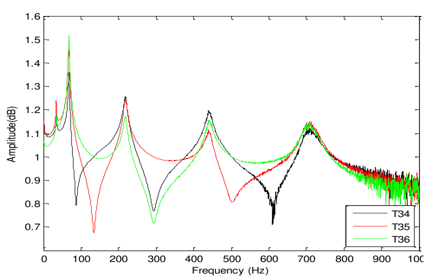

Figure 5.7– The TFs, damage in node 6, 1% stiffness reduction

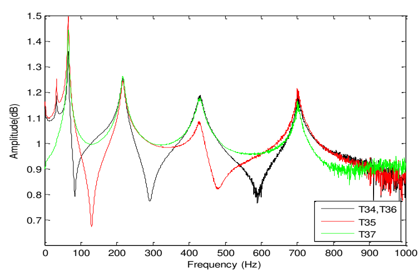

Figure 5.8– The TFs, damage in node 6, 50%stiffness reduction

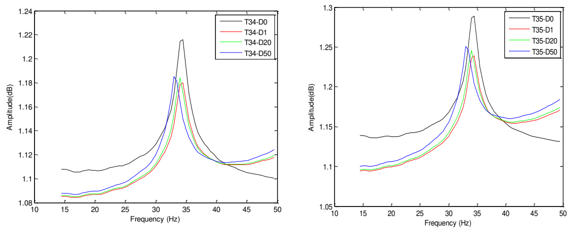

Figure 5.9– The comparison of the first peak at the TFs with difference scenarios, damage in node 6

As discussed above, beams will be damaged at different levels by changing the stiffness of each element. This is done at positions close to points 4, 5, 6 and 7. TI indicator is calculated and used as input data for AANN network. 70% sample of the data is used to train the network, which is adjusted according to its error. 15% sample is used to measure the network generalization, and to halt training when generalization stops improving. 15% sample is used to test the network, which has no effect on training and so provides an independent measure of network performance during and after training.

Figure 5.10 shows the network outputs with respect to targets for training, validation and test sets. The results are perfectly fit, the data falls along 45-degree line, where network outputs are equal to the targets, with R value in each case of slightly above 0.99.

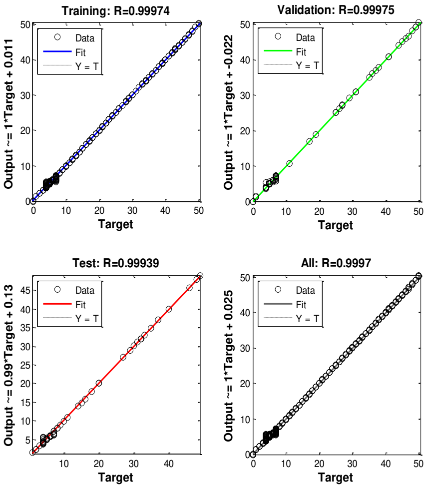

Figure 5.10– Correlation between actual and predicted values in training phase, validation phase and test phase

Figure 5.11 shows the predicted results of AANN function with 4 damage positions and 50 levels. The vertical axis indicates the location of the damage section (at 4 nodes 4, 5, 6 and 7) and the horizontal axis is 50 degrees of damage respectively (from D1 to D50). The graph shows that if the stiffness decreased by less than 5%, the results are less accurate. However, with more severity of damage, the network's predicted results are relatively accurate. This is understandable because the structure needs enough changes to be identifiable and distinguishable. With the above results, we can confirm that after training the AANN network, we can completely detect the degree of damage and its location.

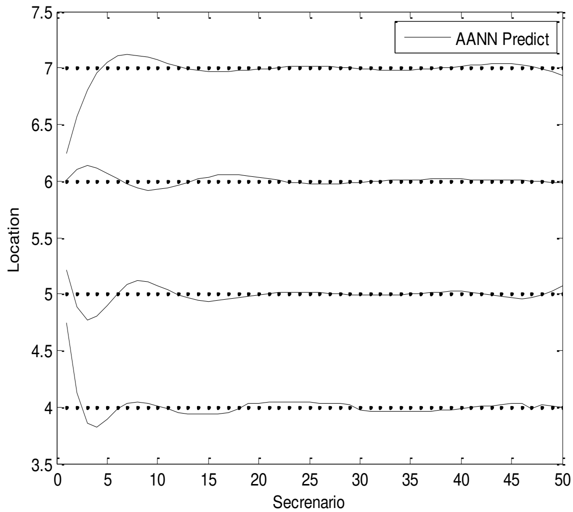

Figure 5.11– Comparison between actual damage location and AANN prediction

5.2.1.6 Discussion

This study proved that transmissibility together with AANN could be used to detect and localize damage. It uses the response measurements only, and the use of AANN make it possible to detect damage once the base-line is defined.

The object of this study is simply supported beams that are simulated with various degrees of failure, i.e. damage positions and severities. Research has shown that, with the data collected, the network after learning was completely capable to identify damage. It should be noted, however, that the selection of input parameters greatly influences the results. Using this method requires large number of data sets to train and test the network, which is a drawback. In this chapter, we analyse each of the single damage cases, however many cases may contain multiple damages. To solve this problem, we need a very large data set. However, today with the development of structural analysis software, the structure can be modeled using FEA and then get data to train the network, thus opening a new direction for SHM technology.

5.2.2 Free-free beam

5.2.2.1 Introduction

This section deals with damage detection in a laboratory beam using the GSM- CNN method. CNN input layer is a tensor with shape (number of images) × (image width) × (image height) × (image depth). An activation function is applied each time to this tensor passing through a hidden layer and the last layer is the fully connected layer. After the fully connected layer, the output layer, which is the final layer, is predicted by CNN. In this section, a complete machine learning system is introduced. The training data was taken from a FE model. The input images were the contour plots of curvature gapped smooth damage index. A free-free beam was used as a case study. In the first step, the FE model of the beam was used to generate data. The collected data were then divided into two parts, i.e. 70% for training and 30% for validation. In the second step, the proposed CNN was trained using training data and then validated using available data. Furthermore, a vibration experiment on steel damaged beam in free-free support condition was carried out in the laboratory to test the method. A total number of 15 accelerometers were set up to measure the mode shapes and calculate the modal curvature of the damaged beam. Two scenarios were introduced with different severities of the damage. The results showed that the trained CNN was successful in detecting the location as well as the severity of the damage in the experimental damaged beam.

Four damage detection steps procedure of the GSM-CNN methods presented in section 4.6 are applied below to assess the damage of a free-free beam.

5.2.2.2 Numerical experiment and data collection (step 1 and 2)

A steel beam, having dimensions of 1 m long × 70 mm wide × 10 mm thick, density of 7820 kg/m^3, Young modulus $E = 2.00 \times 10^{11}$ N/m^2 was modelled in Matlab. The beam was divided into 17 nodes and 16 elements (Figure 5.12). Damaged was introduced in 14 elements (from element 1 to element 14) by reducing the stiffness of each element, from 1% to 60%. For each element, 60 scenarios exist. In total, 14 × 60 = 840 scenarios were created using FEM. Figure 5.13 shows the contour plot of damage index for 3 different damage locations and severities. This figure is plotted using the same technique as shown in Figure 4.2. The vertical axis represents the frequency of damaged beam and the horizontal axis represents the grid points. The axis labels are not shown in Figure 5.13, because the input images of CNN does not contain them. The colour indicates the value of the damage index (as in Figure 4.2). 840 scenarios created 840 images, which were used as input for CNN.

Figure 5.12– Structure of a Convolutional Neural Network

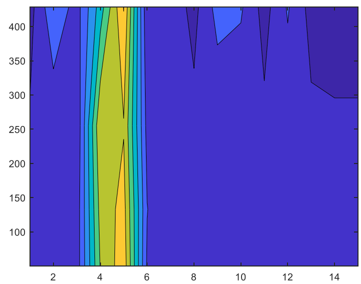

a. Damaged in element 3 with 54% stiffness reduction

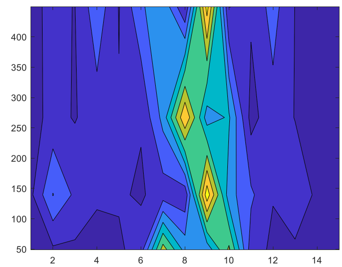

b. Damage in element 8 with 35% stiffness reduction

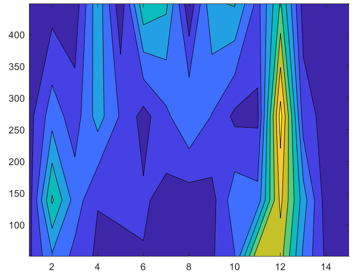

c. Damage in element 12 with 15% stiffness reduction

Figure 5.13– Input images of CNN

5.2.2.3 Build, train and validate CNN architecture (step 3)

CNN with three convolutional layers is used in this work. 16, 32 and 64 different filters are used in the first, second and third convolutional layer, respectively. After each convolution, a ReLU function (Eq. (5.1)) is applied as the activation function. The softmax function (Eq. (5.2)) is applied as the activation function in the last layer to convert to probability distribution across all labels. In this equation, n is the number of neurons, and x_j is the value of the last layer in the jth time neuron. Softmax activation function used to convert this number into the percentage $\sigma(x_j)$ (0< $\sigma(x_j)$<1 and $\sum \sigma(x_j) = 1$), then $\sigma(x_j)$ is considered as the probability that the image belongs to class jth. The categorical_crossentropy function is used as the loss function.

$$ReLU\ (x) = \begin{cases} 0\ if\ x < 0 \\ 1\ if\ x > 0 \end{cases} \tag{5.1}$$

$$\sigma(x_j) = \frac{e^{x_j}}{\sum_{i=1}^{n} e^{x_i}} \tag{5.2}$$

To identify the location of the damage, the output layer with 14 nodes is used. Each node corresponds to a damaged element. The structure of this network is presented in Figure 5.14. Besides, the dropout is applied to the first and last max pooling layer to avoid overfitting in the training data set. After applying dropout, randomly 20% of the neurons are set to zero after one epoch. 840 images are labelled and used to train and valid the network. 70% of data is used for training and 30% of data is used for validation. Figure 5.15 presents the training accuracy and validation accuracy of the proposed network. From the plots, the accuracy is higher than 90% after 10 epochs, and very stable during 20 epochs. The accuracy of 90% means for 100 images, 90 images were predicted correctly by CNN. This is considered as a very good result. The CNN was restored and could be used for new cases.

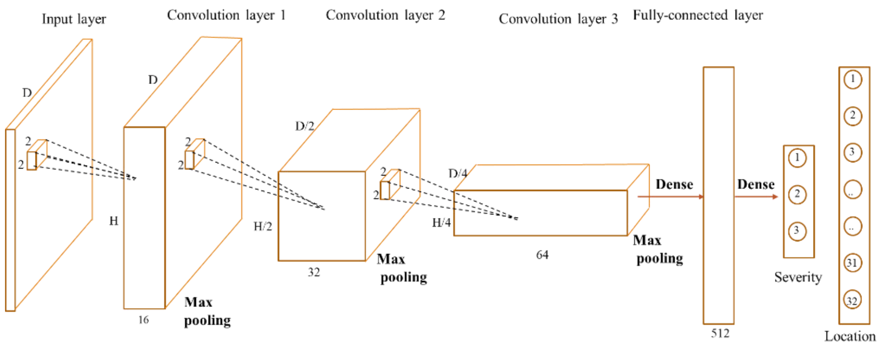

Figure 5.14– The proposed CNN architecture

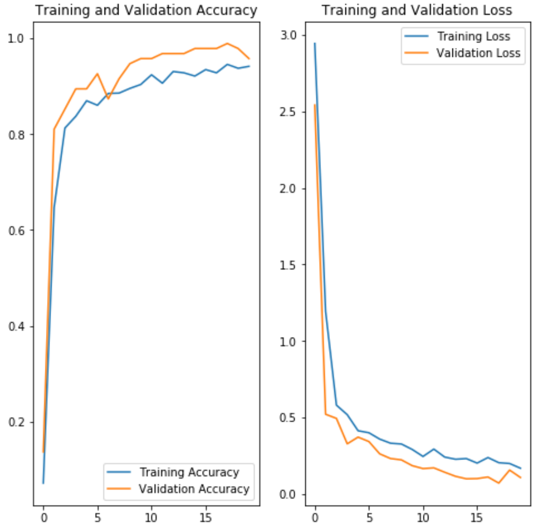

Figure 5.15– The accuracy and loss of training and validation data from CNN used in finding the damage location

Figure 5.16– The accuracy and loss of training and validation data from CNN used in finding the severity of the damage

The severity of the damage is grouped into three levels:

- Level 1: The stiffness reduction is less than 20%.
- Level 2: The stiffness reduction is from 21% to 50%
- Level 3: The stiffness reduction is more than 50%

840 images are labelled in three groups. We changed the output layer in the proposed CNN in three nodes corresponding to three levels of damage. After training and validation, the accuracy of the proposed CNN is over 95% after 15 epochs (Figure 5.16). After epochs 15, reviewing the plot of training and validation loss, we can see a slight trend of overfitting. In this case, the best model should be chosen back to epochs 11 to 13. Overfitting also can be solved by increasing the dropout fraction in the dropout layer.

The proposed CNN is successful in finding the location and classifying the damage in the free-free beam based on simulated data. The image of the damage index contour plots calculated from the gapped smoothing method are used as the input of the network. The processing of building, training, and validation of network was successful with accuracy higher than 90%.

5.2.2.4 Experimental validation of the GSM-CNN approach (step 4)

To verify the proposed method, an experimental modal analysis test has been performed on a steel beam (Figure 5.17) at the 'Bridge and Tunnel lab of NUCE' (Vietnam). The length of the beam is 1.0 m and the boundary conditions approximate the ones of a free-free beam. For that purpose, the beam was hanged on two cables. The cross section is the same as numerical beam described in section 5.2.2.2. The beam was excited by a hammer, one impact a time.

Fifteen accelerometers, each weighs approximately 7.8 g with sensitivity from $10.13 - 10.50\ \mathrm{mV/m/s2}$, were attached to the top of the beam (Figure 5.18). The sampling frequency was $fs = 2560$ Hz. The sampling time was 300 seconds.

The frequency domain decomposition method (FDD) [169] was used to analyse all data. FDD technique is simple and robust. This technique is based on computing the singular value decomposition of the power spectral densities estimated with the periodogram (also known as "Welch's" periodogram) approach to identify the natural frequencies and mode shape vectors. Seven bending modes were extracted by using the FDD technique (Figure 5.19). On the other hand, Matlab was used to model the beam. For the numerical model, different mesh refinements were conducted as shown in Figure 5.20. The natural frequencies trend to converge when the number of elements in the FE model of the beam is more than 30. Therefore, the FE model of the beam with 30 elements is used. Excellent correspondence with FE calculated modal properties is observed.

a. Instrumented steel beam

b. Computers and NI device

c. Hammer

Figure 5.17– Experimental setup

Figure 5.18– Accelerometers setup - top view

Moreover, the mesh size of 30 elements is used to detect damage in 14 elements along the beam. This mesh size is enough for the convergence of natural frequencies. However, it should be noted that the mesh size depends on the number of damaged locations along the beam. For example, if we want to detect the damage location of 30 elements along the beam, the mesh size should be more than 30 elements. Table 5.1 lists the first seven bending frequencies for the free-free beam. The differences between experimental data and FEM is less than 1% for all modes.

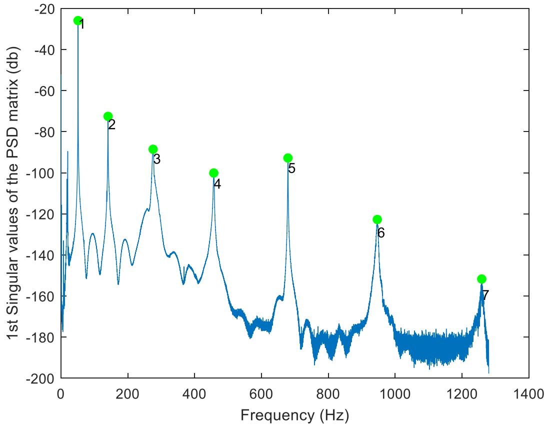

Figure 5.19– Natural Frequencies - Peak picking method

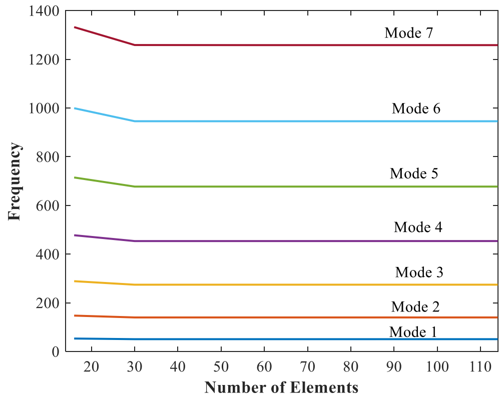

Figure 5.20– Frequencies extracted from FEM of the beam for different mesh sizes

Table 5.1 – Natural frequencies from measurement and FEM for the free-free beam

Mode	FEM (Intact)	Experiment (Intact)	Differences (%) (FEM & Exp.)
1	50.78	50.83	0.11
2	140.02	140.64	0.44
3	274.48	275.42	0.34
4	453.61	457.01	0.74
5	677.39	678.90	0.22
6	945.78	946.42	0.06
7	1258.60	1258.94	0.02

The mode shapes of the first seven bending modes after employing modal scale factor [170] to normalize with FEM mode shapes are shown in Figure 5.21. The continuous black line is the mode shape identified by FEM and the red nodes correspond to experimental results at the 15 sensors locations. Not only the natural frequencies, but also the mode shapes from experimental data fit the FEM results well.

In this research, 15 sensors were attached to the beam. Therefore, 14 damage locations can be detected. The number of damage locations depends on the number of sensors in reality. The more sensors were used the more damage locations can be detected. It should be noted that the training data of CNN must be changed to suite the testing data in reality.

The beam is damaged by making a notch on the edge and adding mass. We considered two scenarios. In the first scenario, two notches are introduced on both sides of the beam, the dimension of the notches are 5×12.5 (mm) and 5×13.3 (mm), respectively. In the second scenario, a 1.5 kg weight mass is added. The notches and the added mass are located between sensors 5 and 6 (Figure 5.22). The mode shapes of the intact and damaged beam were plotted in Figure 5.23. The frequencies of the damaged beam can be seen in Table 5.2. The changes in mode shapes are very small and cannot be used to detect the damage in the beam. Frequencies of all modes decrease when the beam is damaged, but the location of the damaged element cannot be obtained directly from them. The contour plots of damage indexes for the first 4 modes were considered in Figure 5.24 based on the experimental data. These images are used as input of trained CNN. Figure 5.25 shows the prediction of CNN for the two scenarios. The CNN predicted element 5 as the damaged element, with the percentage of 99.32% and 99.95% for scenario 1 and scenario 2, respectively. For scenario 1, the stiffness reduction was 36%, the CNN predicted that the damage level belongs to level 2 (91.38%), whereas, level 1 got only 8.6%. For scenario 2, an added mass of 1.5 kg in weight on the beam, CNN predicted the damage level as level 3 (99.29 %). The experimental data used to evaluate the method show that trained CNN can predict the damage location and damage severity perfectly.

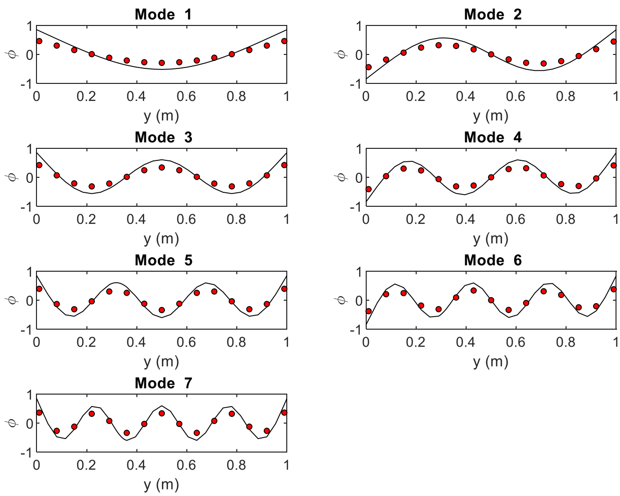

Figure 5.21– The first seven bending mode shapes - *y*-axis is along the beam length

Figure 5.22– The introduction of the notches

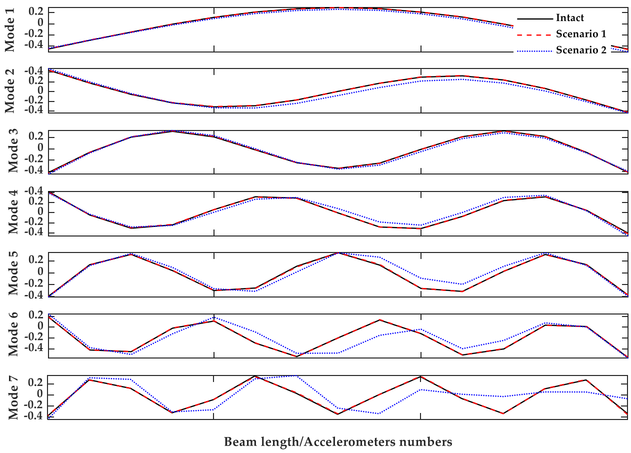

Figure 5.23– The experimentally measured mode shapes

Table 5.2 – Natural frequencies from measurement for free-free beam

Mode	Intact	Experiment (Scenario 1)	Differences (%) (Scenario 1)	Experiment (Scenario 2)	Differences (%) (Scenario 2)
1	50.83	50.35	0.94	49.06	3.60
2	140.64	138.78	1.32	127.58	10.23
3	275.42	273.75	0.60	263.57	4.49
4	457.01	454.99	0.44	426.21	7.22
5	678.90	672.60	0.92	624.82	8.65
6	946.42	944.60	0.19	793.45	19.28
7	1258.94	1252.71	0.49	1071.23	17.52

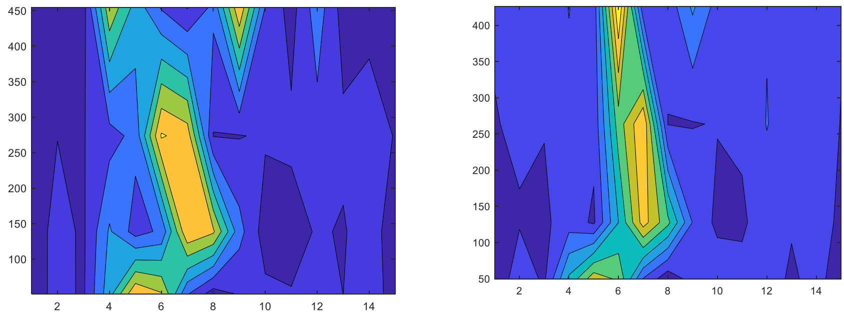

a. Scenario 1 b. Scenario 2

Figure 5.24– The contour plot images from experiment data

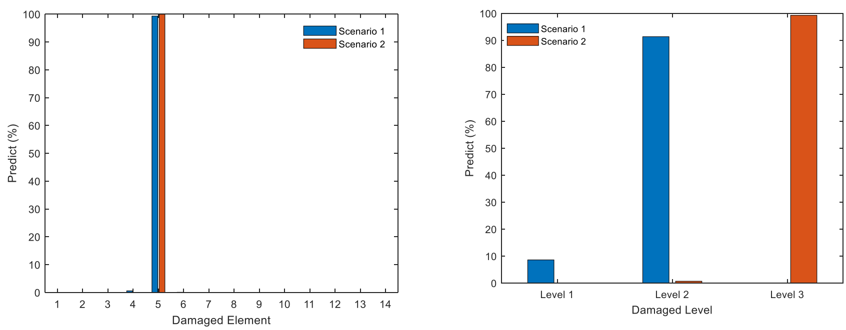

a. Damaged location b. Level of damage

Figure 5.25– The predicted results from the trained CNN

5.2.2.5 Discussion

In this section, we have proposed a novel method for detecting and estimating the severity of the structural damage. The damage index calculated based on the gapped smoothing method, then the contour plots of these are used as the input of Convolutional Neural Networks. A real machine learning system is introduced to evaluate the method. Data collection from FE model is the first step of the machine learning process. A CNN architecture is proposed for training and validation.

The testing data are obtained from vibration measurements. The results showed that the location and the severity of the damage are perfectly predicted by CNN.

The proposed method is elegant and robust to identify structural damage location and its severity. The location of damage can be identified and its severity can be estimated by using output only (response) vibration measurements. The prediction process was automatically done by machine learning. For the development of technology, the modal curvature of structure can be found by measuring displacement mode shapes or from direct modal strain measurements [171].

5.3 Damage detection in bridges

5.3.1 Ca-Non bridge

5.3.1.1 Introduction

This section deals with damage detection in a girder bridge using transmissibility and ANN method. The damage was simulated in a real bridge in Vietnam, i.e. Ca-Non Bridge. Finite Element Method (FEM) of this bridge was used to show the reliability of the proposed technique. The vibration responses at some points of the bridge under a moving truck are simulated and used to calculate the transmissibility functions. These functions are then used as input data to train the ANN, in which the target is the location and the severity of the damage in the bridge. After training successfully, the network can be used to assess the damage. Although simulated response data are used in this section, the practical application of the technique to real bridge data is potentially high.

5.3.1.2 Ca-Non bridge description

For the simulations, the Ca-Non bridge is used. The bridge is located at Km 359 + 724 of the Ho Chi Minh Road (West branch), in the A Luoi district, Thua Thien Hue province, and put into operation in 1979. Two pictures of the bridge are shown in Figure 5.26.

The bridge consists of a simply supported span, composed of steel girders and concrete slab. The length of the bridge is 27.3 m (from the end of right abutment to the end of left abutment). The cross-section of the bridge consists of eight steel girders having the length of 18 m and height of 80 cm. The top and bottom flange are 270 mm wide and 20 mm thick, respectively, the web is 760 mm high and 13 mm thick. The distance between two girders is 1000 mm. Figure 5.27 is the drawing of bridge cross section. The bridge has eight cross-beams including two beams at the abutments. Each cross-beam is the combination of two C-shape, each C-shape steel is 205 mm high and 60 mm wide. The cross-beams are located equally along the girders. The width of the bridge is 8.6 m including 7.6 m for the traffic lane and two barriers having 0.5 m width each. The bridge deck is overlayed by asphalt concrete, the two abutments are made of concrete, and the bearings are made of steel. The dimensions of the bearing are 20 × 50 × 8.5 cm.

Figure 5.26– Ca-Non Bridge location

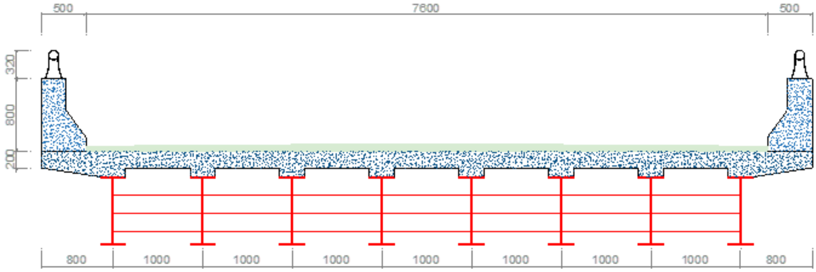

Figure 5.27–The Ca-Non bridge cross section (dimensions in mm)

5.3.1.3 Finite Element Model

Finite element model of the Ca-Non bridge is established in a CSiBridge FEM [172], as shown in Figure 5.28. The reinforced concrete slab is supported by eight I-shape steel girders, which are connected by eight cross beams in the transverse direction. Different types of finite elements have been used to model bridge superstructure. The bridge deck is modeled by shell elements. The girder is modeled using beam elements [173]. The composite action between the concrete deck and the steel girders is modeled as shown in Figure 5.29. Beams and shell elements are connected using rigid body constraint. Separated body constraints are used for each pair of connected nodes. The bridge model contains 735 elements, 813 nodes, and 432 constraints. The mesh size is 0.2 × 0.2 m and 1 m for the deck and I girder, respectively. The barrier, deck surface was modeled as added mass. The material properties are summarized in Table 5.3.

The boundary conditions are simply supported at the two ends of the eight I-shape girders bearings. Rotations in all directions are allowed in order to simulate the simply supported structure. Vertical restraint is placed at the two bearings, while longitudinal and transverse restraints are assigned at one. Modal analysis is conducted for calibration of the bridge model. The first two mode shapes of FEM are shown in Figure 5.29, the numerical frequency is 6.25 Hz for mode 1 and 9.9 Hz for mode 2.

After obtaining the most appropriate numerical results from modal analysis, we introduced a truck passing through the bridge, then the displacement responses of 72 nodes in the bridge are calculated (Figure 5.30). The truck characteristics are listed in Table 5.4.

Table 5.3 –Material properties of Ca-Non Bridge

$E_{concrete}$	$\rho_{concrete}$	$\upsilon_{concrete}$	E_{steel}	ρ_{steel}	υ_{steel}
(GPa)	(kg/m^3)	-	(GPa)	(kg/m^3)	-
27	2400	0.2	190	7800	0.3

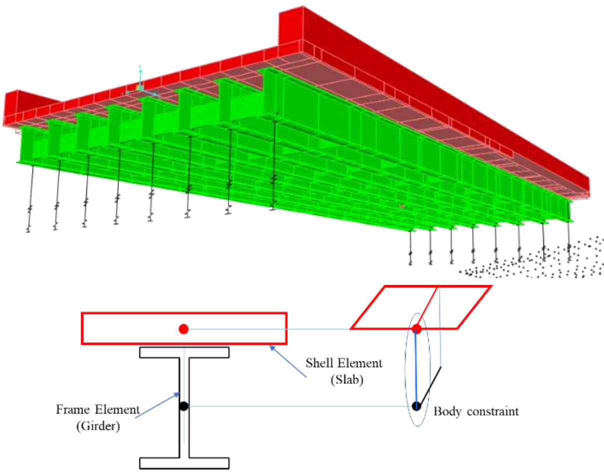

Figure 5.28– The Ca-Non bridge FE model

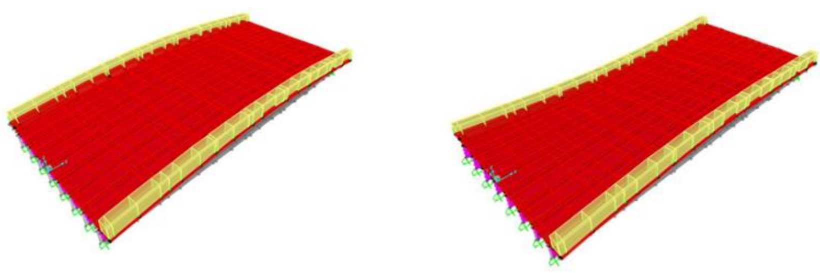

(a) Mode 1- freq.: 6.25 Hz

(b) Mode 2- freq.: 9.9 Hz

Figure 5.29– The two first mode shapes and the corresponding frequencies

Table 5.4 – Truck characteristic

Distance between 2 axles in vertical direction	Distance between first axle and middle axle	Distance between middle axle and last axle	First axle load P_1	Middle axle load P_2	Last axle load P_3
(m)	(m)	(m)	(ton)	(ton)	(ton)
1.8	2.7	1.35	5.07	10.14	10.14

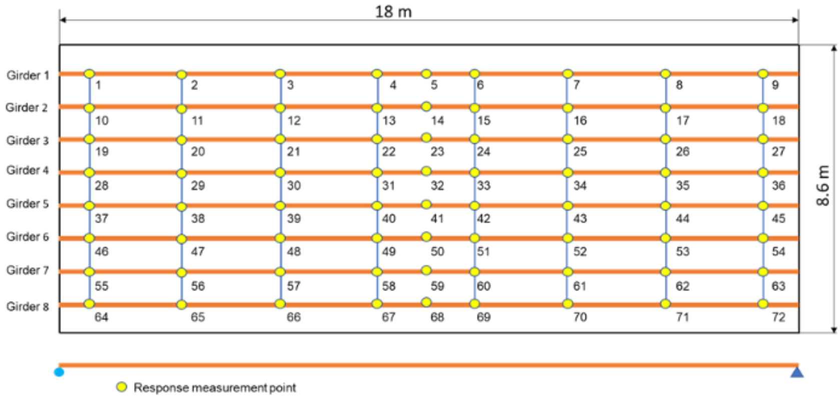

Figure 5.30–Location of the considered nodes

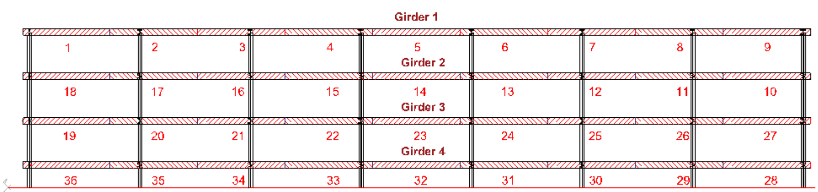

Figure 5.31–Damage locations in Ca-Non Bridge FEM

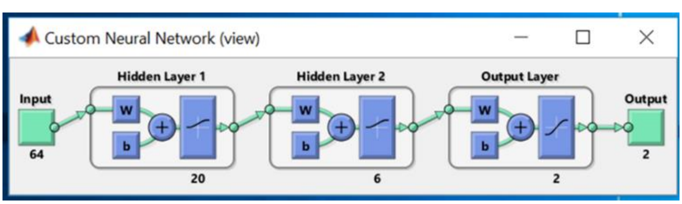

Figure 5.32–The structure of neural network

5.3.1.4 Damage detection procedures

To detect damage in the Ca-Non bridge, the following steps are followed.

Step 1: Responses determination

Calculate the responses of 72 nodes in the bridge.

Step 2: ANNs targets

The targets of the networks in this section are the locations and the severity of the damage in the bridge girders. The severity of damage is shown by the percentage of stiffness decrease in the damaged section. Each bridge girder is divided into 9 elements, with two meters in length for one element. Damages are introduced in half of the bridge in four girders. The 36 locations of damaged are presented and counted by number and shown in Fig. 31.

Step 3: Transmissibility evaluation

The transmissibility functions in each girder could be evaluated directly from the simulated measurements of the responses at 72 analyzing nodes using Eq. (3.7). The load excitation is the moving truck, run across the bridge with the constant velocity. The weight of the truck is assumed to be constant. An amount of 2% random Gaussian noise was added to the simulated responses.

In girder 1, we consider 9 nodes (from 1 to 9), using node 1 as the reference node, 8 transmissibility functions (from $T_{1,2}$ to $T_{1,9}$) and 8 indicators (from TI_1 to TI_8) are calculated using Eq. (3.8) and Eq.(3.15), respectively.

This procedure is repeated for all girders from 2 to 8. Sum up, we got 64 indicators to be used as input for ANNs, which are calculated based on 36 damaged locations. Each damage location has 26 scenarios of damage severity. The damage locations and damage severity are saved as the target of the ANNs corresponding with ANNs inputs.

Step 4: ANNs training and testing

All the ANNs data are divided into three part. One part is taken for ANNs training, one part to valid the network and one part is used for testing. The number of neurons is chosen and the value of the weights are adjusted to obtain the best performance networks.

Step 5: Result analysis

This step is to confirm that the trained ANNs can predict the location and the severity of the damage.

5.3.1.5 Results

The general neural network design process has seven primary steps, namely collect data, create the network, configure the network, initialize the weights and biases, train the network, validate the network and use the network. As discussed above, we use simulated transmissibility functions to collect data. This step is critical to the success of the design network. To create the network, the most important is to choose the number of the hidden layers and number of the neurons in each layer. These may depend on some factors such as the complexity of function to be learned, the training algorithm, the number of neurons in the input layer, the output layer. Using too few neurons in the hidden layer will result in something called under fitting. There are too few neurons in the hidden layers to adequately detect the signals in a complicated data set. Using too many neurons in the hidden layers can result in overfitting. The information contained in the training set is not enough to train all the neurons in the hidden layers. A large number of neurons in the hidden layers can increase the time it takes to train the network. By trial and error, the correct number of neurons to be used in the hidden layers can be selected. In this work, the network with two hidden layers, hidden layer 1 has 20 neurons and hidden layer 2 has 6 neurons are proposed (Figure 5.32). This network then will be trained and validated using *mse* performance network, and Levenberg-Marquardt training algorithm. The results will be shown in the next section.

a. Intact bridge

For the intact girder, Figure 5.33 show the $T_{1,3}$ before and after using Generalized regression neural network (GRNN) to approximate. Before approximation, the result shows oscillation because the numerical response being calculated every 0.005 s, instead of being a continuous variable. GRNN was suggested by D.F. Specht in 1991 [174]. GRNN is a single-pass associate memory feed-forward type ANNs and available in Matlab. Based on observations, the trend of both curves is similar, as the peak and valley appear at the same frequencies. Using this method, we got the results for other transmissibility functions as shown in Figure 5.34. The moving truck is 25 ton weight and runs with 30 km/h velocity on the bridge. Figure 5.35 shows the transmissibility functions when we change the velocity of the truck. From Figure 5.35, when the velocity of the truck changes, the transmissibility function between node 1 (near the bearing) and node 5 (in the middle span) changes, especially at high frequencies. We observe the same remarks when we compare the transmissibility in the same location, with the same velocity of the truck, but with different truck weight (Figure 5.36).

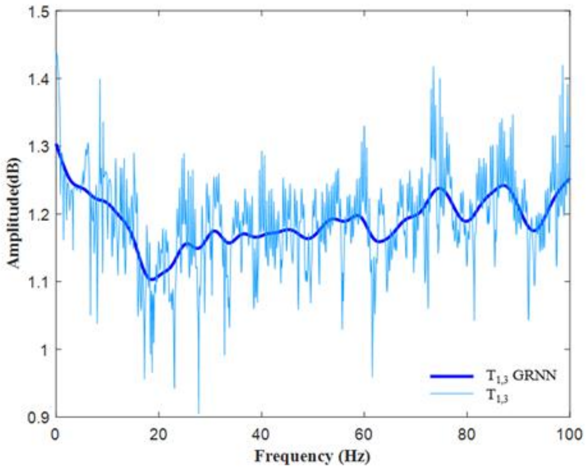

Figure 5.33–$T_{1,3}$ transmissibility from numerical model and approximation function using GRNN

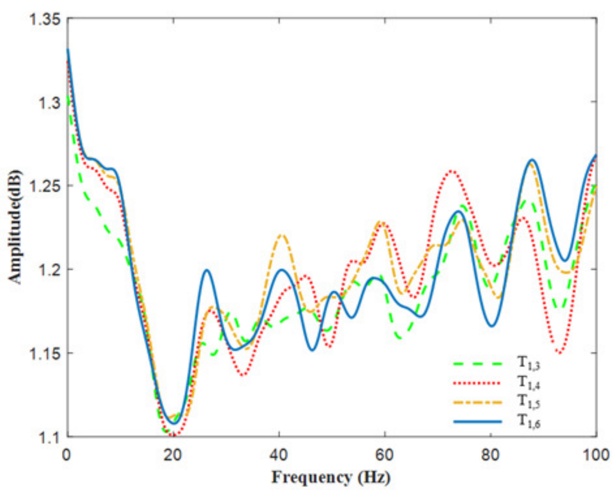

Figure 5.34–Transmissibility of intact girder 1

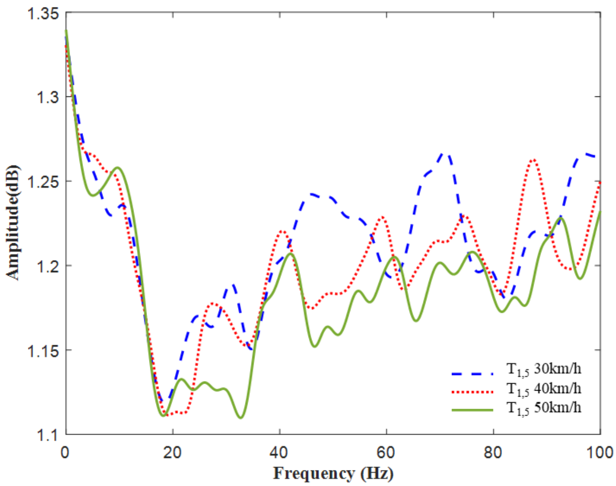

Figure 5.35–T1,5 with different velocity of truck -truck weight 25 ton

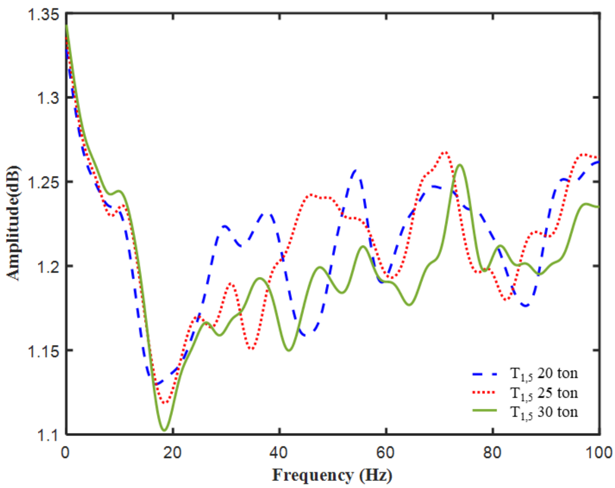

Figure 5.36–$T_{1,5}$ with difference weight of truck, truck velocity 30km/h

b. Damaged bridge

The advantage of using steel in constructing a bridge is its high strength, easy to fabricate, and fast construction time. The disadvantage is corrosion, which often appears in a part of a steel girder. The severity of the damage depends on the depth and the area of the corrosion. In this section, we reduce the stiffness of each element to reflect the severity of damage in the girder. There are 36 locations of damage in 4 girders as discussed above and shown in Figure 5.31. For each damage location, we have 26 scenarios. The stiffness in the damage element is reduced from 0% to 50% with an interval of 2%. Therefore, there will be 26 scenarios in each damage location, i.e. from D1 to D50 in addition to D0 for an intact case.

The transmissibility for damaged girders 1 and 2 is shown in Figure 5.37 and Figure 5.38. In girder 1, the location of damage is numbered as 1 and in girder 2 as 17. We observe that when the severity of the damage changes, the transmissibility function changes also, especially at high frequencies. This proved that transmissibility function is sensitive to local damage and can be used as a damage indicator. To calculate the input for ANNs, we use Eq. (3.15), and frequency range from 9 Hz to 11 Hz. This frequency range covers the first frequency peak of all transmissibility functions.

As discussed above, 64 *TI* indicators calculated from 26 scenarios in 36 damage locations are used as input data for the ANNs network. Figure 5.39 shows 8 of these indicators when the damage occurs at location 1. These indicators change according to the change of damage location and damage severity. There are 936 simulated data in total. A sample of 70% of the data is used to train the network and a sample of 15% is used to measure the network generalization. A sample of 15% is used to test the network, which has no effect on training and therefore it provides an independent measure of network performance during and after training. The target of the networks is the location of the damage and its severity.

Figure 5.40 shows a regression plot for relationship between the outputs of the network and the targets. There are four plots in Figure 5.40. The first one shows the relationship between outputs of the network and the targets in training data sample. The second is for the validation of data sample, the third is for testing data sample and the last is for all data set. The dashed line in each plot presents the perfect line outputs equal to targets. The solid line represents the best fit linear regression line between outputs and targets. If R=1, this indicates that the network outputs are perfectly fit the targets and there is an exact linear relationship between outputs and targets. In our case, the four R-values are greater than 0.95 indicating a good fit. That means that the network, we proposed before, has successfully built a linear relationship between outputs and targets. After establishing the networks, they can be used for any new case. Therefore, by only using the displacement responses of a bridge, we can predict the location and severity of damage.

The number of considered points can be reduced based on the number of measurement heads. Table 5.5 shows the structure of the chosen ANNs and the R-value of each network, depending on the number of sensors. The more sensors, the bigger the R-value is, and the more neurons should be used in each hidden layer.

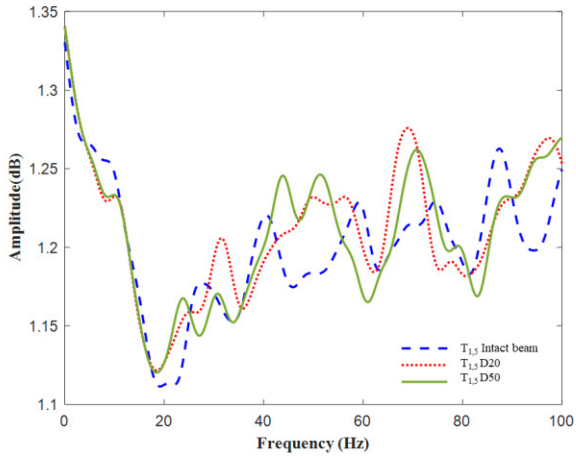

Figure 5.37–$T_{1,5}$ transmissibility with different scenarios -damage at location 1

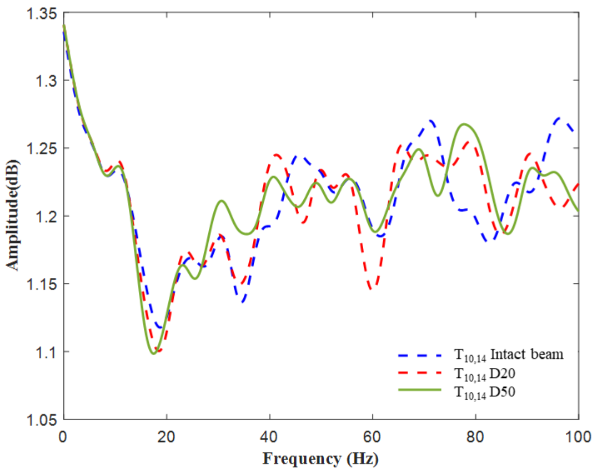

Figure 5.38–$T_{10,14}$ transmissibility with different scenarios - damage at location 17

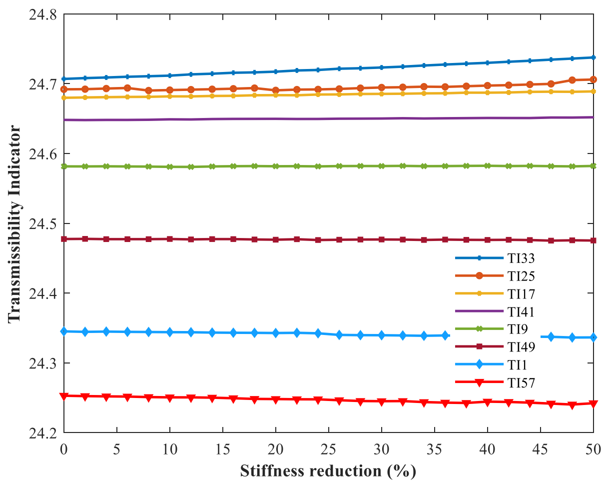

Figure 5.39–Transmissibility Indicators -damage at location 1

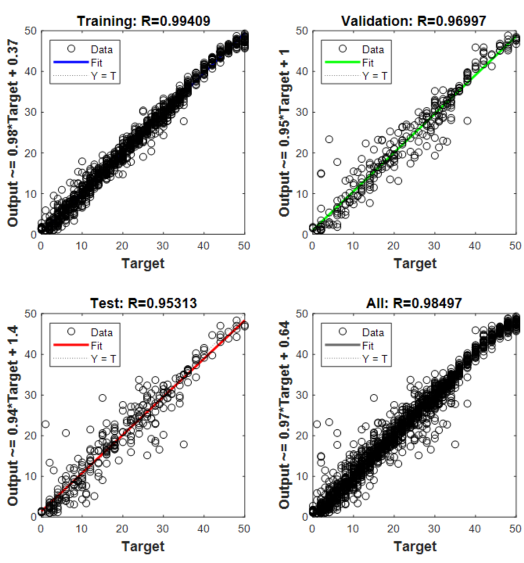

Figure 5.40–Regression analyses of the considered scenarios

Table 5.5 –Number of sensors and R-value of the network

Number of sensors	72	40	24
Number of neurons in Hidden Layer 1	20	10	6
Number of neurons in Hidden Layer 2	6	4	2
All: R-value	0.985	0.956	0.82

5.3.1.6 Discussion

In this section, a damage detection method is proposed using simulated transmissibility together with ANNs. Transmissibility is calculated from the simulated displacement responses of many points on the bridge. The feasibility of this method is assessed through a numerical model of Ca-Non bridge. The results indicate that transmissibility together with ANNs could be used to find out the location and severity of the damage in a bridge with good precision. The use of ANNs provides a suitable methodology for damage detection.

Research has shown that with the collected data, the network after training was completely capable to identify damage. However, this method requires a large number of datasets to train and test the network. The most important is that we have a well calibrated FE model to reflect all the responses of the bridge. The proposed method utilized the displacement responses under a moving truck. The response of the bridge should be recorded at as many points as possible. Thanks to modern technology, this work can be performed without difficulties. The life of a bridge can be extended if it is regularly inspected, then repaired after damage detection.

5.3.2 Nam O bridge

5.3.2.1 Introduction

In section 5.3.1, only single damage was considered and multi damages were pointed out as the subject of future work. In this section, multi damages will be taken into account. The bridge is damaged in one, two, and three elements. Ca-Non is a simply supported concrete girder bridge, whereas Nam O is a truss bridge. The structural behaviour of these two bridges is different. Therefore, this section proposes the use of transmissibility functions combined with a ANN to assess damage in a truss bridge. Moreover, in this section, a classifying algorithm was added to distinguish different types of damage (damaged at one, two, or three elements).

Sensors are installed on the truss joints in order to measure the bridge vibration responses under train and ambient excitations. A finite element (FE) model is constructed for the bridge and updated using FE software and experimental data. Both single damage and multiple-damage cases are simulated in the bridge model with different scenarios. In each scenario, the vibration responses at the considered nodes are recorded and then used to calculate the transmissibility functions. The transmissibility damage indicators are calculated and stored as ANNs inputs. The outputs of the ANNs are the damage type, location and severity. Two machine learning algorithms are used; one for classifying the type and location of damage, whereas the other for finding the severity of damage. The measurements of the Nam O bridge, a truss railway bridge in Vietnam, is used to illustrate the method. The proposed method not only can distinguish the damage types, but also it can accurately identify damage level.

5.3.2.2 The overview of Nam O bridge

Nam O bridge is a long-span railway bridge opened in 2011, under the support of the Ho Chi Minh City - Hanoi Line traffic Safety Improvement Project. The Nam O bridge is located at Da Nang city, Vietnam. The bridge across Cu De river, hold the train traffic from the North to the South. The bridge consists of four simply supported spans, with the length of 75 m for each span. The rail track is directly fastened to the stringers of the bridge deck. The view of the bridge from the downstream side is shown in Figure 5.41 while Figure 5.42 shows the main structural elements of the bridge. Main structural elements included top chords, bottom chords, verticals, diagonals, portal frames, and stringers. The cross-sectional properties of the truss members are presented in Table 5.7. The material properties of steel are elastic modulus 2.05×10^{11} N/m^2, density 7850 kg/m^3 and Poisson's ratio 0.3.

Figure 5.41– The Nam O bridge [175]

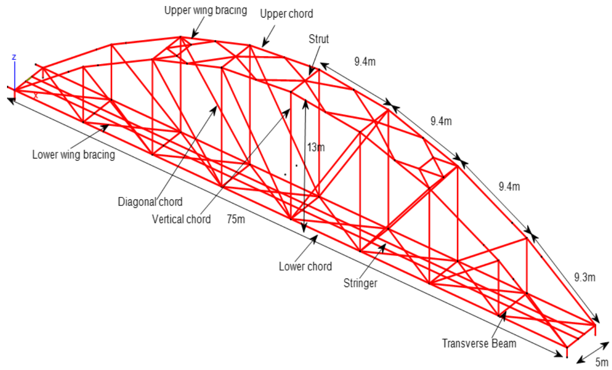

Figure 5.42– The Nam O bridge main structural elements [175]

Table 5.6 – Cross-sectional properties of main structural members

Member		Area A (m^2)	Moment of Inertia Iz (m^4)	Moment of Inertia Iy (m^4)
Upper Chord	Type 1	0.056	6.70×10^{-04}	3.1×10^{-03}
	Type 2	0.054	6.46×10^{-04}	2.93×10^{-03}
	Type 3	0.034	4.30×10^{-04}	1.90×10^{-03}
	Type 4	0.034	4.3×10^{-04}	1.90×10^{-03}
Lower Chord		0.020	2.10×10^{-04}	6.30×10^{-04}
Vertical Chord	Type 1	0.010	5.49×10^{-05}	1.15×10^{-04}
	Type 2	0.023	1.60×10^{-04}	6.50×10^{-04}
	Type 3	0.014	1.24×10^{-04}	2.78×10^{-04}
Diagonal Chord	Type 1	0.014	1.24×10^{-04}	2.78×10^{-04}
	Type 2	0.015	1.20×10^{-04}	3.40×10^{-04}
	Type 3	0.015	1.20×10^{-04}	4.00×10^{-04}
Stringer		0.020	2.07×10^{-04}	6.27×10^{-04}
Transverse Beam	Type 1	0.026	2.03×10^{-04}	3.61×10^{-03}
	Type 2	0.026	9.25×10^{-04}	3.20×10^{-03}
Strut	Portal Frame	0.053	6.25×10^{-04}	2.80×10^{-03}
	Type 1	0.020	1.48×10^{-04}	1.86×10^{-03}
	Type 2	0.022	1.50×10^{-04}	3.20×10^{-03}
	Type 3	0.021	1.60×10^{-04}	2.00×10^{-03}
Upper Wind Bracing	Type 1	0.0036	8.00×10^{-04}	1.09×10^{-05}
	Type 2	0.0019	1.90×10^{-06}	1.40×10^{-06}
Lower Wind Bracing		0.0049	2.38×10^{-06}	4.38×10^{-06}

5.3.2.3 Experimental Measurements and FEM updating

The ambient vibration was performed on the first span from the upstream side of the river. The bridge free vibration after train passage was measured. Eight setups were carried out with four fixed reference sensors, distributed on the two-bay of the span at both lower node and upper one as shown in Figure 5.43. Accelerometers and LVDT sensors are set up on the bridge to measure 40 DOFs (Figure 5.44). The DOFs in each setup can be found in Figure 5.43, where the x-axis is in the longitudinal direction of the bridge, the y-axis is in the transverse direction (to the river flow direction) and the z-axis is in the vertical direction. Nodes 100, 300, 308 and 108 are the location of bearings. Three sensors in the x-axis direction were placed at three nodes 100, 300 and 308. Two sensors along y-axis were placed at three nodes 100, 300 and no sensor at the fixed node 108. The real bearings operational conditions are updated by using these five sensors. The measurement time was about ten to twenty minutes per setup and the sampling rate was 1651 Hz.

Table 5.7 shows the summary of the first 10 extracted mode shapes, within the frequency range from 1.45 Hz to 6.05 Hz. In order to solve the model updating problem, these ten modes are enough. The finite element model of Nam O Bridge was built based on the geometry from the as-built drawings using the MATLAB toolbox StaBil [176]. The FE model includes 137 nodes and 227 beam elements. The elements are Timoshenko beams, which estimate the impacts of shear-deformation. Each node of elements includes 6 degrees of freedom consisting of translations in the x, y, and z axes and rotations around the x, y, and z axis. Rotational springs were used to model the connections between truss members and the springs were employed to model the bearings. Tran-Ngoc et al. [175] used the Particle Swarm Optimization algorithm to update the model so that the frequencies from the FE model and from measurement match. Considering Table 5.7, the results from modes 1 to 3 perfectly match and the differences between FEM and measurement for other natural frequencies are less than 10%. More details about the measurement, FEM bridge, and model updating can be found in Ref. [175].

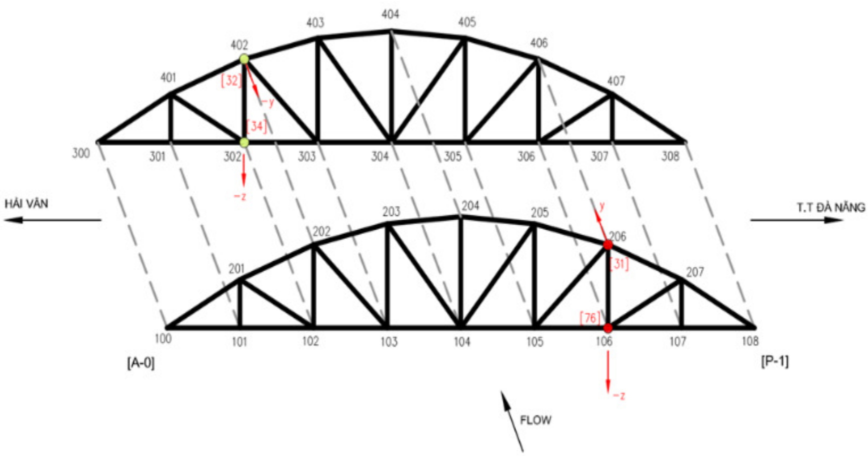

Setup 1: 106*z* 206*y* 302*z* 402*y* 101*z* 103*z* 301*z* 303*z* 305*z*
Setup 2: 106*z* 206*y* 302*z* 402*y* 102*z* 104*z* 107*z* 304*z* 306*z* 307*z*
Setup 3: 106*z* 206*y* 302*z* 402*y* 102*y* 103*y* 104*y* 304*y* 306*y* 307*y*
Setup 4: 106*z* 206*y* 302*z* 402*y* 101*y* 105*y* 107*y* 301*y* 303*y* 305*y*
Setup 5: 106*z* 206*y* 302*z* 402*y* 102*y* 103*y* 104*y* 304*y* 306*y* 307*y*
Setup 6: 106*z* 206*y* 302*z* 402*y* 100*x* 100*y* 300*y* 300*x* 308*x*
Setup 7: 106*z* 206*y* 302*z* 402*y* 403*y* 404*y* 405*y* 406*y*
Setup 8: 106*z* 206*y* 302*z* 402*y* 201*y* 207*y* 401*y* 407*y*

Figure 5.43–The measurement grid, the position of reference sensors and setups

Figure 5.44– Placement of accelerometers and LDVTs at one node of Nam O bridge

Table 5.7 – The first ten natural frequencies from FEM updating compared to the measurement

Mode No	FEM updating – PSO (Hz)	Measurement (Hz)	Differences (%)	Mode type
1	1.45	1.45	0	Transverse mode
2	3.10	3.11	0.3	Transverse mode
3	3.27	3.28	0.3	Lateral torsion
4	4.66	4.62	0.8	First bending
5	6.55	6.05	7.6	Local mode of the two bays at ends
6	7.15	7.12	0.4	Local mode of the two bays at ends
7	7.33	7.30	0.5	Transverse mode
8	8.10	7.46	8.57	Transverse mode
9	9.00	8.29	7.94	Combination mode
10	9.57	8.89	7.10	Second vertical bending

5.3.2.4 The proposed ANNs method

In the Nam O bridge, each span has got two main trusses as shown in Figure 5.44. Each main truss has 29 elements and 16 nodes, which have been labeled. In the experiment, eight setups were used to measure 40 DOFs. Therefore, in the first step of detecting damage, we proposed to find the displacement responses of these DOFs for all damage scenarios. Damage in all lower chords was taken into account in this paper. Three cases of damage including damage in single element (DC1), damage in two elements (DC2) and damage in three elements (DC3) were introduced. We reduced the stiffness of each element to reflect the damage severity. In DC1, the stiffness is reduced from 10% to 60% with an interval of 1%. In DC2, the stiffness is reduced from 1% to 60% with an interval of 5% for both elements and we use the same reduction and interval for three elements in DC3. We use 16 single damaged elements from S1 to S16 in DC1, so that we have 800 sampling data. Six cases of DC2; from M1 to M6 are introduced and 864 sampling data are restored. Only one case of 3 elements damage (M7) is considered, and then 1728 scenarios and sampling data are restored. Table 5.8 shows the damaged elements in the three cases, where one element is denoted by two nodes, for example element 100-101 connects nodes 100 and 101. All the damage scenarios are simulated using FEM in Matlab.

As Nam O bridge is a railway bridge, a locomotive is proposed as an excitation force. Three locomotive weights (35 tons, 33 tons, and 30 tons) are used to get the data for training the network. This locomotive has three axels and the distance between the two axels is 1.5 m. The weight is divided equally on the three axels. The displacement responses at 40 DOFs are calculated based on FE results. The axle load is modelled using a forced matrix in the finite element model. When the locomotive runs on the bridge, the force is transmitted to the longitudinal beam, and then transmitted to the truss joints in the direction of DOF. Gaussian noise is considered in the numerical displacement response. The signal to noise ratio ranges from 70 dB to 50 dB.

Table 5.8 –Details of damage elements in three damaged cases

S1	S2	S3	S4	S5	S6	S7	S8
100-101	101-102	102-103	103-104	104-105	105-106	106-107	107-108
S9	S10	S11	S12	S13	S14	S15	S16
300-301	301-302	302-303	303-304	304-305	305-306	306-307	307-308
M1		M2		M3		M4	
101-102	104-105	104-105	106-107	303-304	304-305	302-303	304-305
M5		M6		M7			
102-103	300-301	300-301	303-304	101-102	102-103	103-104	

There are four fixed sensors in the measurements. These reference sensors are located at the points of significant modal displacements of many modes that measure 4 DOFs 106z, 206y, 302z, 402y. To calculate the transmissibility indicators, these 4 DOFs are used as reference joints. The displacement responses are transformed to frequency domain to calculate the transmissibility. Those transmissibility functions are:

Reference node 106 in z direction: $T_{100,106}$, $T_{101,106}$, $T_{102,106}$, $T_{103,106}$, $T_{104,106}$, $T_{107,106}$.

Reference node 206 in y direction: $T_{100,206}$, $T_{101,206}$, $T_{102,206}$, $T_{103,206}$, $T_{104,206}$, $T_{105,206}$, $T_{201,206}$, $T_{207,206}$.

Reference node 302 in z direction: $T_{301,302}$, $T_{303,302}$, $T_{304,302}$, $T_{305,302}$, $T_{306,302}$, $T_{307,302}$.

Reference node 402 in y direction: $T_{300,402}$, $T_{301,402}$, $T_{303,402}$, $T_{304,402}$, $T_{305,402}$, $T_{306,402}$, $T_{307,402}$, $T_{401,402}$, $T_{403,402}$, $T_{404,402}$, $T_{405,402}$, $T_{406,402}$, $T_{407,402}$.

In *x* direction: $T_{100,308}$.

In total, from 40 DOFs, 34 transmissibility functions $T_{i,j}(\omega)$ are calculated using Eq.(3.8). The transmissibility indicators are then calculated using Eq.(3.15) at frequency band from 0.8 Hz to 2.5 Hz. Finally, 34 damage indicators DI's are determined using Eq.(3.16) and restored as input of ANNs. This procedure is repeated for all scenarios.

The combination of two machine learning algorithms are proposed for detecting damage in Nam O bridge. The ANNs using pattern recognition algorithm is trained to classify the damage. The ANNs using regression algorithm is trained to find the severity of the damage. The classification problems can be solved by using a two-layer feed-forward network. From the input data and desired output, the network divides data into training, validation, and testing sets, which define the network architecture and train the network. The three classes used are DC1, DC2, and DC3. We choose the network with two hidden layers. Hidden layer 1 has 350 neurons and hidden layer 2 has 50 neurons. The network architecture is shown in Figure 5.45. This network then will be trained and validated using *trainscg* (Scaled conjugate gradient back propagation) training function in Matlab, *cross entropy* are used as loss function. After classifying the damage case, the severity of the damage can be found by using the second machine learning algorithm. The structure of this ANNs is shown in Figure 5.46, Figure 5.47 and Figure

5.48 for DC1, DC2 and DC3, respectively. The number of hidden layers and neurons should be taken into account [177]. In this work, the structure of ANNs is chosen by trial and error. These regression networks were trained by using mean square error (*mse*) performance and Levenberg-Marquardt training algorithm. The results of these networks will be shown in the next section. Figure 5.49 shows the procedure to create ANNs from the numerical model data set. These networks can be stored and used for any new cases.

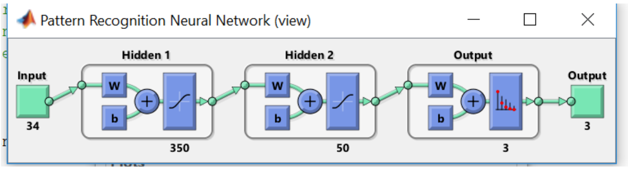

Figure 5.45– The structure of the pattern recognition neural network

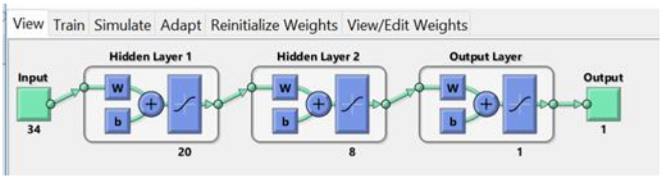

Figure 5.46– The structure of the regression neural network for DC1

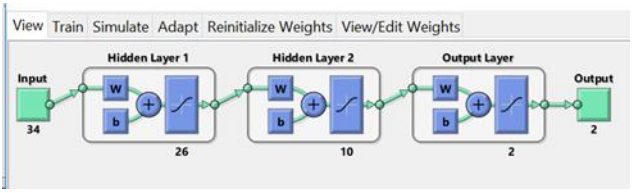

Figure 5.47– The structure of the regression neural network for DC2

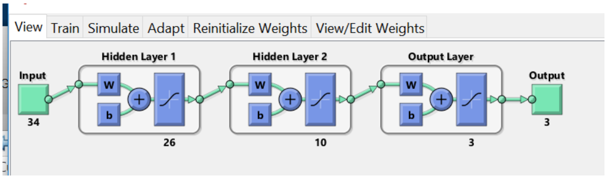

Figure 5.48– The structure of the regression neural network for DC3

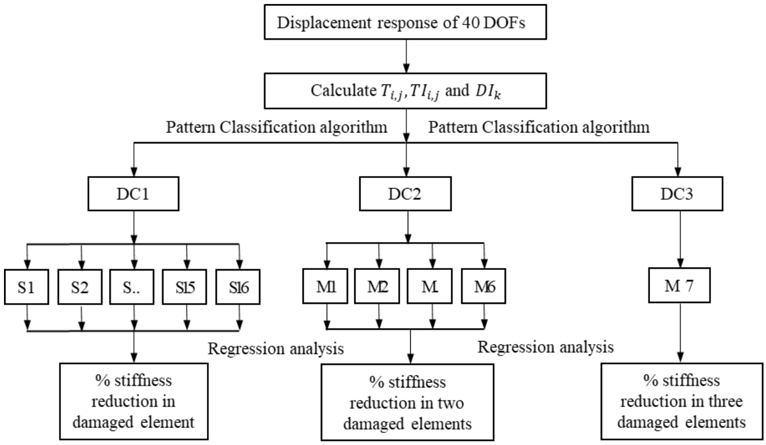

Figure 5.49– The procedure for create ANNs used in damage detection of the Nam O Bridge

5.3.2.5 Results

a. Intact bridge

The transmissibility function is calculated following the procedure discussed in Section 5.3.2.4. These transmissibility functions are taken from the simulated responses of the considered DOFs and locomotive weight. Figure 5.50 shows the function $T_{100,106}$ before and after using the GRNN function for approximation. The load excitation is the 35-ton locomotive. The peaks and the valleys of these two functions appear at the same frequencies instead of the oscillation of the functions got from the numerical model. This function is oscillating because of the numerical response and the moving load being calculated every 0.005 s, instead of being a continuous variable. GRNN are single-pass associate memory feed-forward type ANNs suggested by Specht [174].

Using this method, we can calculate 34 transmissibility functions as described above for the intact bridge. Only three functions $T_{100,106}$, $T_{102,106}$, $T_{104,106}$ are plotted in Figure 5.51. Other functions have similar shape.

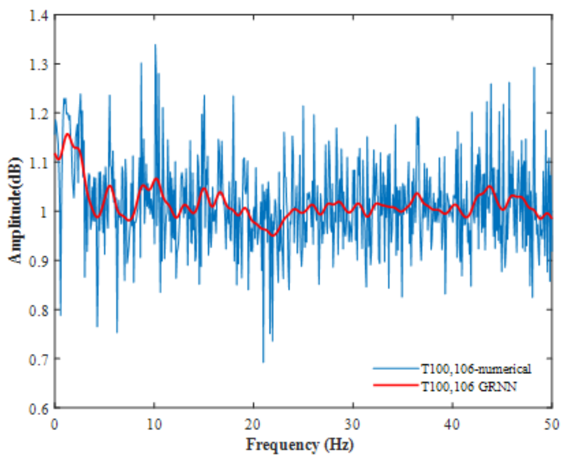

Figure 5.50–$T_{100,106}$ calculated from numerical model and GRNN approximation function, excited by 35 ton locomotive

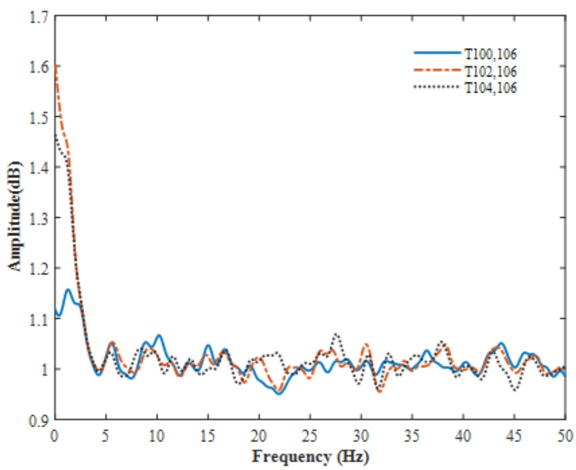

Figure 5.51–Transmissibility functions of intact bridge excited by 35 ton locomotive

b. Damaged bridge

Steel bridges are often selected in a case where the live load is large or the effective span is long, as in railway bridges. Steel truss bridges have higher adaptability than other kinds of bridges. For example, when one truss member is damaged, it's not difficult to replace it by a new one. There are various types of damages in steel truss bridges including damage in joints [149] and main members [148, 178, 179]. Most metals exist in the form of oxides. Therefore, corrosion may appear on steel material in the atmosphere, water and seawater. The appearance of corrosion in a truss member reduces its stiffness. Defining k_i as the stiffness reduction in the truss member i, the undamaged truss and completely damaged truss are represented by $k_i = 0$ and $k_i = 1$, respectively. Eq.(5.3) expresses this definition, where K_i and K_i^d are the undamaged and damage stiffness of the *i* element, respectively.

$$K_i^d = K_i(1 - k_i) \tag{5.3}$$

As discussed in section 5.3.2.4, 34 transmissibility functions are calculated and the damage indicators (DI's) are determined based on the TI indicator. Figure 5.52 shows the transmissibility functions $T_{102,106}$. The percentages, 10%, 40%, and 60%, are the stiffness reduction of the element 307-308. The first peak is chosen for the calculation of TI, frequency range from 0.8 Hz to 2.5 Hz. We can see that when the severity of the damage increases, the transmissibility function changes and then increases.

There are three cases of damage DC1, DC2, and DC3 as discussed above. In the first task, we use ANNs shown in Figure 5.45 to classify these 3 damage cases. There are 2400 samples of DC1, 2592 samples of DC2 and 5184 samples of DC3. These data are divided into 3 parts:

70% for training, 15% for validation and 15% for a test. In the confusion matrix shown in Figure 5.53a, the numbers 1, 2, 3 means DC1, DC2 and DC3, respectively. There are 57.0% of the times in the training confusion matrix, 53.5% of the times in the validation confusion matrix, 57.4% of the times are classified DC1 correctly. The performance progress in Figure 5.53b indicates that the iteration at which the validation performance reached a minimum is epoch 104. The training progresses well, the cross-entropy loss decreases when the number of epoch increases. Similarly, ANN classifies DC2 correctly for 71.3% of the times in the training confusion matrix, 71.0% of the times in the validation confusion matrix, 70.6 % of the times in the test confusion matrix. The DC3 has the biggest samples and the highest percentage of correct classification, too. 92.8% of the times in the training confusion matrix, 92.2% of the times in the validation confusion matrix, 92.3 % of the times in the test confusion matrix are classified correctly. In all cases, the percentage of right prediction is 78.7%. As discussed above, DC1 have 16 cases of damage, from S1 to S16, DC2 have 8 cases of damage from M1 to M6. Pattern networks are used again for classification. Figure 5.54 shows the ROC curves and performance progress from M1 to M6. Figure 5.55a draws some ROC curves, each corresponding to different scenario S1 to S16. The area under the ROC curve, which is close to 1, means that the method's accuracy is high. The correct percentage, in this case, is 80.0% of 2598 samples classified correctly in DC2 and the correct percentage for DC1 is 77.8%. The figures of performance progress indicate a very similar curve between validation and test data (Figure 5.54b, Figure 5.55b). The overfitting does not occur in this case. These results proved that ANNs are successful in finding out the type of damage and the location of the damage.

To find out the damage severity, we use regression networks as shown in Figure 5.56. The output of this network is the severity of the damage. For DC1, the inputs of the network are the 34 transmissibility indicators and the target of the network is the percentage of the stiffness reduction in the damaged element. For DC2, there are two targets of the network that are the percentages of the stiffness reduction at the two damaged elements. Similarly, for DC3, there are three targets corresponding to 3 damaged elements. Figure 5.56a shows a relationship between the outputs of the network and the target in S1 scenario. There are four plots corresponding to the training data sample, validation data sample, testing data sample, and all datasets. The dashed line in each plot presents the perfect line *outputs=targets*. R-value is the correlation coefficient between the outputs and targets. It is a measure of how well the variation in the output is explained by the targets. R=1 indicates that the network outputs are perfectly fit the targets. All four R-values in Figure 5.56a are approximately 0.9 indicating a nearly perfect fit. The variation of mean square error versus the different number of epochs was plotted in Figure 5.56b. The mse decreases with the increase in the number of epochs. The best performance is in epoch 3. The training continued for six more iterations before the training stopped. The validation and test curves are similar. No problem occurred in the training progress. Table 5.9 shows the R-value of the networks for all damaged scenarios. M7 is the most complicated scenario with 3 damaged elements having the lowest R-value. All the R-value is larger than 0.75, most of them larger than 0.90. This proves that ANNs are successful in finding out the severity of the damage in each damaged element. This ANNs then can be stored and used for any new case. Therefore, we can conclude that using machine learning algorithms with the different type of machine learning algorithm can help us in assessing the damage of the Nam O bridge.

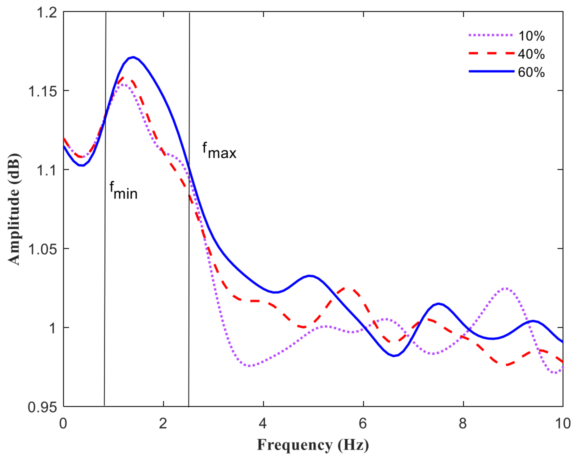

Figure 5.52– Transmissibility functions $T_{102,106}$ for the case of damage at element 307-308

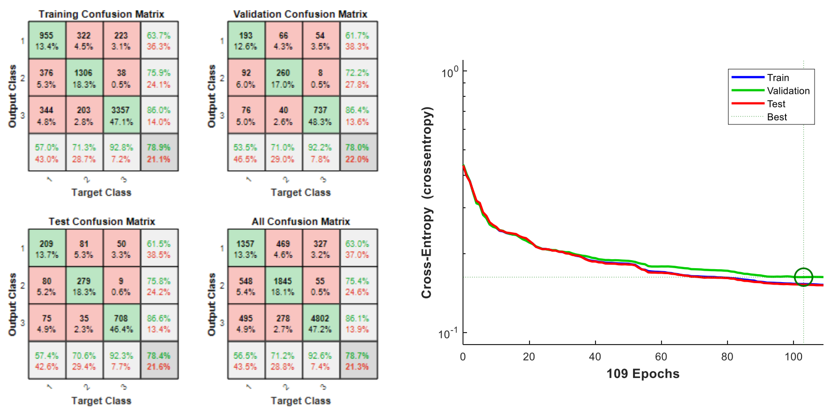

a. Confusion matrix b. Performance progress

Figure 5.53– DC1, DC2, DC3 classification results

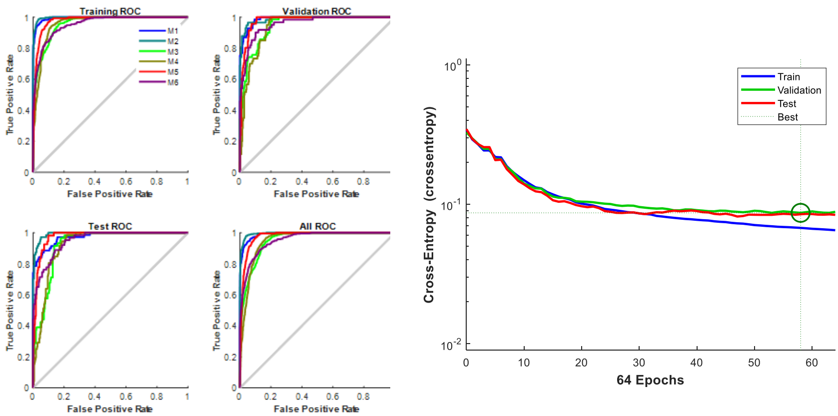

a. ROC curves b. Performance progress

Figure 5.54– DC2 classification results

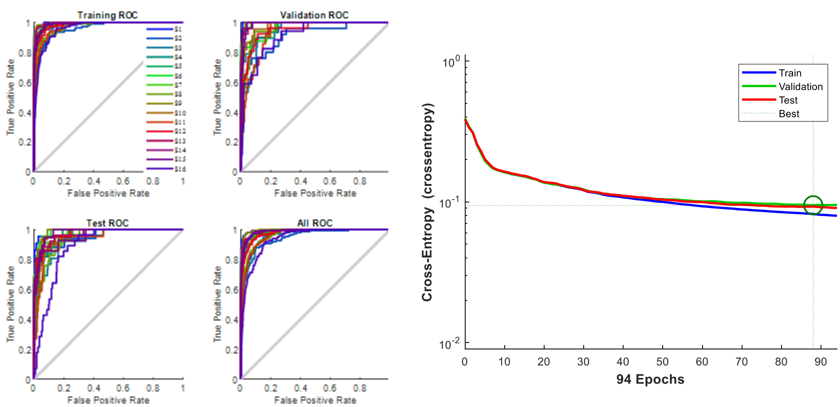

a. ROC curves b. Performance progress

Figure 5.55– DC1 classification results

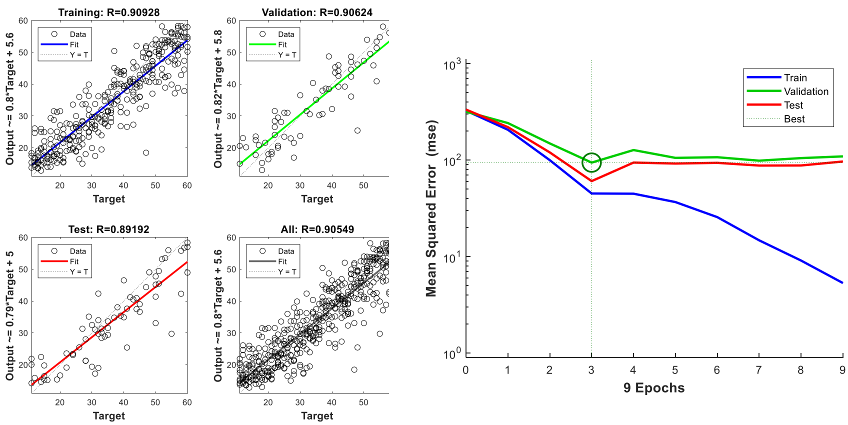

a. Regression analyses b. Performance progress

Figure 5.56– S1 scenario regression analysis results

Table 5.9 – R-value of the network

Scenario	S1	S2	S3	S4	S5	S6
R-value	0.905	0.918	0.852	0.938	0.940	0.981
Scenario	S7	S8	S9	S10	S11	S12
R-value	0.983	0.944	0.981	0.953	0.85	0.968
Scenario	S13	S14	S15	S16	M1	M2
R-value	0.980	0.935	0.965	0.90	0.867	0.86
Scenario	M3	M4	M5	M6	M7	
R-value	0.901	0.956	0.871	0.942	0.773	

5.3.2.6 Discussion

A novel methodology has been here proposed based on the machine learning algorithm to assess damage in a truss bridge with acceptable accuracy. The transmissibility damage indicator was calculated from an updated FE model of the bridge and then used as the input data of

ANNs. There are many kinds of machine learning algorithms that can be used depending on the desired purpose. In this section, the Pattern Recognition algorithm was used to classify the type and location of damages and the Regression algorithm was applied to find the damage severities. First, the FEM is used to train the network. Then, the user provides the input data (the damage indicators calculated from experiments). The results indicated that the ANNs could distinguish the damage appearing at one element, two elements or three elements and found out the severity of the damages.

Transmissibility and machine learning algorithm are two methods that are only based on output responses only. Therefore, the combination of these two methods is very interesting. It is important to note that the proposed method needs a large number of measurement points. The more DOFs we consider, the more accurate the networks. The actual technology permits this to occur. The vibration response of the bridge can be measured at many points.

This shows a promising future in real applications of SHM. Several excitation loads are used to train the network in this research. The results are still good. This proved that if the number of samples is big enough, the real excitation load does not have to be the same as the load used for the numerical simulations. The real excitation load should be in the range of trained excitation load. This research does not consider the effect of temperature, the roughness of the bridge slab, humidity, wind load, etc. But ANNs work very well with big data. All of the conditions that influence the response of the bridge can be considered in the input of the network.

5.3.3 Bo Nghi bridge

5.3.3.1 Introduction

This section addresses a damage detection method based on changes in modal curvatures combined with Convolutional Neural Network (CNN). Bo Nghi bridge is used as an illustrative example. This bridge consists of four T-shaped concrete simply supported girders. One single beam with the same length and cross-section of the bridge girder is modeled and used to extract numerical data to train the CNN. A CNN is trained by using images from the damage index of the GSM to classify the damage location in the numerical beam model. Finally, the finite element model of the bridge is built and used to model damage scenarios and to test the trained CNN. The results indicate that the combination of GSM and CNN can be used for damage detection and localization.

5.3.3.2 Bo Nghi bridge structure

Bo Nghi bridge was constructed in 2005. This bridge is located along the Ho Chi Minh Road, Quang Binh Province, Vietnam. The bridge has three simply supported concrete spans. The length of each span is 32.00 m. One span consists of four T-shaped concrete girders. Each girder has a height of 1.7 m (including 0.15 m of slab/flange thickness) and the web is 170 mm thick. The bridge has two traffic lanes that are 7.0 m in width and two 0.5 m wide barriers. Five cross-beams including two beams at the supports are distributed equally along the span length. Each cross-beam is 250 mm wide and 1350 mm high. Bridge overview pictures and cross-section are presented in Figure 5.57 and Figure 5.58, respectively.

In order to find out the dynamic characteristics of the bridge, 5 accelerometers were employed to measure the bridge's vibrational response under ambient load (Figure 5.59). The 5 accelerometers have sensitivities in the range from 850 to $1000\ \mathrm{mV/m\ s^{-2}}$. The vibration data was recorded by National Instruments (NI) equipment. Sampling frequency is 200 Hz during 300 seconds. The collected data then was treated by using Fast Fourier Transfer (FFT) to convert from time to frequency domain. In general, for a simply supported girder bridge, frequency values of interest are often in an interval from 0 to 30 Hz. Therefore, system identification was restrained to this interval [0, 30] Hz.

Covariance-based Stochastic System identification SSI-COV [180] was used to analyze and identify modes from the dynamic response. Parameters used for system identification were: half number of block rows for Hankel matrix i=100 and model order 2:2:100. Stabilization criteria: 1% for frequency, 5% for damping, 1% for mode shapes. Using these criteria, stable poles can be extracted from the stabilization diagram (Figure 5.60).

Figure 5.57– Overview of Bo Nghi bridge

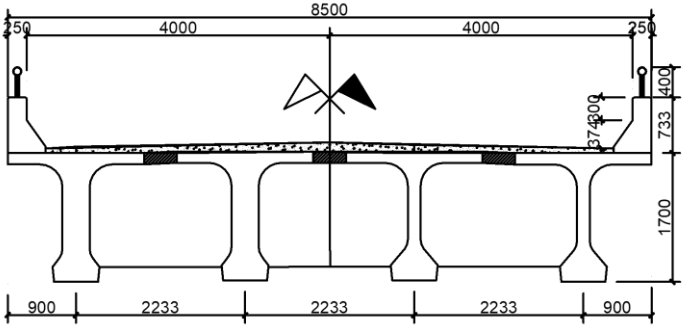

Figure 5.58– A half of cross-section of Bo Nghi bridge at the support (left) and at mid-span (right), (all dimensions are in mm)

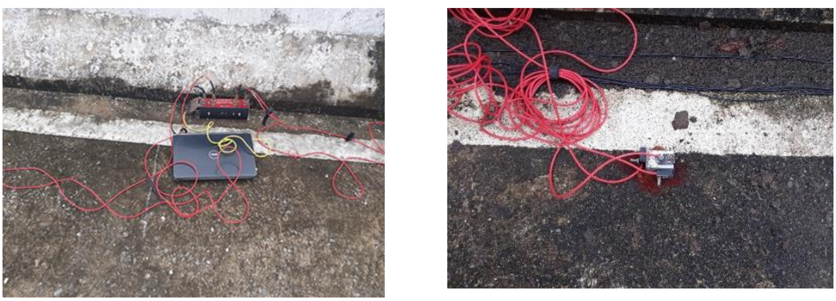

Figure 5.59– Accelerometers in the deck

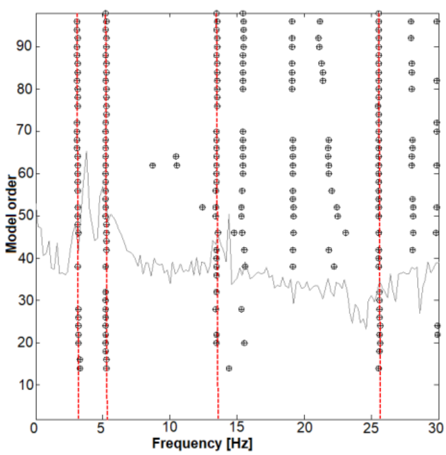

Figure 5.60– Stabilization diagram in the interval from 0-30 Hz.

The bridge was modelled using CSiBridge 20, "SAP2000 Integrated Software for Structural Analysis and Design," Computers and Structures Inc., Berkeley, California. Beam elements were used to model the girder. The boundary conditions of four girders are simply supported. The location of bearing is at the two ends of the four T-shaped girders. Four girders were connected by five cross beams in the transverse direction and by the deck. The barriers and the wearing surface of the deck were modeled as added masses. The bridge was made of concrete material, which has 40 MPa compression strength, density 2400 kg/m^3, and Young Modulus $E = 29$ GPa. Table 5.10 shows that the differences in natural frequencies between FEM and measurements are below 15%.

The displacement mode shapes of the first three bending modes are presented in Figure 5.61. These figures show the displacement mode shapes of the four main girders.

To verify the proposed damage detection method, some damage scenarios were introduced in the FEM by reducing the stiffness of cross-section of a main girder.

Table 5.10 – Frequencies from measurements and FEM for Bo Nghi bridge

Mode	FEM	Experiment	Differences (%)	
1	3.09	3.06	0.98	1st bending
2	5.25	5.33	-1.50	1st torsion
4	11.39	13.16	-13.45	2rd bending
5	27.35	25.52	7.17	3th bending

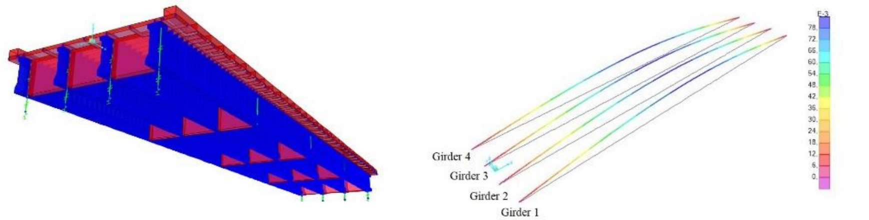

(a) Bo Nghi bridge FEM (b) 1st bending mode, *f*= 3.06 Hz

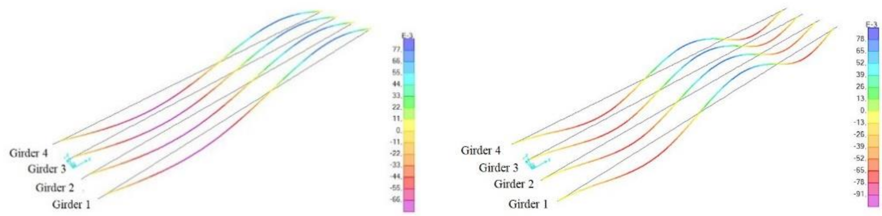

(c) 2rd bending mode, *f*= 11.21 Hz (d) 3th bending mode, *f*=27.35 Hz

Figure 5.61– Bo Nghi bridge FEM and first three bending mode shapes of four girders

5.3.3.3 Procedure of applying GSM-CNN method

The bridge is a complex structure and has many components such as girders, slab, transverse girders, abutment, etc. FEM can be used to model all components of the complete bridge, but it takes time to run. As discussed, CNN is a deep learning method and needs a large amount of data to train. Therefore, this study proposed a method that only uses one single girder to train the network. Then, afterwards the trained network is used to detect damage in a bridge girder. Furthermore, the network will point out which girder is damaged and identify the location of the damage. The following steps are considered.

Step 1: One single simply supported girder in the bridge is modeled using FEM.

Step 2: Damage scenarios are simulated in the girder. The stiffness of each girder element is reduced from 1% to 60%.

Gapped smoothing method is used to calculate the damage indices, then convert them to images. All these images are labeled and used as inputs for CNN.

Step3: Create a CNN model, trained by collecting data from the simply supported girder in step 2.

Step 4: Collect data from the real bridge and calculate the damage indices based on GSM and convert them to images.

Step 5: Use images collected in step 4 as the input of the CNN created in step 3. The output of the network is the damage location.

5.3.3.4 Numerical model of a single simply supported girder

A single girder is modeled using FEM toolbox in Matlab [176]. The length is 32 m and the cross-section is the one of the bridge girder. The girder is divided into 50 elements and 103 nodes (Figure 5.62). The damage is introduced in this FEM by reducing the stiffness of each element from 1% to 60%. In total, $50 \times 60 = 3000$ scenarios are created. Figure 5.63a shows the damage index of the first three vertical bending modes when the damage occurs in element 12. The damage index is calculated using Eq. (4.10) for the first three bending modes based on the modal curvatures extracted from Eq.(4.2) and then normalized. GSM helps to locate the damage between node 21 and 26, but the exact damaged element could not be found. To improve the method, the GSM is combined with CNN. The damage index based on GSM is calculated for each scenario, converted to a contour plot as shown in Figure 5.63b and saved as an image. These are input images of the CNN. Therefore, 3000 images are used to train the network for identifying 50 locations of damage. Each image is labeled with the corresponding damage location.

To create data of an intact girder for training the network, noise is added to the numerical data. One hundred noise levels are added to the data of intact girders. If the girder is intact, CNN will put it to the damage location 0. In total 51 classes are created.

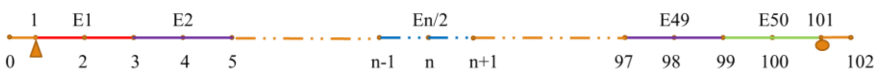

Figure 5.62– FEM of the simply supported girder (Ei means element i).

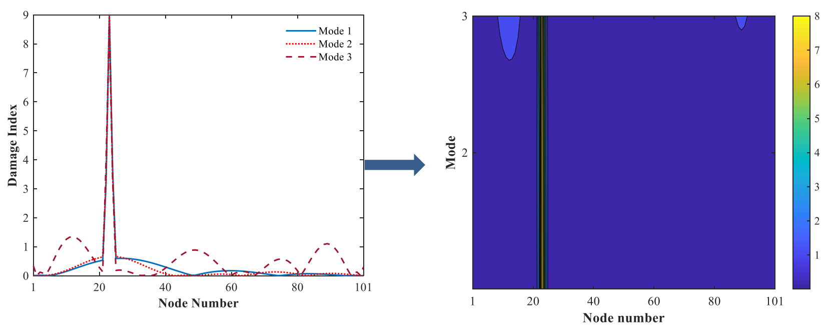

a. Damage index b. Contour plot

Figure 5.63– Damage index and input CNN trained image for damaged element 12

5.3.3.5 Build, train and validate the CNN architecture

Three convolution layers of CNN are proposed for training. Convolution layer 1 contains 16 filters with a kernel size of 3×3. The number of filters is 32 and 64 in convolution layer 2 and 3, respectively (Figure 5.64). To avoid overfitting, dropout layers are applied [181]. A ReLU (Rectified Linear Unit) activation function is used after each layer. After each convolution layer, the max-pooling layer is applied. The pooling layer aggregates the learned parameters from the previous convolution layer, reduces the resolution of filters, but still keeps the main features. After going through three convolution layers and pooling layers, the model can learn the most important feature then the last layer is flattened and turn to a vector in fully connected layers. CNN classifies the input images into pre-defined categories using fully-connected layers.

Instead of classifying the input images into which categories, as we want to predict the percentage of that image in each category, The activation function, softmax is used. For example, when training the location of the damage, one image will belong to one class: undamaged, damaged at E1, damaged at E2 (3 classes). Then the output layer has three nodes. The output of the last layers is the real number z_1, z_2, z_3. Softmax function used to convert these numbers into the percentages a_1,a_2, a_3 (Eq (5.4)). $\sum a_i$ =1 and $0 < a_i < 1$ then a_i is considered as the probability that the image belongs to class i.

To define the loss function, let's come back to our previous example. If there is only one image from the undamaged girder, it must belong to class 1. Then the target is: $a_1 = 1$, $a_2 = 0$, a_3=0 ($y_{target} = [1\ 0\ 0]$), whereas the output from CNN is a_1,a_2, a_3 ($y_{predict} = [\,a_1\ \ a_2\ \ a_3]$). The loss function is defined in Eq. (5.5). Using this equation for this example, $L = \log(a_1)$. If the model predicts right then $a_1 = 1$ or 100% and $L = 0$. In contrast, if the model predicts wrong then $a_1 = 0$ and $L = \infty$. Therefore, the weights and biases are obtained by minimizing L, which is called 'categorical_crossentropy' function.

$$a_k = \frac{e^{z_k}}{\sum_i e^{z_i}} \tag{5.4}$$

$$L = \sum_i y_{target\ i} * \log(y_{predict\ i}) \tag{5.5}$$

The proposed CNN architecture is trained using numerical data. The network detects the location of damage based on the numerical data of 50 damage locations with different levels of severity (section 5.3.3.4). The CNN is also trained to recognize the intact girder and put in the damage location 0.

The accuracy is the fraction of predictions that our model got right. The loss value is calculated using Eq.(5.5). The accuracy and the loss are updated after each step as shown in Figure 5.65. The horizontal axis is the step number. The proposed CNN model succeeds in classifying the damage location. The accuracy of training and validation data is approximately 100%.

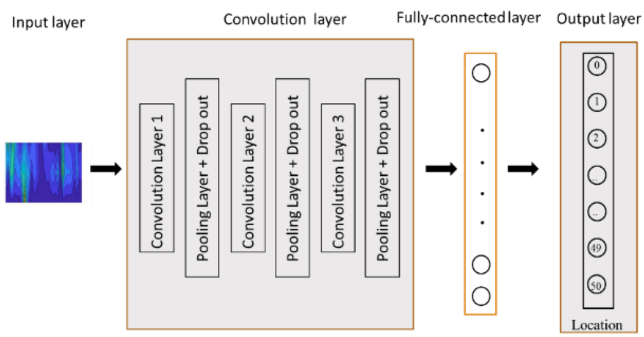

Figure 5.64– The proposed CNN architecture

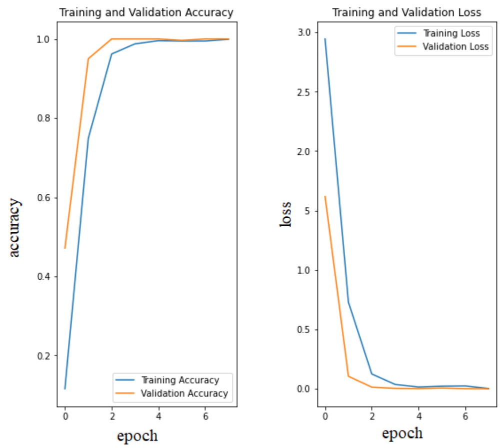

Figure 5.65– Training and validation accuracy/loss of the proposed CNN

5.3.3.6 Testing the CNN architecture

As discussed in section 5.3.3.2, to test the trained CNN, damage scenarios were created in the FEM of the bridge. As an example, the scenario in which the stiffness of E20 at girder 2 is reduced by 50% is described below.

The images from each girder in the Bo Nghi bridge were extracted from mode shapes. The mode shape of each girder was obtained from the FEM of the damaged bridge. In section 5.3.3.4, 103 nodes were used to build the trained girder. However, using so many nodes is not according to reality as vibration measurements cannot be available at all nodes. Therefore, in the FEM of the bridge, the mode shape is only extracted from 51 nodes. This implies that accurate measurements are performed in 51 (nodes) × 4 (girders) = 204 locations. The number of nodes in the trained girder and the real bridge can be adjusted depending on the real case. Eq.(4.2) was used to calculate the modal curvatures and then

Eq.(4.8) was employed to calculate the damage index for the three first bending modes. This damage index is plotted and converted into images as shown in Figure 5.63. Figure 5.66 shows four images from the four girders. These images were the test input images of trained CNN, which do not require the axis labels of images. Trained CNN will predict the damage location of each girder.

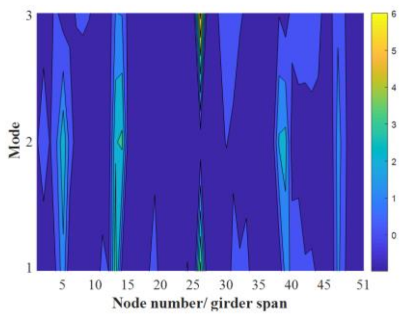

a. Girder 1

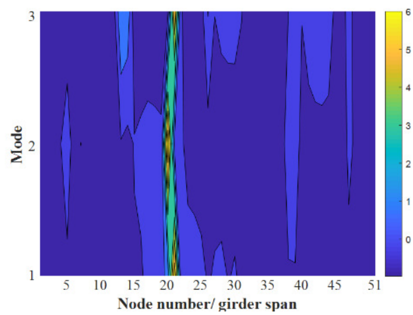

b. Girder 2

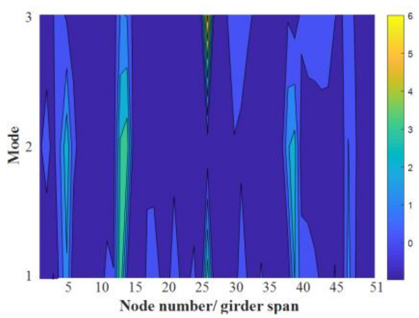

c. Girder 3

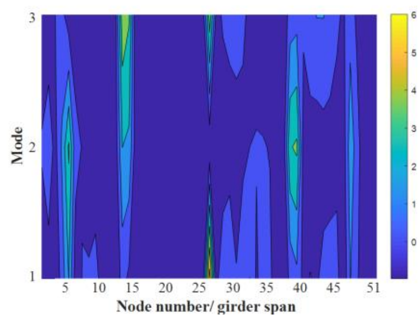

d. Girder 4

Figure 5.66– The input images from Bo Nghi bridge

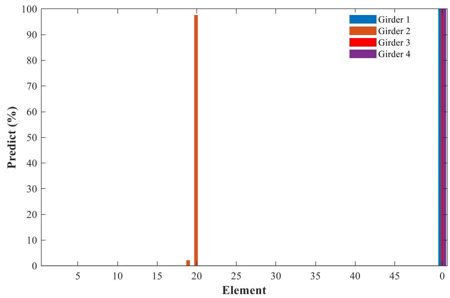

Figure 5.67– The predicted results from trained CNN about the location of damage

Figure 5.67 presents the predicted results from CNN. The GSM-CNN predicted approximately 100% that girder 1, girder 3, girder 4 belong to damage location 0, and 98% that girder 2 belongs to damage location 20. The proposed CNN after trained with images from GSM can predict the location of damage in bridge girders and recognizes the undamaged ones.

One hundred scenarios with different damage severities and locations are created in the FE model of the bridge to verify the method, considering both exterior girder (1, 4) and interior girder (2, 3). They are summarized in Table 5.11. If a false position is found, this scenario will be denoted as "W". CNN predicts the right damage location of 82 scenarios. The accuracy of the total test is 82%. In the 18 scenarios that CNN made the wrong prediction: 13 scenarios had the damage severity less than 20%, and 5 scenarios had the damage severity from 20% to 30%. Therefore, if the severity of the damage is more than 30%, the accuracy of the model will be 100%. Moreover, if the severity of the damage is less than 10%, the model will locate that girder in class 0, which corresponds to an undamaged girder. It can be observed that for low values of the severity (2% to 6%), the assessment is successful. For an increased severity, more than 10%, some assessments fail because this girder is damaged and the model has to predict the correct damage location.

Table 5.11 – Predicted results from trained CNN for test scenarios

Sc*	Lo*	Se*	Re*	Sc*	Lo*	Se*	Re*	Sc*	Lo*	Se*	Re*	Sc*	Lo*	Se*	Re*
1	9/1*	5	R*	26	20/2	5	R	51	28/3	3	R	76	37/4	3	R
2	9/1	15	W*	27	20/2	12	W	52	28/3	12	W	77	37/4	15	R
3	9/1	20	R	28	20/2	20	R	53	28/3	20	R	78	37/4	25	R
4	9/1	25	R	29	20/2	30	R	54	28/3	30	R	79	37/4	30	R
5	9/1	45	R	30	20/2	45	R	55	28/3	45	R	80	37/4	45	R
6	12/1	3	R	31	22/2	5	R	56	30/3	2	R	81	38/4	5	R
7	12/1	16	R	32	22/2	13	W	57	30/3	16	W	82	38/4	18	R
8	12/1	25	R	33	22/2	20	W	58	30/3	22	R	83	38/4	25	R
9	12/1	30	R	34	22/2	25	R	59	30/3	30	R	84	38/4	30	R
10	12/1	50	R	35	22/2	50	R	60	30/3	48	R	85	38/4	45	R
11	14/1	8	R	36	24/2	5	R	61	32/3	5	R	86	40/4	3	R
12	14/1	15	R	37	24/2	14	W	62	32/3	15	W	87	40/4	12	W
13	14/1	22	R	38	24/2	20	W	63	32/3	20	R	88	40/4	20	W
14	14/1	35	R	39	24/2	25	R	64	32/3	25	R	89	40/4	25	R
15	14/1	45	R	40	24/2	45	R	65	32/3	45	R	90	40/4	45	R
16	16/1	3	R	41	25/2	5	R	66	34/3	2	R	91	41/4	5	R
17	16/1	17	R	42	25/2	15	R	67	34/3	12	W	92	41/4	12	W
18	16/1	28	R	43	25/2	25	R	68	34/3	20	R	93	41/4	20	W
19	16/1	35	R	44	25/2	30	R	69	34/3	30	R	94	41/4	25	R
20	16/1	50	R	45	25/2	45	R	70	34/3	50	R	95	41/4	45	R
21	18/1	6	R	46	26/2	8	R	71	36/3	8	R	96	42/4	5	R
22	18/1	12	W	47	26/2	12	W	72	36/3	15	R	97	42/4	15	W
23	18/1	30	R	48	26/2	22	W	73	36/3	20	R	98	42/4	20	R
24	18/1	35	R	49	26/2	25	R	74	36/3	25	R	99	42/4	30	R
25	18/1	45	R	50	26/2	50	R	75	36/3	45	R	100	42/4	45	R

Sc* : The number serial of damage Scenario

Lo*: Location of damage element as shown in Figure 5.62. 9/1 means damage in E9 at girder 1.

Se*: Severity of the damage

Re*: The predicted results from CNN, R*: Right, and W*: Wrong

5.3.3.7 Discussion

A novel method that combines GSM and CNN was proposed in this section to detect the damage in a girder bridge. A CNN was proposed and trained to predict whether the girder is damaged or not, and to find the damage location. The training and validation images are the contour plots of the damage index obtained from GSM. Damage scenarios were introduced in a single girder to train the network. GSM-CNN method was applied to Bo Nghi bridge. This bridge has four girders and damage was simulated in one girder. GSM-CNN has successfully predicted the location of damage in this girder. Moreover, GSM-CNN can predict that other girders are healthy, which is difficult to realize if only GSM is used. If the severity of the damage is more than 30%, the accuracy of this method is 100%. Most of the wrong predictions occur in the girder that has a severity of damage in the range of 12% to 25%. The model can predict the healthy girder that has a severity of the damage less than 10%. The accuracy of the model for all tests is 82 %.

In this section, CNN was trained to locate the damage in a bridge girder using the numerical data from a single girder. This means that a simple model was used to train the network. The trained data do not need to be extracted from the complete and complex bridge model when using the data from FEM of the complete bridge to train the network, the results will be better and the severity of the damage can be found. However, using training data from a simple model, it is demonstrated that this method can be applied afterwards to complex bridges.

GSM-CNN is simple, automated, and easy to employ in real structures. The displacement mode shapes of the bridge can be measured using operational modal analysis. The number of considered points in the girder can be adjusted based on available sensors. Nowadays, several methods have been developed to measure the bridge vibration such as accelerometers [182], wireless sensors [183], direct modal strain measurements [184]. Therefore, this method has a high potential to be applied to a real damaged bridge.

In this research, only damage in the main girder is considered, and we do not consider damage in other components of the bridge. Applying this method to different types of bridges and to other types of damages will be the subject of future research.

Chapter 6

Conclusions and future work

6.1 Conclusions

This thesis has successfully proposed two damage detection methods, which have been verified for beams and bridges. VBDD methods worked well with machine learning algorithms. The vibration measurement data has been used to calculate the input of the neural network. The neural network was trained and validated based on big data from the numerical model. Those non-destructive methods would assess the bridge condition without the knowledge about the intact structure, the excitation load, or a deep understanding of structural behavior.

Firstly, the literature review on VBDD and SHM using machine learning was generally discussed.

Secondly, the method that combines transmissibility and ANN was proposed in Chapter 3. The results of applying this method to a simply supported beam was presented in Chapter 5, section 5.2.1. Four damage locations with different damage levels in the beam were successfully identified with high accuracy. Then, this method was verified with a simply supported girder bridge, Ca-Non bridge. A moving truck was used as an excitation force and the TFs were calculated from the displacement responses of the considered points in the main bridge girders. This research only considers single damage in the main girder, therefore, the method was improved further in the research with a truss bridge, Nam O bridge. Multiple damages were investigated. The pattern classification algorithm was used to classify the damage type and the damage severity was identified using regression analysis. The results obtained from both bridges were great. The proposed method not only can be applied for a beam, but also for different kinds of bridges with high level of accuracy.

Moreover, the potential of this method for practical application is promising. First, a well calibrated FE model is created. Then, the model is updated using the measured modal properties. The responses of some considered points are used to calculate the simulated transmissibility functions. The number of considered points in the bridge depends on the measurement points on site. The simulated truck is the same moving truck as in the experiment. If we want to use different trucks, the truck characteristics such as the axle weight, number of axles, the distance between two axels and the velocity of the truck could be added as input to the networks. Damage scenarios are introduced in the FE model and used to train the ANNs. The ANNs input parameters are obtained from the simulated transmissibility functions. The ANNs targets are the locations and the severity of the damage. In the second step, an experiment is carried out to measure the responses at all considered points due to a truck moving on the real damaged bridge. Then the measured transmissibility functions and transmissibility indicators are calculated. These parameters are put into the ANNs established before. The outputs of the created ANNs are the locations and the severity of the damaged bridge.

The second method proposed in this thesis is the method that combines GSM and CNN in Chapter 4. Single damage in a laboratory free-free beam in section 5.2.2 was located using this method. The vibration measurement has been done in this beam to validate the proposed method. The results showed that, when combining with CNN, the damage was located correctly and the level of severity of the damage can be identified. Section 5.3.3 showed the procedure to apply the GSM-CNN method to a simply supported girder bridge, Bo Nghi bridge. To calibrate the FE model of the Bo Nghi bridge, the onsite vibration experiment was carried out. Based on learning images converted from GSM, CNN can predict the damage location in the main girder correctly. The accuracy of the method is more than 80%.

The research has been validated through numerical examples, and experimental measurments of real bridges. The results reveal the good performance of the proposed methodology and its high potential application to real bridges.

6.2 Future work

The methodologies and applications presented in this thesis have shown that machine learning and VBDD are promising directions in SHM. To improve the method and to validate the application to real bridges, some possible future extension of the present research is presented below.

1. Laboratory scale bridges should be set up to verify the methodology.

2. Extending the VBDD methods to include other techniques, such as flexibility matrix method, matrix update based method, non-linear method, etc.

3. Optimizing the number of sensors and the location of sensors used in each method.

4. Improving machine learning algorithms to increase network accuracy and to reduce process time.

5. Examine the bridges under the influence of temperature, wind, and traffic.

References

1. Farrar, C. and S. Doebling, *Damage detection II: field applications to large structures.* Modal Analysis and Testing, Nato Science Series. Dordrecht, Netherlands: Kluwer Academic Publishers, 1999.
2. Aktan, A., F. Catbas, K. Grimmelsman, and C. Tsikos, *Issues in infrastructure health monitoring for management.* Journal of Engineering Mechanics, 2000. **126**(7): p. 711-724.
3. Catbas, F.N. and A.E. Aktan, *Condition and damage assessment: issues and some promising indices.* Journal of Structural Engineering, 2002. **128**(8): p. 1026-1036.
4. Frýba, L. and M. Pirner, *Load tests and modal analysis of bridges.* Engineering Structures, 2001. **23**(1): p. 102-109.
5. Brownjohn, J. and P. Carden. *Real-time operation modal analysis of Tamar Bridge*. in *26th International Modal Analysis Conference (IMAC XXVI)*. 2008.
6. Carden, E.P. and P. Fanning, *Vibration based condition monitoring: a review.* Structural health monitoring, 2004. **3**(4): p. 355-377.
7. Catbas, F.N., D.L. Brown, and A.E. Aktan, *Use of modal flexibility for damage detection and condition assessment: case studies and demonstrations on large structures.* Journal of Structural Engineering, 2006. **132**(11): p. 1699-1712.
8. Alvandi, A. and C. Cremona, *Assessment of vibration-based damage identification techniques.* Journal of sound and vibration, 2006. **292**(1-2): p. 179-202.

9. Doebling, S.W., C.R. Farrar, M.B. Prime, and D.W. Shevitz, *Damage identification and health monitoring of structural and mechanical systems from changes in their vibration characteristics: a literature review*. 1996, Los Alamos National Lab., NM (United States).

10. Mazurek, D.F. *Modal sensitivity to damage in multigirder bridges*. in *SPIE*. 1997.

11. Doebling, S.W. and C.R. Farrar, *Statistical damage identification techniques applied to the I-40 bridge over the Rio Grande River*. 1998, Los Alamos National Lab., NM (United States).

12. Alvandi, A., *Contribution à l'utilisation pratique de l'évaluation dynamique pour la détection d'endommagements dans les ponts*. 2003.

13. Foti, S. and D. Sabia. *Dynamic behavior of bridges affected by scouring: numerical simulations and experimental evidence*. in *Proceedings 3rd International Conference on Scour and Erosion (ICSE-3). November 1-3, 2006, Amsterdam, The Netherlands*. 2006.

14. Ruocci, G., K. Worden, and A. De Stefano. *Damage detection in a masonry arch bridge model using outlier analysis*. in *Fifth European Workshop on Structural Health Monitoring 2010*. 2010. DEStech Publications, Inc.

15. Jaishi, B., H.-J. Kim, M.K. Kim, W.-X. Ren, and S.-H. Lee, *Finite element model updating of concrete-filled steel tubular arch bridge under operational condition using modal flexibility.* Mechanical Systems and Signal Processing, 2007. **21**(6): p. 2406-2426.

16. Wahab, M.A. and G. De Roeck, *Damage detection in bridges using modal curvatures: application to a real damage scenario.* Journal of Sound and vibration, 1999. **226**(2): p. 217-235.

17. Dilena, M., M. Limongelli, and A. Morassi, *Damage localization in bridges via the FRF interpolation method.* Mechanical Systems and Signal Processing, 2015. **52**: p. 162-180.

18. Chang, K.-C. and C.-W. Kim, *Modal-parameter identification and vibration-based damage detection of a damaged steel truss bridge.* Engineering Structures, 2016. **122**: p. 156-173.

19. Tan, Z.X., D.P. Thambiratnam, T.H. Chan, M. Gordan, and H. Abdul Razak, *Damage detection in steel-concrete composite bridge using vibration characteristics and artificial neural network.* Structure and Infrastructure Engineering, 2020. **16**(9): p. 1247-1261.

20. Yang, Y. and J.P. Yang, *State-of-the-art review on modal identification and damage detection of bridges by moving test vehicles.* International Journal of Structural Stability and Dynamics, 2018. **18**(02): p. 1850025.

21. Kong, X., C.-S. Cai, and J. Hu, *The state-of-the-art on framework of vibration-based structural damage identification for decision making.* Applied Sciences, 2017. **7**(5): p. 497.

22. Johnson, T.J. and D.E. Adams, *Transmissibility as a differential indicator of structural damage.* J. Vib. Acoust., 2002. **124**(4): p. 634-641.

23. Chen, Q., Y. Chan, K. Worden, and G. Tomlinson. *Structural fault detection using neural networks trained on transmissibility functions*. in *Proceedings of the International Conference on Vibration Engineering*. 1994.

24. Worden, K., *Structural fault detection using a novelty measure.* Journal of Sound and vibration, 1997. **201**(1): p. 85-101.

25. Worden, K., G. Manson, and N.R. Fieller, *Damage detection using outlier analysis.* Journal of Sound and vibration, 2000. **229**(3): p. 647-667.

26. Worden, K., G. Manson, and D. Allman, *Experimental validation of a structural health monitoring methodology: Part I. Novelty detection on a laboratory structure.* Journal of sound and vibration, 2003. **259**(2): p. 323-343.

27. Manson, G., K. Worden, and D. Allman, *Experimental validation of a structural health monitoring methodology: Part II. Novelty detection on a Gnat aircraft.* Journal of Sound and Vibration, 2003. **259**(2): p. 345-363.

28. Sampaio, R., N. Maia, A. Ribeiro, and J. Silva. *Transmissibility techniques for damage detection*. in *Proceedings of the International Modal Analysis Conference*. 2001.

29. Maia, N.M., R.A. Almeida, A.P. Urgueira, and R.P. Sampaio, *Damage detection and quantification using transmissibility.* Mechanical Systems and Signal Processing, 2011. **25**(7): p. 2475-2483.

30. Zhou, Y.-L., N.M. Maia, and M. Abdel Wahab, *Damage detection using transmissibility compressed by principal component analysis enhanced with distance measure.* Journal of Vibration and Control, 2018. **24**(10): p. 2001-2019.

31. Fontul, M., A. Ribeiro, J. Silva, and N. Maia, *Transmissibility matrix in harmonic and random processes.* Shock and Vibration, 2004. **11**(5, 6): p. 563-571.

32. Zhou, Y.-L., N.M. Maia, R.P. Sampaio, and M.A. Wahab, *Structural damage detection using transmissibility together with hierarchical clustering analysis and similarity measure.* Structural health monitoring, 2017. **16**(6): p. 711-731.

33. Johnson, T.J., R.L. Brown, D.E. Adams, and M. Schiefer, *Distributed structural health monitoring with a smart sensor array.* Mechanical Systems and Signal Processing, 2004. **18**(3): p. 555-572.

34. Johnson, T.J. and D.E. Adams, *Rolling tire diagnostic experiments for identifying incipient bead damage using time, frequency, and phase plane analysis.* SAE Transactions, 2006: p. 984-990.

35. Lage, Y., M. Neves, N. Maia, and D. Tcherniak, *Force transmissibility versus displacement transmissibility.* Journal of Sound and Vibration, 2014. **333**(22): p. 5708-5722.

36. Kong, X., C. Cai, and B. Kong, *Damage detection based on transmissibility of a vehicle and bridge coupled system.* Journal of Engineering Mechanics, 2015. **141**(1): p. 04014102.

37. Nguyen, H.D., T.T. Bui, G. De Roeck, and M.A. Wahab. *Damage Detection in Simply Supported Beam Using Transmissibility and Auto-Associative Neural Network*. in

International Conference on Numerical Modelling in Engineering. 2018. Springer.

38. Nguyen, D.H., T.T. Bui, G. De Roeck, and M.A. Wahab, *Damage detection in Ca-Non Bridge using transmissibility and artificial neural networks.* Structural Engineering and Mechanics, 2019. **71**(2): p. 175-183.

39. Cofre-Martel, S., P. Kobrich, E. Lopez Droguett, and V. Meruane, *Deep convolutional neural network-based structural damage localization and quantification using transmissibility data.* Shock and Vibration, 2019. **2019**.

40. Nguyen, D.H., H. Tran-Ngoc, T. Bui-Tien, G. De Roeck, and M.A. Wahab, *Damage detection in truss bridges using transmissibility and machine learning algorithm: Application to Nam O bridge.* Smart Structures and Systems, 2020. **26**(1): p. 35-47.

41. Maia, N.M., J.M. Silva, and A.M. Ribeiro, *The transmissibility concept in multi-degree-of-freedom systems.* Mechanical Systems and Signal Processing, 2001. **15**(1): p. 129-137.

42. Ribeiro, A., N. Maia, and J. Silva, *Experimental evaluation of the transmissibility matrix.* Proceedings of IMAC, Kissimmee (FL), USA, 1999.

43. Devriendt, C. and P. Guillaume, *The use of transmissibility measurements in output-only modal analysis.* Mechanical Systems and Signal Processing, 2007. **21**(7): p. 2689-2696.

44. Devriendt, C., G. De Sitter, and P. Guillaume, *An operational modal analysis approach based on parametrically identified multivariable transmissibilities.* Mechanical Systems and Signal Processing, 2010. **24**(5): p. 1250-1259.

45. Devriendt, C., G. De Sitter, S. Vanlanduit, and P. Guillaume, *Operational modal analysis in the presence of harmonic excitations by the use of transmissibility measurements.* Mechanical systems and signal processing, 2009. **23**(3): p. 621-635.

46. Canales, G., L. Mevel, and M. Basseville. *Transmissibility based damage detection.* in *Proceedings of the 27th*

International Modal Analysis Conference (IMAC-XXVII'09). 2009.

47. Sun, Q., W.-J. Yan, W.-X. Ren, and L.-L. Liu, *Application of transmissibility measurements to operational modal analysis of railway, highway, and pedestrian cable-stayed bridges.* Measurement, 2019. **148**: p. 106880.

48. Devriendt, C., P. Guillaume, E. Reynders, and G. De Roeck. *Operational modal analysis of a bridge using transmissibility measurements*. in *Proceedings of IMAC-25: A Conference and Exposition on Structural Dynamics*. 2007.

49. Papatheou, E., G. Manson, R.J. Barthorpe, and K. Worden, *The use of pseudo-faults for novelty detection in SHM.* Journal of Sound and Vibration, 2010. **329**(12): p. 2349-2366.

50. Siebel, T. and D. Mayer. *Damage detection on a truss structure using transmissibility functions*. in *Proceedings of the 8th International Conference on Structural Dynamics, EURODYN*. 2011.

51. Zhou, Y.L., E. Figueiredo, N. Maia, R. Sampaio, and R. Perera, *Damage detection in structures using a transmissibility-based Mahalanobis distance.* Structural Control and Health Monitoring, 2015. **22**(10): p. 1209-1222.

52. Zhou, Y.-L. and M.A. Wahab, *Cosine based and extended transmissibility damage indicators for structural damage detection.* Engineering Structures, 2017. **141**: p. 175-183.

53. Li, J., H. Hao, Y. Xia, and H.-p. Zhu, *Damage detection of shear connectors in bridge structures with transmissibility in frequency domain.* International Journal of Structural Stability and Dynamics, 2014. **14**(02): p. 1350061.

54. Feng, L., X. Yi, D. Zhu, X. Xie, and Y. Wang, *Damage detection of metro tunnel structure through transmissibility function and cross correlation analysis using local excitation and measurement.* Mechanical Systems and Signal Processing, 2015. **60**: p. 59-74.

55. Meruane, V. and A. Ortiz-Bernardin, *Structural damage assessment using linear approximation with maximum entropy*

and transmissibility data. Mechanical Systems and Signal Processing, 2015. **54**: p. 210-223.

56. Zhou, Y.-L., M. Abdel Wahab, and R. Perera. *Damage detection by transmissibility conception in beam-damage detection by transmissibility conception in beam-like structures*. in *4th International Conference on Fracture Fatigue and Wear*. 2015.

57. Schulz, M.J., A.S. Naser, P.F. Pai, M.S. Linville, and J. Chung. *Detecting structural damage using transmittance functions*. in *SPIE*. 1997.

58. Zhang, H., M. Schulz, A. Naser, F. Ferguson, and P. Pai, *Structural health monitoring using transmittance functions.* Mechanical Systems and Signal Processing, 1999. **13**(5): p. 765-787.

59. Ghoshal, A., M.J. Sundaresan, M.J. Schulz, and P.F. Pai, *Structural health monitoring techniques for wind turbine blades.* Journal of Wind Engineering and Industrial Aerodynamics, 2000. **85**(3): p. 309-324.

60. Zhou, Y.-L., E. Figueiredo, N. Maia, and R. Perera, *Damage detection and quantification using transmissibility coherence analysis.* Shock and Vibration, 2015. **2015**.

61. Chesné, S. and A. Deraemaeker, *Damage localization using transmissibility functions: a critical review.* Mechanical systems and signal processing, 2013. **38**(2): p. 569-584.

62. Maia, N., A. Urgueira, and R. Almeida, *Whys and Wherefores of Transmissibility.* Vibration Analysis and Control: New Trends and Developments, 2011: p. 197.

63. Pandey, A., M. Biswas, and M. Samman, *Damage detection from changes in curvature mode shapes.* Journal of sound and vibration, 1991. **145**(2): p. 321-332.

64. WILLIAMS, C. and O. SALAWU, *Bridge Assessment Management and Design (BIG Barr et al., editors London*. 1994, Elsevier. Concepts of condition assessment of bridges using vibration ….

65. Farrar, C.R. and D. Jauregui, *Damage detection algorithms applied to experimental and numerical modal data from the I-40 bridge*. 1996: Los Alamos National Laboratory.

66. Ratcliffe, C.P., *Damage detection using a modified Laplacian operator on mode shape data.* Journal of Sound and Vibration, 1997. **204**(3): p. 505-517.

67. Ratcliffe, C.P. and W.J. Bagaria, *Vibration technique for locating delamination in a composite beam.* AIAA journal, 1998. **36**(6): p. 1074-1077.

68. Yoon, M.K., D. Heider, J.W. Gillespie, C.P. Ratcliffe, and R.M. Crane. *Local damage detection using a global fitting method on mode shape data*. in *IMAC-XIX: A Conference on Structural Dynamics*. 2001.

69. Yoon, M., D. Heider, J. Gillespie Jr, C. Ratcliffe, and R. Crane. *Spatial damage detection in composite structures using a global fitting method on curvature operating shapes*. in *American Society for Composites 16th Annual Technical Conference*. 2001.

70. Yoon, M., D. Heider, J. Gillespie Jr, C. Ratcliffe, and R. Crane, *Local damage detection using the two-dimensional gapped smoothing method.* Journal of Sound and Vibration, 2005. **279**(1-2): p. 119-139.

71. Oh, B.H. and B.S. Jung, *Structural damage assessment with combined data of static and modal tests.* Journal of Structural Engineering, 1998. **124**(8): p. 956-965.

72. Meruane, V., I. Fernandez, R.O. Ruiz, G. Petrone, and E. Lopez-Droguett, *Gapped Gaussian smoothing technique for debonding assessment with automatic thresholding.* Structural Control and Health Monitoring, 2019. **26**(8): p. e2371.

73. Ahmad, S., A. Waleed, U.S. Virk, M.T. Riaz, A. Sharjeel, and N. Ahmad, *Multiple damage detections in plate-like structures using curvature mode shapes and gapped smoothing method.* Advances in Mechanical Engineering, 2019. **11**(5): p. 1687814019848921.

74. Nguyen, D.H., Q.B. Nguyen, T. Bui-Tien, G. De Roeck, and M.A. Wahab, *Damage detection in girder bridges using modal curvatures gapped smoothing method and Convolutional Neural Network: Application to Bo Nghi bridge.* Theoretical and Applied Fracture Mechanics, 2020. **109**: p. 102728.

75. SUN, K., *Damage identification of small radius curved bridge based on curvature of displacement influence line.* Journal of ZheJiang University (Engineering Science), 2016. **50**(4): p. 727-734.

76. Dilena, M. and A. Morassi, *Dynamic testing of a damaged bridge.* Mechanical Systems and Signal Processing, 2011. **25**(5): p. 1485-1507.

77. Sohn, H., C.R. Farrar, F.M. Hemez, D.D. Shunk, D.W. Stinemates, B.R. Nadler, and J.J. Czarnecki, *A review of structural health monitoring literature: 1996–2001.* Los Alamos National Laboratory, USA, 2003. **1**.

78. Fan, W. and P. Qiao, *Vibration-based damage identification methods: a review and comparative study.* Structural health monitoring, 2011. **10**(1): p. 83-111.

79. Liu, Y. and S. Nayak, *Structural health monitoring: State of the art and perspectives.* Jom, 2012. **64**(7): p. 789-792.

80. Worden, K. and J.M. Dulieu-Barton, *An overview of intelligent fault detection in systems and structures.* Structural Health Monitoring, 2004. **3**(1): p. 85-98.

81. Chen, H.-P. and Y.-Q. Ni, *Structural health monitoring of large civil engineering structures*. 2018: Wiley Online Library.

82. Brownjohn, J.M.W. and T.C. Pan, *Response of tall buildings to weak long distance earthquakes.* Earthquake engineering & structural dynamics, 2001. **30**(5): p. 709-729.

83. Brownjohn, J.M., A. De Stefano, Y.-L. Xu, H. Wenzel, and A.E. Aktan, *Vibration-based monitoring of civil infrastructure: challenges and successes.* Journal of Civil Structural Health Monitoring, 2011. **1**(3-4): p. 79-95.

84. Wong, K., *Structural health monitoring and safety evaluation of Stonecutters Bridge under the in-service condition.* Bridge maintenance, safety, management and life-cycle optimization: IABMAS10, Philadelphia, 2010: p. 2641-2648.

85. Le Diourion, T. and G. Hovhanessian, *The health monitoring of Rion Antirion Bridge.* IMACXXIII, Orlando, 2005.

86. Dallard, P., A. Fitzpatrick, A. Flint, S. Le Bourva, A. Low, R. Ridsdill Smith, and M. Willford, *The London millennium footbridge.* Structural Engineer, 2001. **79**(22): p. 17-21.

87. ICOLD, C., *Dam monitoring general considerations. International Commission on Large Dams.* Bulletin, 1988. **60**.

88. Grimmelsman, K.A. and A.E. Aktan. *Impacts and mitigation of uncertainty for improving the reliability of field measurements*. in *The 2nd International Conference on Structural Health Monitoring of Intelligent Infrastructure, Shenzhen, China*. 2005.

89. Grimmelsman, K.A., Q. Pan, and A.E. Aktan, *Analysis of data quality for ambient vibration testing of the Henry Hudson Bridge.* Journal of Intelligent Material Systems and Structures, 2007. **18**(8): p. 765-775.

90. Macdonald, J. *Pedestrian-induced vibrations of the Clifton Suspension Bridge, UK*. in *Proceedings of the Institution of Civil Engineers-Bridge Engineering*. 2008. Thomas Telford Ltd.

91. Macdonald, J.H., P.A. Irwin, and M.S. Fletcher, *Vortex-induced vibrations of the Second Severn Crossing cable-stayed bridge—full-scale and wind tunnel measurements.* Proceedings of the Institution of Civil Engineers-Structures and Buildings, 2002. **152**(2): p. 123-134.

92. Moutinho, C., W.-H. Hu, E. Caetano, and A. Cunha. *Implementation of a dynamic monitoring system at Coimbra footbridge*. in *International Modal Analysis Conference, XXVI IMAC, Orlando, USA*. 2008.

93. Moyo, P. and R. Tait, *Structural assessment and performance prediction of a railway bridge.* Struct. Infrastruct. Eng, 2010. **6**.

94. Wong, K.Y., *Instrumentation and health monitoring of cable-supported bridges.* Structural control and health monitoring, 2004. **11**(2): p. 91-124.

95. Worden, K. and G. Manson, *The application of machine learning to structural health monitoring.* Philosophical Transactions of the Royal Society A: Mathematical, Physical and Engineering Sciences, 2007. **365**(1851): p. 515-537.

96. Chen, Q., Y. Chan, and K. Worden, *Structural fault diagnosis and isolation using neural networks based on response-only data.* Computers & Structures, 2003. **81**(22-23): p. 2165-2172.

97. Hakim, S. and H. Abdul Razak, *Adaptive neuro fuzzy inference system (ANFIS) and artificial neural networks (ANNs) for structural damage identification.* Struct Eng Mech, 2013. **45**(6): p. 779-802.

98. Nanthakumar, S., T. Lahmer, X. Zhuang, G. Zi, and T. Rabczuk, *Detection of material interfaces using a regularized level set method in piezoelectric structures.* Inverse Problems in Science and Engineering, 2016. **24**(1): p. 153-176.

99. Zapico, J., M. Gonzalez, and K. Worden, *Damage assessment using neural networks.* Mechanical Systems and Signal Processing, 2003. **17**(1): p. 119-125.

100. Shu, J., Z. Zhang, I. Gonzalez, and R. Karoumi, *The application of a damage detection method using Artificial Neural Network and train-induced vibrations on a simplified railway bridge model.* Engineering structures, 2013. **52**: p. 408-421.

101. Na, S. and H.-K. Lee, *Neural network approach for damaged area location prediction of a composite plate using electromechanical impedance technique.* Composites Science and Technology, 2013. **88**: p. 62-68.

102. Nguyen, H.D., T.T. Bui, G. De Roeck, and M.A. Wahab. *Damage Detection in Simply Supported Beam Using Transmissibility and Auto-Associative Neutral Network*. in *International Conference on Numerical Modelling in Engineering*. 2018. Springer.

103. Tran-Ngoc, H., S. Khatir, G. De Roeck, T. Bui-Tien, and M.A. Wahab, *An efficient artificial neural network for damage detection in bridges and beam-like structures by improving training parameters using cuckoo search algorithm.* Engineering Structures, 2019. **199**: p. 109637.

104. Zhou, Y.-L. and M.A. Wahab, *Damage detection using vibration data and dynamic transmissibility ensemble with auto-associative neural network.* Mechanics, 2017. **23**(5): p. 688-695.

105. Zhao, Z.-Q., P. Zheng, S.-t. Xu, and X. Wu, *Object detection with deep learning: A review.* IEEE transactions on neural networks and learning systems, 2019.

106. Sarkar, S., K.K. Reddy, M. Giering, and M.R. Gurvich. *Deep learning for structural health monitoring: A damage characterization application*. in *Annual Conference of the Prognostics and Health Management Society*. 2016.

107. Cha, Y.J., W. Choi, and O. Büyüköztürk, *Deep learning-based crack damage detection using convolutional neural networks.* Computer-Aided Civil and Infrastructure Engineering, 2017. **32**(5): p. 361-378.

108. Verstraete, D., A. Ferrada, E.L. Droguett, V. Meruane, and M. Modarres, *Deep learning enabled fault diagnosis using time-frequency image analysis of rolling element bearings.* Shock and Vibration, 2017. **2017**.

109. Abdeljaber, O., O. Avci, S. Kiranyaz, M. Gabbouj, and D.J. Inman, *Real-time vibration-based structural damage detection using one-dimensional convolutional neural networks.* Journal of Sound and Vibration, 2017. **388**: p. 154-170.

110. Yu, Y., C. Wang, X. Gu, and J. Li, *A novel deep learning-based method for damage identification of smart building structures.* Structural Health Monitoring, 2019. **18**(1): p. 143-163.

111. Khodabandehlou, H., G. Pekcan, and M.S. Fadali, *Vibration-based structural condition assessment using convolution neural networks.* Structural Control and Health Monitoring, 2019. **26**(2): p. e2308.

112. Salawu, O., *Detection of structural damage through changes in frequency: a review.* Engineering structures, 1997. **19**(9): p. 718-723.

113. Gillich, G.-R., H. Furdui, M.A. Wahab, and Z.-I. Korka, *A robust damage detection method based on multi-modal analysis in variable temperature conditions.* Mechanical Systems and Signal Processing, 2019. **115**: p. 361-379.

114. Yang, C. and S.O. Oyadiji, *Damage detection using modal frequency curve and squared residual wavelet coefficients-based damage indicator.* Mechanical Systems and Signal Processing, 2017. **83**: p. 385-405.

115. Doebling, S.W., C.R. Farrar, and M.B. Prime, *A summary review of vibration-based damage identification methods.* Shock and vibration digest, 1998. **30**(2): p. 91-105.

116. Cao, H., Y.-L. Zhou, Z. Chen, and M. Abdel Wahab, *Form-finding Analysis of Suspension Bridges using an Explicit Iterative Approach.* Structural Engineering and Mechanics, 2017. **62** (1): p. 85–95.

117. Tiachacht, S., A. Bouazzouni, S. Khatir, M. Abdel Wahab, A. Behtani, and R. Capozucca, *Damage assessment in structures using combination of a modified Cornwell indicator and genetic algorithm.* Engineering Structures, 2018. **177**: p. 421-430.

118. Samir, K., B. Brahim, R. Capozucca, and M. Abdel Wahab, *Damage detection in CFRP composite beams based on vibration analysis using proper orthogonal decomposition method with radial basis functions and cuckoo search algorithm.* Composite Structures, 2018. **187**: p. 344-353.

119. Qin, S., Y.-L. Zhou, H. Cao, and M.A. Wahab, *Model Updating in Complex Bridge Structures using Kriging Model Ensemble with Genetic Algorithm.* KSCE Journal of Civil Engineering, 2018. **22**(9): p. 3567-3578.

120. Khatir, S., K. Dekemele, M. Loccufier, T. Khatir, and M. Abdel Wahab, *Crack identification method in beam-like structures using changes in experimentally measured frequencies and*

Particle Swarm Optimization. Comptes Rendus Mécanique, 2018. **346**(2): p. 110-120.

121. Khatir, S. and M. Abdel Wahab, *Fast simulations for solving fracture mechanics inverse problems using POD-RBF XIGA and Jaya algorithm.* Engineering Fracture Mechanics, 2018.

122. Zheng, T., J. Liu, W. Luo, and Z. Lu, *Structural damage identification using cloud model based fruit fly optimization algorithm.* STRUCTURAL ENGINEERING AND MECHANICS, 2018. **67**(3): p. 245-254.

123. Yin, Z., J. Liu, W. Luo, and Z. Lu, *An improved Big Bang-Big Crunch algorithm for structural damage detection.* STRUCTURAL ENGINEERING AND MECHANICS, 2018. **68**(6): p. 735-745.

124. Yang, Z., Z. Yu, and H. Sun, *On the cross correlation function amplitude vector and its application to structural damage detection.* Mechanical Systems and Signal Processing, 2007. **21**(7): p. 2918-2932.

125. Gul, M. and F.N. Catbas, *Damage assessment with ambient vibration data using a novel time series analysis methodology.* Journal of Structural Engineering, 2010. **137**(12): p. 1518-1526.

126. Posenato, D., F. Lanata, D. Inaudi, and I.F. Smith, *Model-free data interpretation for continuous monitoring of complex structures.* Advanced Engineering Informatics, 2008. **22**(1): p. 135-144.

127. Khuc, T. and F.N. Catbas, *Computer vision-based displacement and vibration monitoring without using physical target on structures.* Structure and Infrastructure Engineering, 2017. **13**(4): p. 505-516.

128. Shi, J., X. Xu, J. Wang, and G. Li, *Beam damage detection using computer vision technology.* Nondestructive Testing and Evaluation, 2010. **25**(3): p. 189-204.

129. Neves, A., I. González, J. Leander, and R. Karoumi, *Structural health monitoring of bridges: a model-free ANN-based approach to damage detection.* Journal of Civil Structural Health Monitoring, 2017. **7**(5): p. 689-702.

130. Vu-Bac, N., T. Duong, T. Lahmer, X. Zhuang, R. Sauer, H. Park, and T. Rabczuk, *A NURBS-based inverse analysis for reconstruction of nonlinear deformations of thin shell structures.* Computer Methods in Applied Mechanics and Engineering, 2018. **331**: p. 427-455.

131. Zang, C. and M. Imregun, *Structural damage detection using artificial neural networks and measured FRF data reduced via principal component projection.* Journal of sound and vibration, 2001. **242**(5): p. 813-827.

132. Gonzalez-Perez, C. and J. Valdes-Gonzalez, *Identification of structural damage in a vehicular bridge using artificial neural networks.* Structural Health Monitoring, 2011. **10**(1): p. 33-48.

133. Meruane, V. and J. Mahu, *Real-time structural damage assessment using artificial neural networks and antiresonant frequencies.* Shock and Vibration, 2014. **2014**.

134. Farrar, C.R. and K. Worden, *An introduction to structural health monitoring.* Philosophical Transactions of the Royal Society A: Mathematical, Physical and Engineering Sciences, 2006. **365**(1851): p. 303-315.

135. Thyagarajan, S., M. Schulz, P. Pai, and J. Chung, *Detecting structural damage using frequency response functions.* Journal of Sound and Vibration, 1998. **1**(210): p. 162-170.

136. Maia, N., J. Silva, E. Almas, and R. Sampaio, *Damage detection in structures: from mode shape to frequency response function methods.* Mechanical systems and signal processing, 2003. **17**(3): p. 489-498.

137. Yan, Y., L. Cheng, Z. Wu, and L. Yam, *Development in vibration-based structural damage detection technique.* Mechanical systems and signal processing, 2007. **21**(5): p. 2198-2211.

138. Kaveh, A. and M. Maniat, *Damage detection based on MCSS and PSO using modal data.* Smart Struct Syst, 2015. **15**(5): p. 1253-70.

139. Nguyen, T.Q., T.T. Nguyen, H. Nguyen-Xuan, and N.K. Ngo, *A Correlation Coefficient Approach for Evaluation of Stiffness*

Degradation of Beams Under Moving Load. Computers, Materials & Continua, 2019. **61**(1): p. 27-53.

140. Cruz, P.J. and R. Salgado, *Performance of vibration-based damage detection methods in bridges.* Computer-Aided Civil and Infrastructure Engineering, 2009. **24**(1): p. 62-79.

141. Nguyen, T.Q., L.Q. Tran, H. Nguyen-Xuan, and N.K. Ngo, *A statistical approach for evaluating crack defects in structures under dynamic responses.* Nondestructive Testing and Evaluation, 2019: p. 1-32.

142. Devriendt, C. and P. Guillaume, *Identification of modal parameters from transmissibility measurements.* Journal of Sound and Vibration, 2008. **314**(1-2): p. 343-356.

143. Zhou, Y.-L. and M.A. Wahab, *Rapid early damage detection using transmissibility with distance measure analysis under unknown excitation in long-term health monitoring.* Journal of Vibroengineering, 2016. **18**(7).

144. Zhou, Y.L., *Structural health monitoringby using transmissibility*. 2015, Industriales.

145. Yan, W.-J., M.-Y. Zhao, Q. Sun, and W.-X. Ren, *Transmissibility-based system identification for structural health Monitoring: Fundamentals, approaches, and applications.* Mechanical Systems and Signal Processing, 2019. **117**: p. 453-482.

146. Deraemaeker, A., A. Preumont, E. Reynders, G. De Roeck, J. Kullaa, V. Lamsa, K. Worden, G. Manson, R. Barthorpe, and E. Papatheou, *Vibration-based structural health monitoring using large sensor networks.* Smart Structures and Systems, 2010. **6**(3): p. 335-347.

147. Weinstein, J.C., M. Sanayei, and B.R. Brenner, *Bridge Damage Identification Using Artificial Neural Networks.* Journal of Bridge Engineering, 2018. **23**(11): p. 04018084.

148. Lee, J.J., J.W. Lee, J.H. Yi, C.B. Yun, and H.Y. Jung, *Neural networks-based damage detection for bridges considering errors in baseline finite element models.* Journal of Sound and Vibration, 2005. **280**(3-5): p. 555-578.

149. Mehrjoo, M., N. Khaji, H. Moharrami, and A. Bahreininejad, *Damage detection of truss bridge joints using Artificial Neural Networks.* Expert Systems with Applications, 2008. **35**(3): p. 1122-1131.

150. Sahin, M. and R. Shenoi, *Quantification and localisation of damage in beam-like structures by using artificial neural networks with experimental validation.* Engineering Structures, 2003. **25**(14): p. 1785-1802.

151. Hakim, S. and H.A. Razak, *Modal parameters based structural damage detection using artificial neural networks-a review.* Smart Structures and Systems, 2014. **14**(2): p. 159-189.

152. Wu, X., J. Ghaboussi, and J. Garrett Jr, *Use of neural networks in detection of structural damage.* Computers & structures, 1992. **42**(4): p. 649-659.

153. Meruane, V., *Online sequential extreme learning machine for vibration-based damage assessment using transmissibility data.* Journal of Computing in Civil Engineering, 2015. **30**(3): p. 04015042.

154. Beale, M.H., M.T. Hagan, and H.B. Demuth, *Neural Network Toolbox™ User's Guide.* The Mathworks Inc, 1992.

155. Demuth, H. and M. Beale, *Matlab neural network toolbox user's guide version 6. The MathWorks Inc.* 2009.

156. Fawcett, T., *ROC graphs: Notes and practical considerations for researchers.* Machine learning, 2004. **31**(1): p. 1-38.

157. Qiao, P., K. Lu, W. Lestari, and J. Wang, *Curvature mode shape-based damage detection in composite laminated plates.* Composite Structures, 2007. **80**(3): p. 409-428.

158. Yoon, M.-K., D. Heider, J.W. Gillespie, C.P. Ratcliffe, and R.M. Crane, *Local damage detection with the global fitting method using mode shape data in notched beams.* Journal of Nondestructive Evaluation, 2009. **28**(2): p. 63-74.

159. Siebel, T., A. Friedmann, M. Koch, and D. Mayer. *Assessment of mode shape-based damage detection methods under real*

operational conditions. in *Proceedings of the 6th European Workshop on Structural Health Monitoring*. 2012.

160. Guo, X., L. Chen, and C. Shen, *Hierarchical adaptive deep convolution neural network and its application to bearing fault diagnosis.* Measurement, 2016. **93**: p. 490-502.

161. Cofré, S., P. Kobrich, E.L. Droguett, and V. Meruane. *Transmissibility based structural assessment using deep convolutional neural network*. in *Proc. ISMA*. 2018.

162. De Oliveira, M.A., A.V. Monteiro, and J. Vieira Filho, *A new structural health monitoring strategy based on PZT sensors and convolutional neural network.* Sensors, 2018. **18**(9): p. 2955.

163. Nguyen, T.Q., L.C. Vuong, C.M. Le, N.K. Ngo, and H. Nguyen-Xuan, *A data-driven approach based on wavelet analysis and deep learning for identification of multiple-cracked beam structures under moving load.* Measurement, 2020: p. 107862.

164. Liang, X., *Image-based post-disaster inspection of reinforced concrete bridge systems using deep learning with Bayesian optimization.* Computer-Aided Civil and Infrastructure Engineering, 2019. **34**(5): p. 415-430.

165. Ali, R. and Y.-J. Cha, *Subsurface damage detection of a steel bridge using deep learning and uncooled micro-bolometer.* Construction and Building Materials, 2019. **226**: p. 376-387.

166. Ciambella, J., A. Pau, and F. Vestroni, *Modal curvature-based damage localization in weakly damaged continuous beams.* Mechanical Systems and Signal Processing, 2019. **121**: p. 171-182.

167. Gu, J., Z. Wang, J. Kuen, L. Ma, A. Shahroudy, B. Shuai, T. Liu, X. Wang, G. Wang, and J. Cai, *Recent advances in convolutional neural networks.* Pattern Recognition, 2018. **77**: p. 354-377.

168. Goodfellow, I., Y. Bengio, and A. Courville, *Deep learning*. 2016: MIT press.

169. Brincker, R., L. Zhang, and P. Andersen, *Modal identification of output-only systems using frequency domain decomposition.* Smart materials and structures, 2001. **10**(3): p. 441.

170. Ewins, D., *Model validation: Correlation for updating.* Sadhana, 2000. **25**(3): p. 221-234.

171. De Roeck, G., E. Reynders, and D. Anastasopoulos. *Assessment of Small Damage by Direct Modal Strain Measurements*. in *International Conference on Experimental Vibration Analysis for Civil Engineering Structures*. 2017. Springer.

172. CSI, S.V., *8. Integrated finite element analysis and design of structures basic analysis reference manual.* Computers and Structures Inc, Berkeley (CA, USA), 2002. **9**.

173. Chung, W. and E.D. Sotelino, *Three-dimensional finite element modeling of composite girder bridges.* Engineering Structures, 2006. **28**(1): p. 63-71.

174. Specht, D.F., *A general regression neural network.* IEEE transactions on neural networks, 1991. **2**(6): p. 568-576.

175. Tran-Ngoc, H., S. Khatir, G. De Roeck, T. Bui-Tien, L. Nguyen-Ngoc, and M. Abdel Wahab, *Model updating for Nam O bridge using particle swarm optimization algorithm and genetic algorithm.* Sensors, 2018. **18**(12): p. 4131.

176. Dooms, D., M. Jansen, G. De Roeck, G. Degrande, G. Lombaert, M. Schevenels, and S. François, *StaBIL: A finite element toolbox for MATLAB.* VERSION 2.0 USER'S GUIDE, 2010.

177. Guo, H., X. Zhuang, and T. Rabczuk, *A Deep Collocation Method for the Bending Analysis of Kirchhoff Plate.* CMC-COMPUTERS MATERIALS & CONTINUA, 2019. **59**(2): p. 433-456.

178. Barai, S. and P. Pandey, *Time-delay neural networks in damage detection of railway bridges.* Advances in Engineering Software, 1997. **28**(1): p. 1-10.

179. Yeung, W. and J. Smith, *Damage detection in bridges using neural networks for pattern recognition of vibration signatures.* Engineering Structures, 2005. **27**(5): p. 685-698.

180. Reynders, E. and G. De Roeck, *Reference-based combined deterministic–stochastic subspace identification for experimental and operational modal analysis.* Mechanical Systems and Signal Processing, 2008. **22**(3): p. 617-637.

181. Srivastava, N., G. Hinton, A. Krizhevsky, I. Sutskever, and R. Salakhutdinov, *Dropout: a simple way to prevent neural networks from overfitting.* The journal of machine learning research, 2014. **15**(1): p. 1929-1958.

182. Gordan, M., H.A. Razak, Z. Ismail, K. Ghaedi, Z.X. Tan, and H.H. Ghayeb, *A hybrid ANN-based imperial competitive algorithm methodology for structural damage identification of slab-on-girder bridge using data mining.* Applied Soft Computing, 2020. **88**: p. 106013.

183. Pham, T., E.J. Kim, and M. Moh. *On data aggregation quality and energy efficiency of wireless sensor network protocols-extended summary*. in *First International Conference on Broadband Networks*. 2004. IEEE.

184. Anastasopoulos, D., M. De Smedt, L. Vandewalle, G. De Roeck, and E.P. Reynders, *Damage identification using modal strains identified from operational fiber-optic Bragg grating data.* Structural Health Monitoring, 2018. **17**(6): p. 1441-1459.

Infrastructure and smart communication network.